uOttawa

L'Université canadienne
Canada's university

FACULTÉ DES ÉTUDES SUPÉRIEURES ET POSTOCTORALES

uOttawa

L'Université canadienne
Canada's university

FACULTY OF GRADUATE AND POSDOCTORAL STUDIES

Jennifer Marie Paterson
AUTEUR DE LA THÈSE / AUTHOR OF THESIS

M.Sc. (Biochemistry)
GRADE / DEGREE

Department of Biochemistry, Microbiology and Immunology
FACULTÉ, ÉCOLE, DÉPARTEMENT / FACULTY, SCHOOL, DEPARTMENT

Investigation of the oncolytic activity of Vesicular stomatitis virus murine cancer models

TITRE DE LA THÈSE / TITLE OF THESIS

J. Bell
DIRECTEUR (DIRECTRICE) DE LA THÈSE / THESIS SUPERVISOR

CO-DIRECTEUR (CO-DIRECTRICE) DE LA THÈSE / THESIS CO-SUPERVISOR

EXAMINATEURS (EXAMINATRICES) DE LA THÈSE / THESIS EXAMINERS

P. Liston

R. Parks

Gary W. Slater
LE DOYEN DE LA FACULTÉ DES ÉTUDES SUPÉRIEURES ET POSTDOCTORALES /
DEAN OF THE FACULTY OF GRADUATE AND POSTDOCORAL STUDIES

Investigation of the oncolytic activity of Vesicular stomatitis virus in murine cancer models

Jennifer Marie Paterson, B.Sc.

Thesis submitted to the
Faculty of Graduate and Postdoctoral Studies
In partial fulfillment of the requirements
for the Master of Sciences degree in Biochemistry

Department of Biochemistry, Microbiology and Immunology
Faculty of Medicine
University of Ottawa

Your file Votre référence
ISBN: 0-494-11377-4
Our file Notre référence
ISBN: 0-494-11377-4

Abstract

Interferon (IFN) inducing strains of Vesicular stomatitis virus (VSV) replicate selectively in transformed cells and exert impressive oncolytic abilities in murine tumour models. Interestingly, in some tumour models, complete tumour cures can only be obtained by administering multiple intravenous doses of virus, indicating that there must be barriers that limit the ability of a single dose of virus to eliminate a tumour. The goal of the current research was to examine the intravenous delivery of IFN inducing VSV to subcutaneous tumours, as well as subsequent spread and tumour killing activity. It was found that intravenous delivery is inefficient and seems to result in preferential delivery of virus to the tumour rim. However, apoptosis is induced throughout the uninfected core of the tumour, indicating that VSV may induce indirect killing of tumour cells. While the specific cause of this apparent bystander effect was not determined, it was observed that VSV treatment also resulted in collapse of functional tumour vasculature.

Acknowledgements

I would like to thank my supervisor John Bell firstly for always being excited about my work, and providing excellent advice (although he thinks I just did whatever I wanted anyway). I would like to thank David Stojdl and Brian Lichty, who's work and guidance provided the rationale for this project. I would like to thank Kelley Parato for sound advice and encouragement, and Anthony Power for stimulating discussion. I would like to thank Jen Reynard for many intravenous injections and entertaining walks to Biohazard, and Alison McGuire for excellent laboratory assistance and friendship over two summers. I would also like to thank Jamie and Grace for helping to make the lab fun, and everyone else in the Bell lab and the Ottawa Regional Cancer Centre for their support. I would like to thank my parents for their generous support and encouragement throughout my life and career. Finally, I would like to thank Matthew for putting up with my frustrating work habits and staying up all night with me many times so I didn't get too tired.

Table of Contents

List of Abbreviations

ATF2	Activating transcription factor 2
CBP/p300	CREB binding protein and p300
CT26	Colon carcinoma 26
Δ51	Deletion of methionine 51 in matrix protein of VSV
DMEM	Dulbecco's modified Eagle's medium
dsRNA	double stranded RNA
G	Glycoprotein (of VSV)
GFP	Green fluorescent protein
GFPLuc	Fusion of GFP and fifefly luciferase (Clontech)
H&E	Hematoxylin and eosin (staining of tissue sections)
HSV	Herpes simples virus
IF	Immunofluorescence
IFN	Interferon
IHC	Immunohistochemistry
IKKi	Inducible IκB kinase
IL-4	Interleukin 4
IN	Intranasal
IP	Intraperitoneal
IPC	Interferon producing cell
IRF	Interferon regulatory factor
ISG	Interferon stimulated gene
IT	Intratumoural
IV	Intravenous
JAK	Janus kinase
L	Large polymerase protein (of VSV)
Luc	Luciferase (Firefly)
M	Matrix protein (of VSV)
M51R	Substitution of methionine 51 for arginine in matrix protein of VSV
MEF	Mouse embryonic fibroblast
MOI	Multiplicity of infection
N	Nucleocapsid protein (of VSV)
NDV	Newcastle disease virus
NFkB	Nuclear factor kB
OAS	2'-5' oligoadenylate synthase
P	Phosphoprotein (of VSV)
PBS	Phosphate buffered saline
PCR	Polymerase chain reaction
PFU	Plaque forming units
PKR	Protein kinase R
RFP	Red fluorescent protein
RLU	Relative light units (for luciferase assay)
RNAseL	Ribonuclease L
SEM	Standard error of the mean
ssRNA	single stranded RNA
STAT	Signal Transducer and Activator of Transcription
TBK1	Tank binding kinase

TK	Thymidine kinase
TLR	Toll like receptor
TNFα	Tumor necrosis factor α
TUNEL	Terminal deoxynucleotidyl transferase-mediated dUTP nick end labeling
TYK2	Tyrosine kinase 2
V221F	Substitution of valine 221 for phenylalanine in matrix protein of VSV
VSV	Vesicular stomatitis virus
WT	Wild type

List of Figures and Illustrations

Introduction

Conventional and novel cancer therapies

Cancer is a disease that occurs when normal cells develop genetic mutations that result in their uncontrolled proliferation. Every year, more than 140,000 Canadians will be diagnosed with cancer, and almost half of these patients will eventually die of their disease(1). The high cancer mortality rate is due to several factors: difficulty in detection and diagnosis, low therapeutic index of current treatments, and the possibility of disease recurrence from a very small number of cancer cells escaping treatment (2).

The most common cancer therapies are surgery, radiation therapy, and chemotherapy (3). Surgeons can successfully remove many primary solid tumours, however malignant cells invading surrounding normal tissue, or metastasizing to distant sites, often lead to disease recurrence. Radiation, which is also targeted to specific tumour sites, suffers from the same limitations as surgery, with the added burden of evolving radiation resistance. Chemotherapy describes a large class of anti-cancer drugs that are applied systemically as opposed to locally. Thus, chemotherapy can target primary tumours as well as metastases, and even disseminated leukemias. However, most chemotherapies kill some normal cells as well as malignant cells, and the resulting toxicity contributes to a relatively small therapeutic window (3).

The past several decades have brought about a dramatic revolution in our understanding of cancer at a molecular level, prompting the development of many novel cancer therapies. These molecular therapies target specific genetic mutations found only in cancer cells, and are thus less toxic to normal tissues than

conventional chemotherapeutics. Examples include radio-labeled recombinant antibodies that bind selectively to tumour-specific antigens, and suicide gene therapy under the control of cancer-specific promoters (3). Despite vast amounts of research, however, cancer mortality rates have changed little since the 1970s(1). Many of the novel molecular cancer therapies (including antibodies and gene therapy vectors) are substantially larger than conventional chemotherapeutics, and it is thought that this difference may lead to very inefficient delivery to solid tumours via the vascular route (4). Oncolytic viruses, which are the subject of this report, have prompted high hopes in the last decade because they can specifically target molecular cancer defects, and also actively replicate and spread throughout solid tumours, thus potentially overcoming inefficient delivery.

Historical overview of oncolytic viruses

Historically, viral infections have occasionally been associated with the remission of cancer in humans, and such observations may have provided the impetus for the deliberate therapeutic testing of viruses in animal cancer models beginning as early as the 1920s, as reviewed by Sinkovics and Horvath (5). Unfortunately, the viruses that were most capable of destroying tumours also proved to be the most lethal in animals (6). For example, in 1937, Levaditi and Haber showed that fowl plague virus (avian influenza) could destroy transplanted tumours in immune-competent mice, although the virus invariably killed the mice within a week of treatment (7). Tumour destruction could only be evaluated histologically, and by the failure of treated tumours to transplant into naïve mice.

Relatively few viruses were found to be able to cure tumours without subsequently killing the mouse. One example, however, is Newcastle disease virus

(NDV), which could prevent the development of lethal Ehrlich ascites tumours if the mouse was treated with virus within 6 days of receiving the tumour cells (8). Interestingly, cured mice were found to be immune to subsequent challenge with high doses of the same tumour cells, suggesting that the virus may have stimulated anti-tumour immunity (9). Vesicular stomatitis virus (VSV), the subject of this report, was also tested for oncolytic ability, although in a less convincing manner. In 1969, Sinkovics and Howe showed that when murine lymphoma cells were infected with VSV in vitro, and then transplanted into mice, about half of the mice receiving infected cells rejected the lymphoma, while all the mice receiving uninfected cells died of cancer (10). Obviously, killing tumour cells before implantation into mice is not as impressive as eliminating a mature tumour *in situ*. At around the same time, it was shown that antigens prepared from VSV-infected Ehrlich ascites cells in vitro (oncolysates) could immunize mice against subsequent challenge with those same cells (11). Again, this suggested that the stimulation of tumour immunity might be an important part of the action of oncolytic viruses.

Promising animal results prompted several small scale human cancer trials using West Nile virus (12) NDV (13), and mumps virus (14) among others. As reviewed by Sinkovics and Horvath (5), convincing remissions occurred rarely among the majority of marginal or unsuccessful attempts(5). As of the mid-1990s, no rigorously controlled human clinical trials had been performed, and oncolytic virus therapy, although popular in some alternative medical circles, was not widely accepted by the mainstream medical community (15, 16).

Oncolytic virus revolution

In the 1990s, two major developments sparked a resurgence of interest in oncolytic viruses. Firstly, in 1991, Martuza and colleagues developed the first genetically engineered oncolytic virus: Herpes Simplex Virus 1 (HSV-1) deleted of its Thymidine Kinase (TK) gene (17). TK is responsible for recycling nucleotides required for DNA synthesis by HSV; specifically, this gene is required for viral replication in non-dividing cells, which have low nucleotide pools. Cancer cells, however, upregulate many enzymes required for DNA synthesis, and thus TK is not required for the replication of HSV in these cells. Martuza hypothesized that TK-deleted HSV would selectively replicate in and kill human brain cancer cells while sparing normal nondividing neurons. Indeed, this virus could be safely injected into the brains of nude mice bearing human glioma xenografts, and prolong the survival of these mice. Although no cures were observed in this study, the strategy of genetically engineering broadly permissive viruses to limit their replication in normal cells (but not cancer cells) has been refined and expanded. Examples include E1B-deleted Adenovirus (18), TK and VGF deleted Vaccinia virus (19), NS1-deleted Influenza A virus (20), and γ34.5-deleted HSV-1 (21).

The second major development in oncolytic virus therapy was the first report of complete durable cures of human cancer xenografts in nude mice (which cannot mount an acquired immune response), using NDV in 1994 (22, 23). This development was important because all previous reports of oncolytic virus cures were in immune competent mice, where virus induced acquired tumour immunity was thought to play a large role. These studies, however, showed that an oncolytic virus could completely destroy a tumour without the aid of acquired immunity. The

role of innate immunity, however, is currently a hot topic in oncolytic virus therapy, and will be discussed further. Although the molecular mechanism by which NDV could selectively replicate in cancer cells was not investigated, these promising preclinical results may have encouraged further research into Reovirus and VSV, both naturally occurring oncolytic viruses whose tumour killing specificity was under investigation (24-26).

Vesicular stomatitis virus: life cycle and epidemiology

As mentioned above, live VSV was briefly experimented with as a cancer therapeutic in mouse models in the 1960s, however its well known neurovirulence may have dampened enthusiasm for further experiments at the time. Recent insights into the mechanism of wild type (WT) Indiana serotype VSV oncolysis (26), as well as the development of neuro-attenuated oncolytic strains (27) have led to a resurgence in interest in VSV, and have provided the foundation for the detailed work described in this thesis. Before discussing the oncolytic potential of VSV, a brief description of the virus biology will be provided.

VSV, a member of the genus *Vesiculovirus* and the family *Rhabdoviridae*, is an enveloped, bullet shaped particle of 180 x 75 nm (28). As shown in Figure 1, the VSV virion contains a nonsegmented negative sense RNA genome of 11kb encoding 5 major genes. Because of its ease of culture, VSV has long been used a model negative sense RNA virus to study viral gene expression, evolution, and host cell interactions (28).

The molecular life cycle of VSV has been reviewed in detail elsewhere (28), and will be discussed here only briefly. Interaction of the trimeric membrane-bound glycosylated VSV Glycoprotein (G) with its ubiquitous cell surface receptor

Figure 1. Virion and genetic structure of VSV.

A: Virion structure. VSV forms a bullet shaped particle, enveloped in a host-derived plasma membrane, containing all five viral proteins and the single stranded negative sense RNA genome. The L (Large) protein forms the major component of the RNA dependent RNA polymerase, along with P (Phosphoprotein) and N (Nucelocapsid) protein, which also has a role in packaging the genome. The G (Glycoprotein) forms a glycosylated trimer that binds the host receptor, phosphatidylserine and mediates pH dependent membrane fusion. The M (Matrix) protein has a role in virus assembly and budding, cytopathic effects, and host cell shut off.

B: Genome structure and gene expression. The viral genome consists of a single negative sense RNA molecule that acts as a template for transcription of positive sense mRNAs in sequential order from the 3' end of the genome. The polymerase pauses at the end of each transcript, and reinitates with imperfect efficiency, such that genes at the 3' end (N) are transcribed more than genes at the 5'end (L) providing a mechanism of regulation of gene expression. The leader (le) and trailer (tr) regions are transcribed but not translated. See text for further details.

A

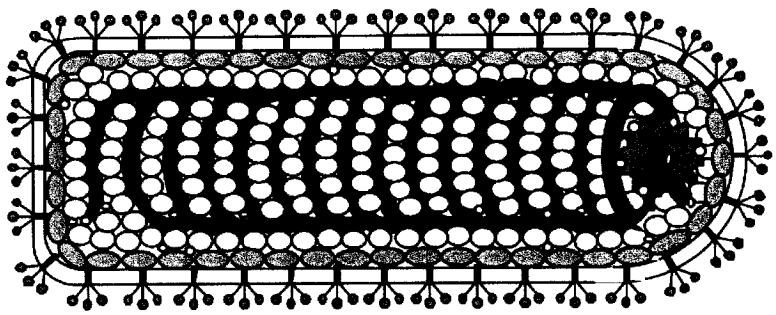

B

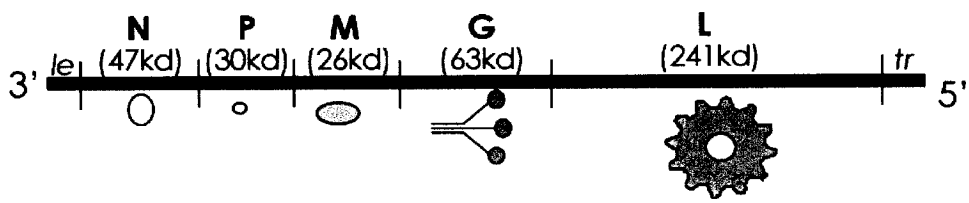

phosphatidylserine triggers endocytosis of the viral particle. Acidification of the endosome prompts the G-protein mediated fusion of the viral and endosome membranes, such that the single copy RNA genome, wrapped in Nucleocapsid (N) protein, is released into the cytoplasm along with the other virally encoded proteins L (Large), P (Phosphoprotein) and M (Matrix). L, P, and N along with host factors (29) form the polymerase, which immediately transcribes capped and polyadenylated mRNAs in sequential order from the 3' end of the negative sense genome, as shown in Figure 1. The polymerase pauses at the end of each transcript, and reinitiates with imperfect efficiency, such that genes at the 3' end (N) are transcribed more than genes at the 5'end (L) providing a mechanism of regulation of gene expression.

Viral mRNAs are translated by host machinery, and the accumulation of viral proteins triggers a switch from transcription of mRNAs to replication of full length positive sense RNA anti-genomes (28). These anti-genomes provide a template for the subsequent generation of negative sense genomes, which can act as further mRNA templates and later be packaged into progeny virus particles.

Throughout the rapid cycles of viral transcription, translation, and replication, the VSV M protein plays a crucial role in controlling the host cell by inhibiting the expression of cellular genes. Host protein synthesis is reduced to less than 10% of normal levels just four hours after infection, and this effect can be reproduced by transfection of M mRNA (30, 31). By shutting off host gene expression, VSV allows its own mRNAs to take full advantage of the cellular translational machinery, and also inhibits the expression of host antiviral proteins (27). This is an important phenomenon that will be discussed in more detail later. The M protein also localizes

to the plasma membrane, where it interacts with newly synthesized G, and plays a crucial role in virus budding (28). Progeny viruses begin to bud just two hours after infection (32).

VSV occurs in two serotypes in nature: New Jersey and Indiana, both of which are found in parts of South America, Mexico, and the southern United States (33). Although the natural ecological life cycle of VSV remains unclear, livestock such as cattle, horses, and pigs, as well as many wild mammals become infected and seroconvert, as reviewed by Rodriguez (34). Symptoms, including fever and ulceration of oral tissues and feet, are short-lived, and persistent infection has not been documented. Epidemics of VSV among livestock occur about every ten years in the southern United States, while yearly endemic infections occur further south. Biting insects, such as mosquitoes, sandflies, and black flies become productively infected with VSV, and may transmit the virus between mammalian hosts (35, 36). In endemic areas, human VSV seropositivity is common, while in the United States, exposure seems to be limited to animal handlers who become infected during epidemics (33). Human symptoms, which may include fever, conjunctivitis, and vesicular lesions, are short-lived (33).

Innate immunity to viruses

As VSV's interaction with the innate immune system is key to recent research into its oncolytic ability, a brief description of this pathway will be provided. The primary innate defense against viruses, present in most cell types of all vertebrates, is the Interferon (IFN) system, illustrated in Figure 2. IFN was first characterized as a secreted factor, produced in response to inactivated influenza virus, that could inhibit the replication of live virus (37). Type I IFN in mammals includes more than 10

Figure 2. The Interferon pathway as characterized in MEFs.

1) Virus is recognized by sensor proteins that trigger the phosphorylation TBK1 and IKKi, which are kinases that then phosphorylate IRF3, resulting in its activation and translocation into the nucleus **(2)**. In the nucleus, IRF3 associates with the cofactors CBP/p300, and along with other transcription factors (NFkB, and ATF2/cJun), induces the transcription of a select set of Type I IFN genes (IFNβ and possibly IFNα4), which are then translated and secreted **(3)**. IFNβ binds to the IFN receptor **(4)**, resulting in dimerization and activation of the JAK1 and TYK2 kinases. These kinases phosphorylate STATs, which form a complex with IRF9. This complex activates the transcription **(5)** of hundreds of IFN stimulated genes (ie. ISG56, ISG20, PKR and OAS), which can severely limit virus replication **(6)**. Some ISGs, including ISG56, can be induced by IRF3 in the first transcriptional wave, followed by IFN mediated amplification in the second wave. IFN also induces the transcription of IRF7 **(7)**, which is then activated by virus-induced phosphorylation in a similar manner to IRF3 **(8)**. IRF7 can then further activate the transcription of IFNβ, as well as all the subtypes of IFNα that were not induced by IRF3 **(9)**. This IRF7 mediated increase in Type I IFN production **(10)** feeds back to further augment ISG synthesis **(11)**, resulting in self-amplifying waves of IFN production. See text for further details.

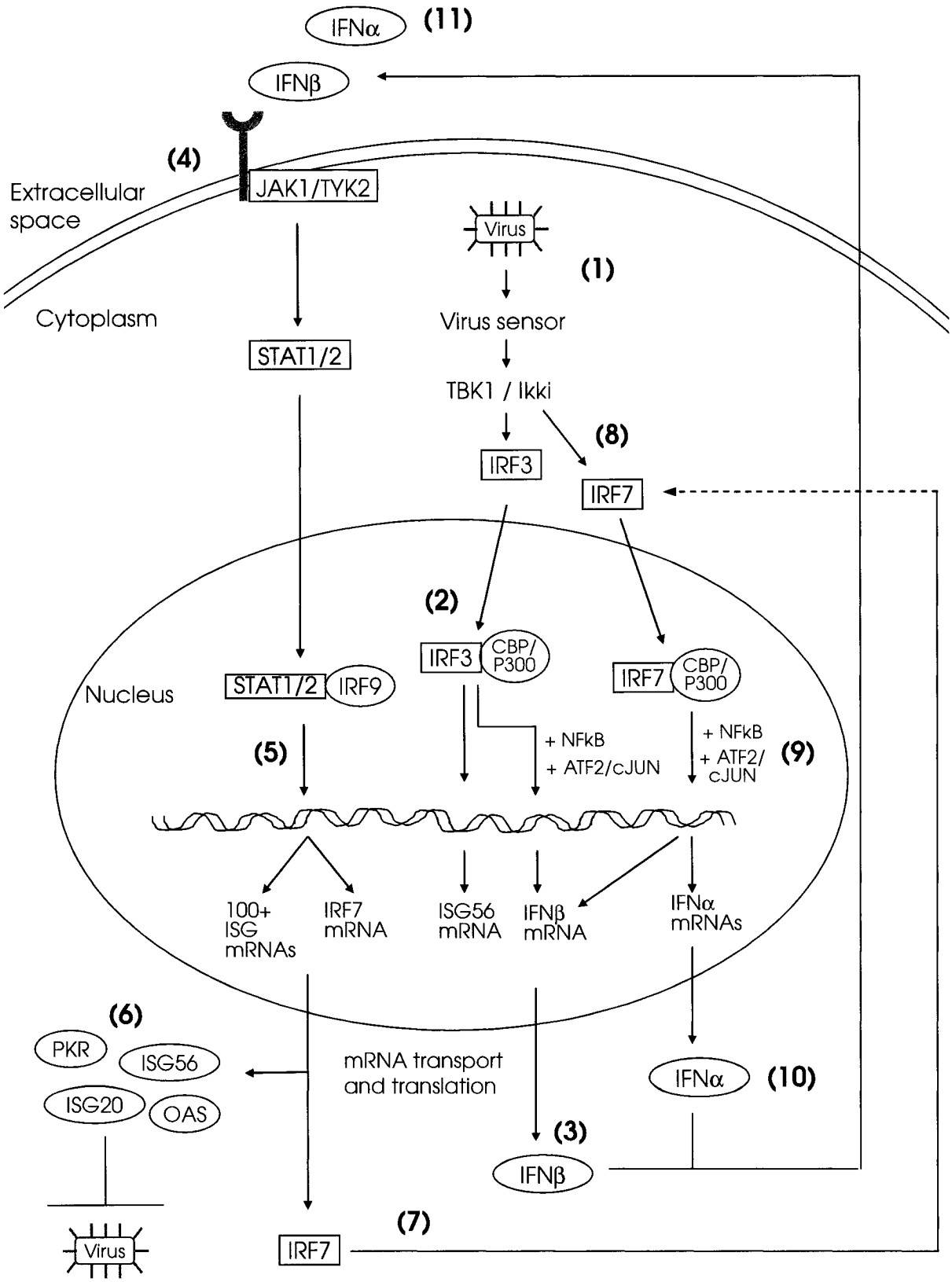
IFNα
(11)
IFNβ
(4)
Extracellular space
JAK1/TYK2
Virus
(1)
Cytoplasm
Virus sensor
STAT1/2
TBK1 / Ikki
(8)
IRF3
IRF7
(2)
IRF3
CBP/ P300
IRF7
CBP/ P300
Nucleus
STAT1/2
IRF9
+ NFkB
+ ATF2/cJUN
+ NFkB
+ ATF2/ cJUN
(9)
(5)
100+ ISG mRNAs
IRF7 mRNA
ISG56 mRNA
IFNβ mRNA
IFNα mRNAs
(6)
PKR
ISG56
ISG20
OAS
mRNA transport and translation
IFNα
(10)
(3)
IFNβ
Virus
IRF7
(7)

IFNα subtypes, one IFNβ, and the less well characterized ω,κ, and δ subtypes, which all bind to the same receptor (38, 39). Type II Interferon (IFNγ) is not structurally related to Type I IFN, and plays a more restricted antiviral role, predominantly in the regulation of acquired immunity (40).

Although Type I IFN was first characterized almost 50 years ago (37), the exact mechanism by which viruses induce its production is still under investigation. Some viruses induce extensive secretion of IFN in cell culture, while others, including VSV, induce little to no IFN because they inhibit host gene expression (41). dsRNA is also a potent IFN inducer; for many years it was assumed that all viruses produced dsRNA as replicative intermediates, and that this was the mechanism by which such a wide diversity of unrelated viruses could trigger similar innate immune responses. Recent research has pointed to the importance of other viral IFN inducers, which will be briefly discussed at the end of this section.

It is currently thought that the transcription factors IFN Regulatory Factor 3 (IRF3) and the related IRF7 play key roles in a positive feedback model of IFN induction which has been well characterized in Mouse Embryonic Fibroblasts (MEFs) (42-44). IRF3 is constitutively expressed in the cytoplasm in an inactive form. Upon virus infection, IRF3 becomes phosphorylated and translocates into the nucleus, where it associates with the cofactors CBP/p300. Active IRF3 cooperates with other virus activated transcription factors (NFκB, and ATF2/cJun) to induce the transcription of a select set of Type I IFN genes (IFNβ and possibly IFNα4), which are then translated and secreted.

This IRF3-induced IFN acts in an autocrine / paracrine manner, binding to the IFN receptor in the plasma membrane and signaling through the activation of the

JAK / STAT pathway. STAT1/2 heterodimers form a complex with IFN Regulatory Factor 9 (IRF9) which activates the transcription of hundreds of IFN stimulated genes (ISGs), which can severely limit virus replication (45). ISG20, for example, degrades viral RNA (46), while ISG56 inhibits translation (47). Although these proteins appear to be active immediately upon synthesis, other ISGs are produced in a latent form, requiring double stranded RNA (dsRNA) mediated enzymatic activation. Examples in this class include Protein Kinase R (PKR), which inhibits translation (48) and 2'5' Oligoadenylate synthase (OAS), which activates Ribonuclease L (RNAseL) to degrade viral RNA (49). Other ISGs have roles in immune modulation, growth inhibition, and apoptosis, as will be discussed in more detail later. While some ISGs strictly require the JAK/STAT pathway for transcription, others, including ISG56, can be induced by IRF3 in the first transcriptional wave, followed by IFN mediated amplification in the second wave (50, 51).

IFN also induces the transcription of IRF7, which is then activated by virus-induced phosphorylation in a similar manner to IRF3. IRF7 is distinct from IRF3, however, in that it can activate the transcription of IFNβ and IFNα4, as well as many of the other subtypes of IFNα that were not induced during the first wave of transcription. Thus, The IFN system in MEFs functions in waves: IRF3 induced IFNβ expression, followed by modest IFNβ induced expression of ISGs, including IRF7, which is then followed by an IRF7-mediated massive amplification in IFNα/β production, which then further stimulates ISG production.

While this positive feedback model is widely supported by studies in cells of fibroblast and epithelial origin, the model must be modified to explain IFN production in leukocytes (52-55). In particular, during systemic virus infection in

mammals, the majority of IFN is produced by specialized subsets of dendritic cells referred to as either Interferon Producing Cells (IPCs) or plasmacytoid dendritic cells. It appears that in these cells, IRF7 is present constitutively, in contrast to MEFS where it is transcriptionally induced only upon stimulation with IFN. Accordingly, IPCs are able to produce large amounts of all subtypes of IFN immediately upon stimulation, as opposed to in amplifying waves.

Recently, important progress has been made defining the mechanism by which viruses induce IFN synthesis. Both viruses and dsRNA have been shown to induce IRF3/7 phosphorylation by TANK-binding kinase 1 (TBK1) and inducible IκB kinase (IKKi) (56, 57). In the case of dsRNA, this signaling pathway has been shown to be mediated through the dsRNA binding Toll Like Receptor 3 (TLR3), as well as through TLR3 independent mechanisms (56, 58). However, recent evidence has suggested that RNA viruses, including VSV, are not recognized by TLR3, but by TLR7, a receptor for endocytosed ssRNA (59-62). At least in IPCs, virus mediated activation of TLR7 is responsible for the vast majority of IFN synthesis (61, 62).

VSV is exquisitely sensitive to IFN

VSV Indiana induces very little IFN production in sensitive cell lines in vitro (27, 63-65), however enough IFN is induced in vivo (probably by IPCs) to significantly curb VSV infection. This was demonstrated by the observation that mice lacking the Type I IFN receptor uniformly succumbed to lethal intravenous (IV) infection with just 30-50 Plaque Forming Units (PFU) of VSV, while control mice could easily tolerate more than 100,000 times that dose (66). This and other evidence has earned VSV a reputation as a virus that is extremely sensitive to IFN. In comparative studies in vitro, VSV was consistently found to be one of the most IFN sensitive viruses, as

summarized in several reviews (41, 67). For example, in Vero monkey kidney cells, just a single unit of IFNβ could inhibit the yield of VSV by half, while 53 units were required to achieve the same effect with HSV1, and 1500 units were required for HSV2 (68). PKR seems to play a crucial role in the IFN induced protection of mice against VSV, especially during intranasal infection. This was revealed by the susceptibility of PKR-/- mice to lethal VSV infection with just 50 PFU, a phenotype which could not be rescued by exogenous IFN (48).

Many cancer cells are resistant to IFN

While we have so far focused on the role of IFN in innate antiviral defense, IFN can also affect cell proliferation, apoptosis, and the immune system in the absence of viral infection (69). Studies in the late 1960s showed that exogenously administered IFN could markedly inhibit the growth of several transplantable tumours in mice (70). Unfortunately, these dramatic results have not been reproduced in human clinical trials, with the exception of certain hematological malignancies (71). In fact, IFN seems to affect most cancer cells much less than normal cells in vitro. For example, studies in our lab have shown that 42 out of 52 human cancer cell lines in the National Cancer Institute 60 cell panel have defects in their response to IFN (27). The widespread resistance of cancer cells to IFN may result from the presence of low levels of endogenous IFN during tumour development that selects for tumour cells that can resist its antiproliferative effects. Indeed, transplanted tumours develop more readily and grow faster in mice treated with anti-IFN antibodies (72) or in IFN receptor knockout mice (73), suggesting that endogenous IFN is sufficient to affect tumour development.

Research has shown that the IFN pathway in general, as well as several specific genes involved in this pathway, can function as tumour suppressors. Overexpression of IFNα (74), the Type I IFN receptor (75), IRF3 (76), or IRF1 (77) reduces cell proliferation and decreases tumorigenicity in mice. Furthermore, deletions of IRF1 have been associated with leukemia and myelodysplasia (78), while deletions in IFNα/β may be common in acute lymphoblastic leukemia (79). Interestingly, a recent survey of 91 patients with a diverse array of neoplasms revealed high circulating levels of secreted IFN receptors, more than 5 times the level present in control subjects (80).

Several specific ISGs have also been implicated in tumour development. Inhibitors of PKR have oncogenic properties (81, 82), and PKR activation was found to be defective in 21 of 28 chronic lymphocytic leukemia patients (83). Deficiencies in STAT1 (84), RNAseL (85), and the novel ISG IFIX (86) have also been documented in human cancers.

Thus, a growing overlap between antiviral defense and anti-tumour defense is being revealed. Proteins thought to function solely in inhibiting viruses (PKR and RNAseL) seem to be involved in inhibiting tumour formation, while several genes thought to be involved in tumour formation are now known to control susceptibility to viruses. An important example is p53, a tumour suppressor gene which is defective in about 50% of human cancers; the p53 and IFN pathways have recently been linked, and p53-/- mice were shown to be extremely susceptible to VSV infection (87). Another example is Ras, an oncogene that is activated in about a third of human cancers; transfection with activated Ras inhibits the activity of PKR and transforms reovirus resistant NIH 3T3 cells into reovirus factories (24). Collectively,

this body of research led to the idea that as tumours progressed, they would develop mutations in growth control pathways that would simultaneously increase their susceptibility to viruses (26).

VSV selectively kills tumour cells with defects in the IFN pathway

As discussed earlier, VSV is well known as a poor inducer of IFN in cell culture, with, however, striking susceptibility to the antiviral effects of exogenous IFN. In 2000, Stojdl and colleagues postulated that because many cancers had defects in their response to IFN, VSV would be able to selectively kill tumour cells while sparing normal cells in the presence of IFN (26). Indeed, IFN pretreatment eliminated detectable virus production from four of five normal human cell cultures, while a diverse sample of human carcinoma cells were partially or totally resistant to the antiviral effects of IFN. Injection of 10^9 PFU of VSV into subcutaneous human melanoma xenografts in nude mice induced partial tumour regression in all animals, with three of 12 animals demonstrating complete cures. In this study, mice had to be treated with IFN to prevent VSV from spreading to the brain and killing the animals. Thus, VSV was shown to be a potent and safe oncolytic virus in the presence of exogenous IFN.

Research by other groups confirmed the specificity of VSV for killing IFN resistant tumour cells, and expanded the number of mouse tumour models in which oncolytic VSV was active (88, 89). In these studies, instead of protecting mice from VSV's neurovirulence using exogenous IFN, lower doses of virus ($2\text{-}5\times10^7$ PFU) were injected into tumours to avoid the neurological side effects. While impressive growth inhibitory effects were observed, no durable cures were obtained. Other important milestones were achieved, however. Firstly, oncolytic VSV activity was

demonstrated by intravenous (IV) as opposed to intratumoural (IT) administration of virus. Systemic treatment with oncolytic viruses is highly desirable because most cancer deaths occur from metastatic disease (2). Unfortunately, although IV administered VSV could inhibit the growth of subcutaneous tumours, mice had to be euthanized prematurely due to neurological complications. The second important experiment showed that VSV (delivered IT) could inhibit the growth of tumours in immune competent mice. All previous studies had used nude mice, which lack an acquired immune system and thus have impaired antiviral defenses. As potential human patients would certainly have an acquired immune system, it was reassuring that VSV could exert antitumoural effects in mice despite the presence of all the natural antiviral defenses.

Building a better oncolytic VSV

There are several reasons why VSV in particular is an attractive candidate oncolytic virus. Firstly, VSV is extensively well characterized, as it has been used for decades as the model virus of its class to study the molecular mechanisms of viral gene expression and cytopathogenesis. Novel recombinant viruses can be engineered and rescued using relatively simple plasmid-based expression systems in cell culture (90). Furthermore, as discussed previously, VSV is not endemic to North America, and thus cancer patients could be treated here without the complication of pre-existing neutralizing anti-VSV antibodies. VSV is also a rapidly replicating virus, a property that might be crucial in a race to spread throughout a tumour before the host immune system becomes fully activated. Lastly, as an RNA virus with no DNA intermediate, VSV has no transforming potential.

Unfortunately, the first studies to test VSV as an oncolytic agent revealed the important limitation of neurotoxicity. In fact, Lindenmann and Klein had previously observed in the 1960s that the most potent oncolytic viruses were also the most neurovirulent (6). As it stood, VSV could either be administered at suboptimal doses to avoid its neurovirulence, or exogenous IFN could be applied to protect the brain. Over the next several years, two different strategies were employed to solve this problem. The first strategy was to increase the tumour-specific toxicity of VSV so that low doses of the virus were more efficacious. The second strategy was to attenuate the virus selectively in normal cells so that very high doses could be delivered systemically without neurotoxicity.

VSVs genetically engineered to induce bystander tumour cell killing

The former strategy, of increasing tumour-specific toxicity, was first exemplified by Fernandez and colleagues, who engineered recombinant VSVs expressing either murine Interleukin 4 (IL-4) or the Herpes Simplex Virus Thymidine Kinase (TK) gene (91). IL-4 is an immune-stimulating cytokine that may play a role in tumour rejection (92), while TK is a suicide gene frequently used in gene therapy (93). As mentioned earlier, TK is responsible for maintaining nucleotide pools for DNA synthesis during Herpes infection. However TK can also convert the non-toxic prodrug Gancyclovir into a toxic metabolite that spreads from cell to cell. Thus TK gene therapy is often used in combination with Gancyclovir to induce bystander cell-killing.

As predicted, these novel viruses were significantly more potent than the Wild Type (WT) non-recombinant VSV in two subcutaneous tumour models in immune competent mice, with IT virus delivery (91). Although durable cures were not

obtained in these tumour models, both novel recombinant viruses were able to completely cure 50% of immune competent animals of metastatic disease. In the metastatic model, both tumour cells and viruses were administered IV. This study was later followed up with the description of another recombinant VSV expressing a more potent suicide gene: a fusion of *Escherichia coli* cytosine deaminase with uracil phosphoribosyltransferase (94). This virus did appear to be more potent than the previous TK version, especially in tumour cells that were relatively resistant to VSV.

Another group has also attempted to improve the oncolytic ability of VSV using a very different mechanism: Ebert and colleagues genetically engineered VSV to express a modified version of the Newcastle Disease Virus Fusion protein (95). This mutant protein was shown to mediate very efficient fusion of infected and non-infected cells into huge multinucleated virus-producing syncytia. It was suggested that the fusion strategy of bystander cell-killing would be more potent than the typical suicide gene / pro-drug systems already tried. Indeed, in a difficult model of *in situ* multifocal hepatocellular carcinoma in immune competent rats, this novel virus could more than double the time to death, and was significantly more efficacious than a non-fusogenic VSV.

In summary, recombinant VSVs designed to induce bystander tumour cell killing have significantly increased oncolytic ability in vivo. These viruses were all administered at relatively low doses to avoid neurological complications. As mentioned above, another strategy to increase the oncolytic ability of VSV is to specifically attenuate the virus in normal cells so that it can be systemically

administered safely at very high doses. This approach was pioneered by Stojdl and colleagues using naturally occurring IFN inducing VSV mutants (27).

IFN inducing mutants of VSV are attenuated in normal tissues, yet retain their tumour killing ability

In the 1970s and 80s, several VSV mutants were isolated that formed small plaques on monolayers of cells that were capable of producing IFN, yet still spread rapidly on cells that could not produce IFN (96, 97). Many of these presumably IFN-inducing mutants were also unable to inhibit host proteins synthesis. Thus, instead of thinking of WT VSV as failing to induce IFN, it was realized that WT VSV might trigger the production of IFN, yet inhibit global host gene expression such that IFN was never secreted. The M protein was subsequently found to be responsible for this attenuated phenotype: of six mutants previously isolated, all were found to have the M protein mutations Methionine 51 to Arginine (M51R), or Valine 221 to Phenylalanine (V221F) (98).

Although the mechanism by which WT M inhibits host gene expression has been debated (99, 100), recent evidence has convincingly shown that WT M protein blocks the nucleocytoplasmic transport of host mRNAs, including the IFNβ mRNA, by binding to nuclear pore complex subunit Nup98 (27, 101). Significantly, site directed mutagenesis studies revealed that M amino acids 52-54 were critical for the binding of M to Nup98 (101). In addition, two of the IFN inducing mutant viruses originally isolated (M51R and V221F/S226R) were also shown to inhibit the nucleocytoplasmic export of host mRNAs (27).

Since exogenously administered IFN seemed to be able to protect nude mice from VSV's neurovirulence without compromising its oncolytic ability, Stojdl

and colleagues hypothesized that the previously isolated IFN-inducing VSV mutants might also retain their oncolytic ability, yet lose the ability to replicate in normal IFN-sensitive tissues such as the brain (27). Indeed, very high doses (10^9 PFU IV) of both the M51R VSV (termed AV1) and the V221F/S226R VSV (AV2) were well tolerated by immune competent and nude mice without any signs of neurotoxicity (27). Side effects, including piloerection and weight loss, were mild and short-lived. Just a tenth of the dose of WT virus still killed half of treated animals. The observed attenuation was solely due to the IFN inducing ability of AV1 and AV2, since Type I IFN receptor knockout animals were equally susceptible to WT, AV1 and AV2 VSV.

Crucially, AV1 and AV2 displayed impressive oncolytic ability in a variety of mouse cancer models (27). The most striking effect was observed in a model of colon carcinoma (CT26) lung metastases in immune competent Balb/c mice. Six intranasal doses of $5x10^7$ PFU of either AV1 or AV2 could durably cure 100% of animals. The WT virus was highly lethal by this route, with just 10^4 PFU killing half the animals.

When these same CT26 tumour cells were established subcutaneously, 6 IV doses of AV2 ($5x10^8$ PFU) could completely cure 5/8 mice. Interestingly, while a single dose of AV2 resulted in partial responses in 7/8 mice, none were completely cured. This suggests that a single dose of virus could reach the tumour and begin oncolysis, but perhaps the amount of virus delivered was not enough to spread throughout the tumour before the activation of host antiviral defenses. Although not mentioned in this report, it was also found that administering 12 doses of VSV rather than 6 could not increase the number of durable cures (D. Stojdl, unpublished

results). It is though that after the 6-dose period of two weeks, the acquired anti-VSV immune response would neutralize further doses of virus.

Since Type I IFN can increase antigen presentation and stimulate the immune system, it is possible that AV1 and AV2 might encourage the development of acquired anti-tumour immunity. Indeed, mice that were cured of subcutaneous CT26 tumours for more than 7 months were uniformly resistant to subsequent rechallenge with the same cells. Importantly, IFN-inducing VSVs could also exert oncolytic effect *without* stimulating of the acquired immune system, as demonstrated by the ability of AV2 to durably cure 7/10 nude mice of intraperitoneal human ovarian carcinoma tumours (27).

Obuchi and colleagues had also realized that a VSV that induced the production of IFN might be able to efficiently kill IFN resistant tumour cells while sparing IFN sensitive normal cells (102). Their approach was to genetically engineer VSV to express the IFNβ cDNA (VSV-IFNβ). This virus was significantly attenuated compared to the non-recombinant WT VSV, however, it was not as attenuated as the AV1 and AV2 mutants. 10^8 PFU of VSV-IFNβ IV still killed 2/5 mice, and the virus was routinely administered at $5x10^7$ PFU IV, as opposed to $5x10^8$-$1x10^9$ for AV1 and AV2. Interestingly, not all of the attenuation seemed to come from the IFNβ cDNA, as recombinant VSV expressing Green Fluorescent Protein (VSV-GFP) was also significantly attenuated in mice. When VSV-IFNβ and VSV-GFP were administered at the same dose, VSV-IFNβ was shown to be able to exert significantly improved oncolytic effect, possibly due to indirect effects such as immune stimulation.

Purpose of the current research, hypothesis, and objectives

At the beginning of this project, both AV1 and AV2 VSV had been developed and characterized in our lab in terms of efficacy in the mouse tumour models described above. However, what was actually going on inside tumours that were either succumbing to VSV oncolysis, or resisting VSV oncolysis, was unknown. In particular, studies in the subcutaneous CT26 model suggested that intravenously administered AV1 VSV could reach tumours and begin to exert some effect (delayed tumour growth), but a single dose was insufficient to exert durable cures. One would assume that an acquired immune response would be able to eliminate VSV from animals within weeks, however, there may also be physiological or innate immune mechanisms that play a role in limiting virus delivery, or spread early on. We thus developed the following hypothesis:

> ***Systemically administered IFN-inducing mutants of VSV selectively replicate and spread within murine tumours in vivo, resulting in tumour cell killing. However, we propose that complete tumour eradication may be limited by innate or physiological barriers to either the delivery of VSV to tumours, or the spread of VSV within tumours, or both.***

The specific objectives of the current work are as follows:

- To characterize the intravenous delivery of VSV to CT26 tumours
- To characterize the spread of VSV within tumours over time
- To characterize VSV induced tumour cell killing
- To investigate the mechanism by which multiple dosing cures more mice than single dosing

- To establish whether findings in the CT26 tumour model system are representative of other mouse tumour models
- To use information about the barriers to VSV therapy to design better treatment protocols

Experimental approach

The highly VSV-sensitive CT26 colon adenocarcinoma model in Balb/c mice is used in most of this research, with a more limited investigation of melanoma and breast cancer models in syngeneic mice. Most experiments follow variations on a general approach: Tumour bearing animals are treated intravenously (or by other routes) with one dose or multiple doses of previously characterized naturally occurring VSVs (WT, AV1, or AV2), or novel recombinant viruses whose construction is described in this report. For example, recombinant viruses expressing GFP or RFP (Green or Red Fluorescent Protein) permit visualization of viral gene expression in whole tumours of freshly euthanized animals. Viral replication can be assessed by plaque titration of tumour homogenates, or by using a recombinant virus expressing the reporter gene luciferase. Alternatively, tumours and other tissues can be frozen, sectioned and immunohistochemically stained for VSV, as well as other antigens of interest including apoptotic markers. Together, these techniques will allow us to assess the delivery, spread, and tumour killing ability of VSV in murine tumours in vivo.

Methods

Cell culture, Interferon treatment, and VSV infections

Cells were cultured in HyQ Dulbecco's Modified Eagle Medium (High glucose) with with L-glutamine and sodium pyruvate (HyClone) supplemented with a 3:1 mixture of bovine serum (Medicorp) : fetal calf serum (CanSera), made up to 10%. Cells were incubated at 37°C in 5% CO_2. IFN sensitivity was assayed by plating cells in 100 U/ml Universal IFNα (PBL Biomedical Laboratories) overnight followed by virus infection. VSV infections were carried out in a minimal volume of serum free media (100 ul for 60 mm dishes), and incubated at 37°C for 45 minutes, at which point fresh serum-containing media was added. When cell culture supernatants were to be titred (Figure 3B, Figure 4C), the virus was washed from plates with three changes of Phosphate Buffered Saline (PBS) before serum-containing media was added.

Preparation and titration of VSV

Virus stocks were prepared by infecting confluent 150 mm plates of Vero cells at a Multiplicity of Infection (MOI) of 0.01 PFU/cell for 24 hours. After pelleting cellular debris, supernatant was filtered at 0.2 um and frozen at –80°C until use for cell culture experiments. For animal studies, VSV was pelleted by centrifugation at 30,000 g for 90 minutes in a Beckman J2-21M Induction Drive Centrifuge. The virus pellet was resuspended in PBS to a concentration of $4x10^{10}$-$3x10^{11}$ PFU/ml, and frozen at –80°C until use. VSV was titred by making serial dilutions in serum free media, and infecting 60 mm plates of confluent Vero cells. After 45 minutes, the virus was overlayed with 0.5% agarose in media, and the plaques were grown at 37°C overnight. Plaques were counted by visual inspection. G-less WT VSV GFP (see

below) was prepared by D. Stojdl by infection of 293-T cells transfected with VSV G protein. This virus was concentrated as described above, and quantified by infecting Vero cells with various dilutions and counting GFP-expressing cells.

Cloning of recombinant viruses

Recombinant viruses were constructed using plasmids originally described by Lawson et al (90), and then modified by Schnell et al (103), and Stojdl et al (27). Reporter genes were inserted in the XhoI / NheI restriction sites of pVSV-XN1 (103) for WT viruses, or the same sites in pΔ51XNDG (27) to generate viruses bearing the ΔM51 mutation. These genome plasmids contain all the viral transcriptional regulatory elements to ensure trangene expression. A plasmid based on pBluescript SK+ (Stratagene) containing the GFP gene from pEFGP-N1 (Clontech) was obtained from B. Lichty. GFP was removed from this plasmid by digestion with XbaI, followed by overhang fill-in, and then digestion with XhoI. This fragment was ligated into pΔ51XNDG that had been digested with NheI, filled in, and then digested with XhoI. A plasmid containing the mRFP1 gene was obtained from R. Tsien (104). This gene was PCR amplified using primers that added a XhoI site and Kozak sequence to the 5' end (CCCCCTCGAGACCATGGCCTCCTCCGAGGACGT), and an NheI site to the 3' end (CCCCGCTAGCTTAGGCGCCGGTGGAGTGGC). The PCR product was gel purified, digested and ligated into both pVSV-XN1 and pΔ51XNDG digested with XhoI/NheI. The GFPLuc gene was PCR amplified from pEGFPLuc (Clontech) using primers that added a SalI site to the 5' end (CACAGTCGACACCATGGTGAGCAAGGGCGAGGA) and an NheI site to the 3' end (CCCCGCTAGCTTACACGGCGATCTTTCCGC). The PCR product was gel

purified, digested and ligated into pΔ51XNDG digested with XhoI/NheI. Plasmids were purified using a Qiagen Maxiprep kit.

Rescue of recombinant viruses

Recombinant VSVs were rescued entirely from DNA, using plasmids encoding the VSV N, P and L genes under the control of T7 promoters as described previously with modifications (90). Briefly, Baby Hamster Kidney cells stably expressing the T7 DNA dependent RNA polymerase (BHK-T7) were grown in media containing 1mg/ml of the selection marker Genetecin (Gibco). Seventy percent confluent BHK-T7 cells in 6-well dishes were co-transfected with VSV N (0.5 ug), P (1.25 ug), L (0.25ug), and genome (0.5 ug) using Lipofectamine 2000 as described by the manufacturer (Invitrogen). After 5 hours, transfection media was removed and replaced with DMEM containing 10% serum and about $5x10^5$ Vero cells per well. Wells in which virus had rescued were identified by cytopathic effects as well as fluorescent transgene expression. Rescued viruses were plaque purified and cDNA was sequenced to confirm M gene sequence. WT VSV GFP was constructed and rescued by B. Lichty, while G-less WT VSV GFP was provided by D. Stojdl.

Flow cytometry

Trypsinized cells were collected for GFP and RFP expression as well as forward scatter and side scatter using a FACScan flow cytometer (BD Biosciences). Ten thousand events were analyzed in each sample and data was analyzed using CellQuest 3.3 software (BD Biosciences). Figure 3 illustrates the method of healthy cell gating used to generate the data in Figure 7B.

Figure 3. Method for gating healthy cells after VSV infection by flow cytometry.

After VSV infection, healthy cells could be identified by the pattern of forward and side scatter using flow cytometry. In this example, 57.9% of uninfected CT26 cells were found in the healthy gate, while less than 2% of cells infected with either WT VSV GFP or Δ51 VSV GFP were found in the healthy gate. Propidium iodide staining for membrane permeability was found to be a less reliable measure of cell viability due to the loss of PI staining at very late stages of death. This method of healthy cell gating was used to generate the data in Figure 7B.

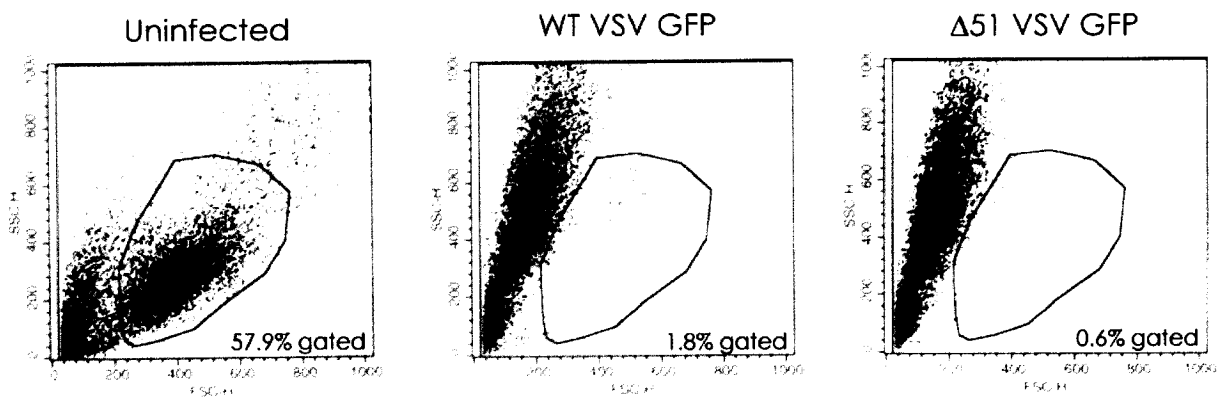
Uninfected
WT VSV GFP
Δ51 VSV GFP
57.9% gated
1.8% gated
0.6% gated

MTS cell viability assay after VSV infection

Cells were plated in 96-well dishes, at $2x10^4$ cells per well. The next day, log dilutions of WT VSV GFP and Δ51 VSV GFP were prepared in DMEM lacking serum and phenol red. Triplicate infections were done in 20 ul volume for 45 minutes at 37°C, and then 150 ul of fresh DMEM with serum without phenol red was added. After 24 hours, cell viability was assessed using the CellTiter 96 AQueous One Solution Cell Proliferation Assay (Promega), as described by the manufacturer. This assay is based on the metabolism of a tetrazolium compound into a product that can be detected colorimetrically. The compound was added directly to infected and uninfected cells in phenol red-free media, as well as control wells containing only media (to generate a blank value). After incubation at 37°C for between one and four hours, accumulation of the metabolized compound was measured by absorbance at 490 nm using a 96-well Dynex Revelation MRX Microplate Reader (Dynex Technologies).

Mouse tumour models and virus treatments

Female 6-8 week old Balb/c and C57Bl6 mice were obtained from Charles River Laboratories. Subconfluent CT26 cells were harvested by trypsinization, pelleted, resuspended in PBS, and assessed for viability by trypan blue staining. Only cultures with >95% viability were used to seed animal tumours. CT26 lung tumours were established by tail vein injection of $3x10^5$ CT26 cells in 100 ul of PBS. Subcutaneous tumours were established by injection of $3x10^5$-10^6 CT26 cells in 100 ul in the left flank. Some mice were seeded with both lung and subcutaneous tumours, as indicated. In this case, lung tumours were seeded first, followed three days later by subcutaneous tumours. B16F10 and EMT6 cells were prepared as

above and injected subcutaneously into the left flanks of C57Bl6 and Balb/c mice, respectively.

Lung tumour-bearing mice were treated with VSV after tumours were confirmed by dissection of test animals (10-16 days). Subcutaneous tumour bearing mice were treated after tumours had reached an easily palpable size (typically 3-10 mm diameter, 10 days after tumour seeding). Intravenous VSV treatments were done by tail vein injection of virus diluted to 100 ul in PBS. Intratumoural injections were done in 35 ul PBS. Intranasal administration was done by lightly anesthetizing animals with halothane (MTC Pharmaceuticals), and pipetting 50 ul of virus directly into the nose. Doses are indicated in the figure legends for each experiment.

Fluorescent imaging of VSV in tumour bearing mice in situ

Tumour-bearing animals were treated intravenously with VSV in 100 ul PBS (doses and viruses for individual experiments described in Figure Legends). Mice were euthanized by halothane overdose. Skin was removed, and the whole mouse carcass (or individual organs) was visualized in a dissecting fluorescent microscope (Leica MZFLIII) with standard GFP and RFP filter sets. Pictures were captured with a Nikon Coolpix 100 digital camera. Fluorescent and white light images were overlayed in Adobe Photoshop 7.0. Exact magnifications cannot be provided because this microscope has a continuous gradient of magnifications, rather than stepwise.

Titration of VSV from mouse tissues

After removal from the animal, tissues were stored at –80°C until they were to be titred. At this point, tissues were thawed, weighed, and homogenized in 1ml of PBS using a homogenizer (Kinematica AG PCU-11). Tissue homogenates were titred

as described for cells, with the exception that gentamycin (10ug/ml, Gibco) was added to overlays. The sensitivity of plaque titration is about 100 PFU/g.

Luciferase assays

Frozen mouse tissues were weighed and homogenized in 1ml PBS as was done for titering. An aliquot of homogenized tissue was mixed with 5x Cell Culture Lysis Reagent (CCLR) (Promega) and incubated at room temperature for 10 minutes. Cellular debris was pelleted for 20 seconds at low speed. 20ul of supernatant was added to 100 ul of Luciferase Assay Reagent (Promega) in BD Falcon polystyrene tubes and luciferase activity in Relative Light Units (RLU) was detected in a luminometer reading for 10 seconds (EG&G Berthold Lumat LB9507). We determined that the background luciferase activity varied among empty tubes; with values up to 4000. Control tissues with no luciferase did not have any background above that found from empty tubes. We thus subtracted 4000 units from every raw value.

The linear range of detection was determined by making ten fold duplicate dilutions of a Δ51 VSV GFPLuc-infected tumour sample (Figure 4). The curve departed from linearity somewhere beyond 10^7 RLU, so samples measured at this level or beyond were diluted in CCLR and measured again. As shown in Figure 4, although the luciferase curve was perfectly linear, its slope was not equal to one (ie. diluting a sample by ten fold results in a decrease in RLU of only 8.8 fold). Thus, the slope of this curve was taken into account when comparing the RLU measured for diluted versus undiluted samples. We also determined informally that varying the

Figure 4. Standard curve of luciferase activity.

CT26 tumour bearing lungs treated with Δ51 VSV GFPLuc were homogenized and assayed for luciferase activity as described *in Materials and Methods*. The undiluted sample could not be measured by the luminometer, and was read as "Overload". Duplicate serial ten fold dilutions in CCLR were assayed, and a standard curve of the log-transformed data shown here (Graphpad Prism 3.0). Error bars are too small to see. The upper point was deemed to be saturated and was not included in calculation of the linear equation ($y = 0.88x + 8.8$). As discussed in the text, this information was used in calculations of luciferase activity in diluted samples.

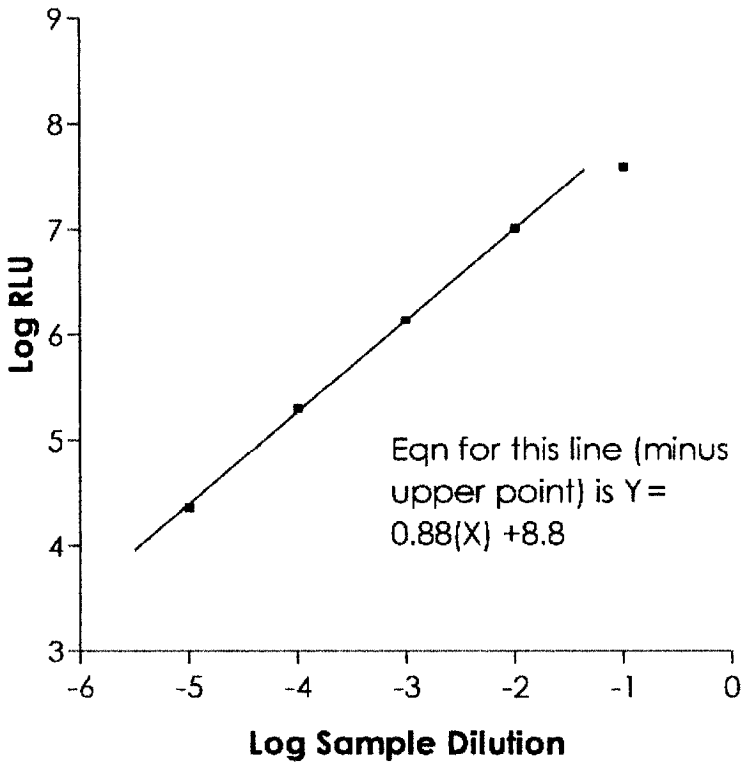
9
8
7
6
5
4
3
Log RLU
-6
-5
-4
-3
-2
-1
0
Log Sample Dilution
Eqn for this line (minus upper point) is Y = 0.88(X) +8.8

total amount of tissue homogenate did not substantially alter the amount of luciferase that could be detected. When different samples from the same experiment were assayed at different time points, a standard control was included to be sure of the consistency of reagents and methods.

Because of the background level of 4000 RLU, it made more sense to plot Log RLU per mg rather than per g of tumour. With these units, background activity was around 0.25 Log RLU/mg, so this value was used in calculations.

Slow intravenous infusion of virus into mice

CT26 subcutaneous tumour bearing mice in both bolus and slow infusion groups were anesthetized with 0.015ml/g 2.5% Avertin (Tribromoethanel, Sigma Chemicals). One group of mice was intravenously injected via tail vein with a bolus of $5x10^8$ PFU of Δ51 VSV GFPLuc in 100 ul. Another group of mice was catheterized in the tail vein and infused with the same dose of virus in 500 ul over 12 minutes using a programmable syringe pump (Harvard 11 Plus Apparatus, Harvard Biosciences). Mice were monitored as anesthesia wore off within one hour.

Frozen tissue preparation and sectioning

Tissues were quickly removed from mice, rinsed with PBS, embedded in Shandon Cryomatrix freezing medium (ThermoElectron Corporation) in plastic molds, and snap frozen in liquid nitrogen cooled isopentane according to standard procedures. Tissues were stored at –80°C until sectioning in a cryostat (Microm HM500 OM). Five micron sections were cut and adhered to Fischer Superfrost Plus slides and kept in the cryostat until transferring into –80 °C, where they were stored until processing. Hematoxylin and eosin staining was carried out as described previously (105).

Immunofluoresence and TUNEL staining

Unless otherwise indicated, dilutions were made in PBS, incubations were carried out at room temperature, and samples were washed several times with PBS between each step. Briefly, frozen tissue sections were fixed in 4% paraformaldehyde (20 minutes), blocked with 1.5% normal goat serum (30 minutes), and incubated with rabbit anti-serum raised against VSV (gift of Dr. Earl Brown) at 1/5,000 dilution for 30 minutes. Then a Cy3-conjugated donkey anti-rabbit antibody (Jackson Immunoresearch Laboratories) was applied (1/500 dilution) for 30 minutes. TUNEL staining was carried out according to the manufacturers instructions (In Situ Cell death Detection Kit – FITC, Roche) with enzyme incubation at 37°C for one hour. Nuclei were counterstained with Hoescht 33242 (2.5 ug/ml), and slides were cover-slipped in PBS / glycerol. Staining was visualized in a Zeiss Axiocam HRM inverted fluorescent microscope and analyzed using Axiovision 4.0 software. Negative control sections were used to set exposures, which were kept constant throughout.

Immunohistochemistry and H&E staining

Immunohistochemistry was performed using the Vectastain ABC kit for rabbit primary antibodies (Vector Labs), according to instructions provided. Unless otherwise indicated, dilutions were made in PBS, incubations were carried out at room temperature, and samples were washed several times with PBS between each step. Briefly, tissue sections were fixed in 4% paraformaldehyde (20 minutes), quenched of endogenous peroxidase activity with 3% H_2O_2 (15 minutes), and then blocked with 1.5% normal goat serum (30 minutes). Endogenous biotin was blocked by incubation with Avidin solution (15 minutes) then Biotin solution (15 minutes) using

an Avidin Biotin Blocking kit (Vector Labs). Primary antibodies (all of rabbit origin) were employed as follows: VSV (gift of Earl Brown) at 1/5,000 for 30 minutes. Acitve caspase 3 (BD Pharmingen) at 1/500 for 1 hour. Pimonidazole (gift of James Raleigh) at 1/5,000 for 30 minutes. CD45 (BD Pharmingen) at 1/25 for two hours. Secondary antibody and ABC reagent provided with the Vectastain ABC kit were applied as instructed. Horseradish peroxidase (HRP) activity was visualized with a Diaminobenze-HRP kit (KPL Biosciences), resulting in formation of a brown precipitate in positive areas. Nuclei were counterstained in hematoxylin (stains DNA blue), and then slides were dehydrated in an ethanol / xylenes series and mounted according to standard protocols (105). For assessment of cell morphology, sections were stained with hematoxylin and eosin (stains proteins pink) according to standard protocols (105). Whole tumour images were obtained with an Epson Perfection 2450 Photo Scanner while magnifications were captured using a Xeiss Axiophot HBO 50 microscope.

Analysis of tumour hypoxia and perfusion

To analyse hypoxia, mice were intraperitoneally injected with pimonidazole (Hypoxyprobe, Promega) at 60 mg/kg. After 30-60 minutes, animals were intravenously injected with 100 ul of a 50% solution of 100 nm diameter orange fluorescent microspheres (Molecular Probes). Five minutes later, animals were sacrificed by cervical dislocation, and tumours were immediately snap frozen as described above. To analyse hypoxia, immunohistochemical staining using an anit-pimonidazole adduct antibody was performed as described above. Tumour perfusion was analyzed by visualizing fluorescent microspheres in the vasculature of

10 um unfixed frozen sections of tumours using a ScanArray Express microarray scanner with a standard Cy3 laser (Packard Bioscience).

Digital quantification of immunohistochemistry by colour thresholding

The positive-staining area in immunohistochemical sections was quantified as described previously, using Adobe Photoshop 7.0 (106). Sections were scanned at 10-fold magnification using an Epson Perfection 2450 Photo Scanner and images were saved JPG format. A collection of positive- and negative-staining tumours were used to manually define a colour threshold setting that consistently selects only positively stained pixels (brown DAB precipitate) in sections stained on different occasions. A setting was also defined to select the total pixels (positive plus blue hematoxylin counterstain). These settings were then used to quantify the percentage of a section staining positive for either VSV or active caspase 3, as shown in Figure 5. Note that the images of all sections quantified are provided in Appendix II, III and IV.

Statistical analysis

All statistical analyses were performed with Graphpad Prism 3.0 software. Data are presented as mean +/- standard error. All virus quantifications (plaque assay and luciferase) were log transformed before statistical analysis and plotting. When no virus was detected, data was analyzed by calculating the maximum amount of virus that could have been present in the sample without being detected by our method. For plaque titration, this value was usually about 100 PFU/g. For luciferase assays, this is about 2 RLU/mg.

Figure 5. Method for digital quantification of immunohistochemistry.

In Adobe Photoshop 7.0, a colour threshold was manually defined that could consistently select only positively stained pixels (brown DAB precipitate) in sections stained on different occasions. A setting was also defined to select the total pixels (positive plus blue hematoxylin counterstain).
A: These threshold settings were used to select the total tissue section area, and the positively stained area, with an example shown here (selected area blacked out). The Adobe Photoshop Histogram command was used to count the selected pixels. Background was estimated from sections stained without 1° antibody.
B: The percentage positive staining area was defined by subtracting the background, and then dividing by the total section area and multiplying by 100%. If sections were scanned at different resolutions (different pixel/area), this was taken into account in calculations.

A

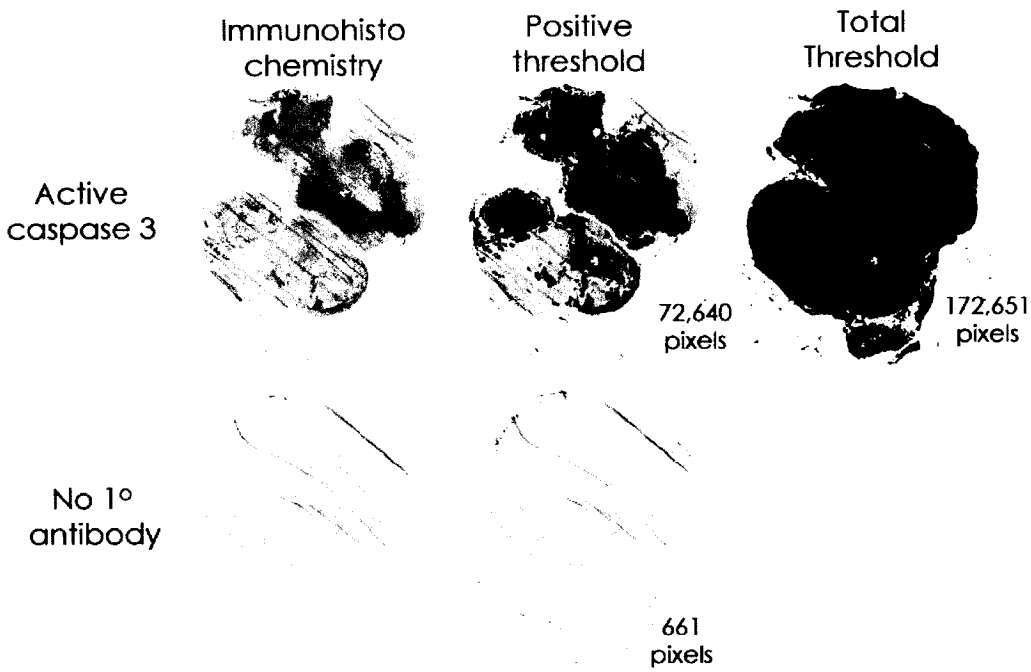

B

% active caspase 3

= (72,640 - 661) / 172,651 x 100%

= 41.7%

Results

Characterization of recombinant VSVs expressing reporter genes

In order to more easily characterize VSV oncolysis in mouse tumour models, several recombinant viruses expressing the reporter genes GFP, RFP, or GFP-Luciferase fusion protein (GFPLuc) were rescued. The cloning strategies, as well as the four-plasmid VSV rescue system are described in the *Materials and Methods* section. Briefly, the pVSV-XN1 genome plasmid (103) was used as a backbone into which foreign cDNAs could be cloned between the G and L genes of a Wild Type (WT) M-containing VSV. Expression of reporter genes in an IFN-inducing VSV backbone was accomplished by cloning into the ΔM51 XNDG genome backbone constructed by others in our lab (27). Viruses rescued from this backbone have a deletion of Methionine 51 of the M protein and display a similar phenotype to the M51R mutant (27).

Figure 6A illustrates the naturally occurring and recombinant viruses used in this report. The viruses constructed specifically for use in this research include Δ51 VSV GFP, WT VSV RFP, Δ51 VSV RFP, and Δ51 VSV GFPLuc. WT VSV GFP was constructed by Brian Lichty (see *Materials and Methods*) and G-less WT VSV GFP was obtained from David Stojdl and will be discussed later. Newly rescued viruses were plaque purified and partially sequenced to confirm M gene status (data not shown).

As shown in Figure 6B, all naturally occurring and recombinant viruses replicated to similar titres in Vero monkey kidney cells, which are incapable of producing IFN (107). Figure 6C illustrates the relative fluorescence of recombinant reporter viruses as assessed by flow cytometry of Vero cells infected for 10 hours.

Figure 6. Characterization of recombinant VSVs expressing reporter genes.

A: Genome organization of engineered and naturally occurring VSVs. As described in the *Introduction*, AV1 VSV is a naturally occurring IFN-inducing mutant of the original Indiana HR strain of VSV. As indicated, the mutation responsible for the AV1 phenotype is a substitution of Methionine 51 to Arginine (M51R) in the M protein. Recombinant viruses were constructed by inserting reporter genes (GFP, RFP, and a GFP-Luciferase fusion protein) between the G and L genes in VSV genome plasmids containing either WT M or M with a deletion of Methionine 51 (ΔM51) as described in *Materials and Methods*. G-less WT VSV GFP encodes GFP in the place of G, and thus can only bud from cells expressing exogenous G protein.
B: Recombinant VSVs expressing reporter genes all replicate with similar kinetics as non-recombinant viruses in tissue culture. Vero monkey kidney cells were infected in duplicate with the various viruses indicated at an MOI of 5, and supernatants harvested after 4, 8 and 12 hours were titred on Vero cells.
C: Flow cytometry analysis of fluorescent protein expression by recombinant VSVs. Vero cells were infected with the viruses indicated at an MOI of 5 and analyzed for GFP or RFP expression by flow cytometry 10 hours after infection.

A

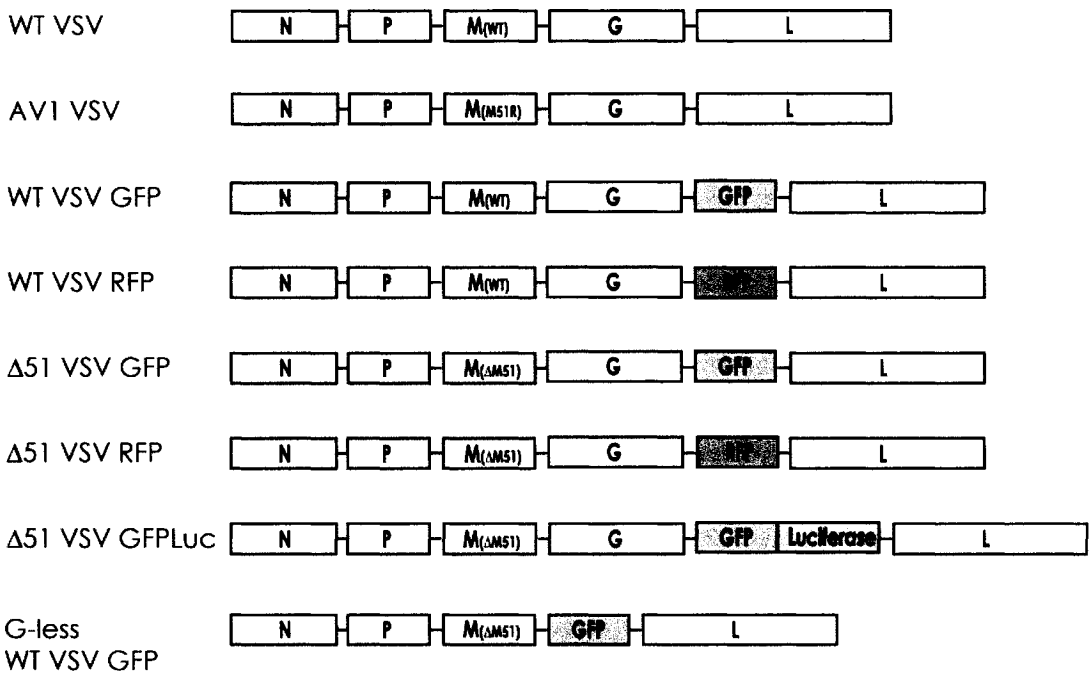
WT VSV
N
P
M(WT)
G
L
AV1 VSV
N
P
M(M51R)
G
L
WT VSV GFP
N
P
M(WT)
G
GFP
L
WT VSV RFP
N
P
M(WT)
G
L
Δ51 VSV GFP
N
P
M(ΔM51)
G
GFP
L
Δ51 VSV RFP
N
P
M(ΔM51)
G
L
Δ51 VSV GFPLuc
N
P
M(ΔM51)
G
GFP
Luciferase
L
G-less
WT VSV GFP
N
P
M(ΔM51)
GFP
L

B

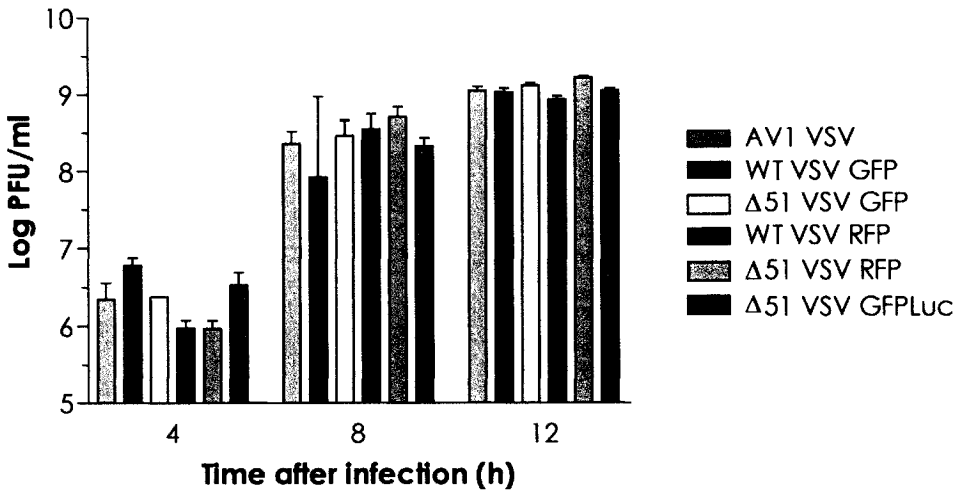
10
9
8
7
6
5
Log PFU/ml
4
8
12
Time after infection (h)
AV1 VSV
WT VSV GFP
Δ51 VSV GFP
WT VSV RFP
Δ51 VSV RFP
Δ51 VSV GFPLuc

C

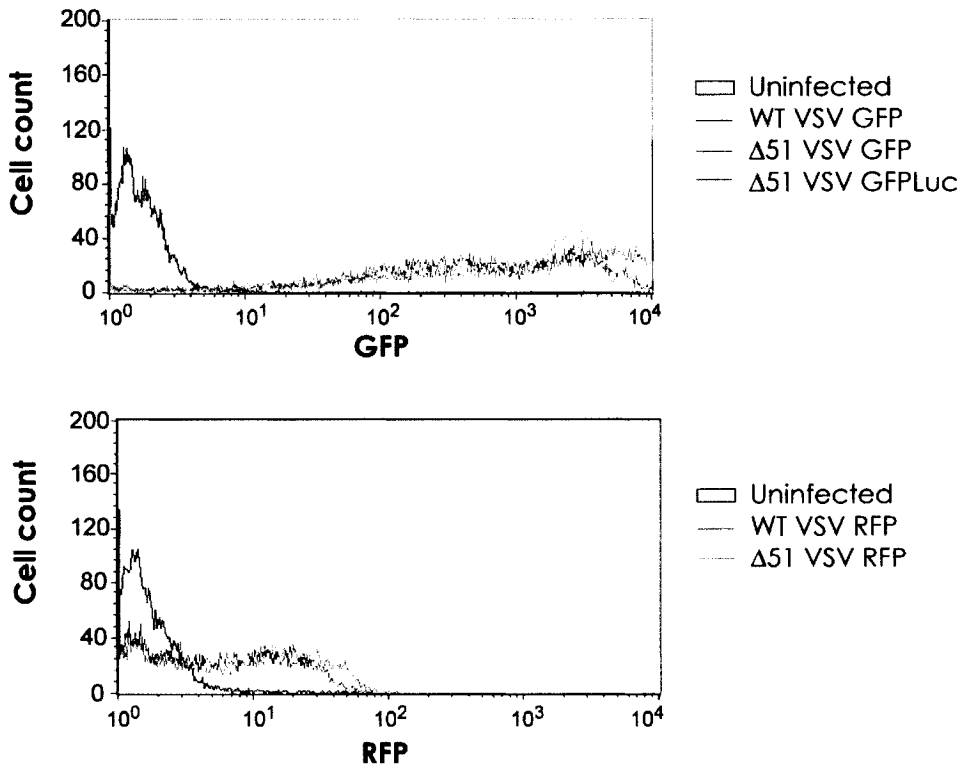
200
160
120
80
40
0
Cell count
10^0
10^1
10^2
10^3
10^4
GFP
Uninfected
WT VSV GFP
Δ51 VSV GFP
Δ51 VSV GFPLuc
200
160
120
80
40
0
Cell count
10^0
10^1
10^2
10^3
10^4
RFP
Uninfected
WT VSV RFP
Δ51 VSV RFP

WT VSV GFP, Δ51 VSV GFP, and Δ51 VSV GFPLuc all produce very bright fluorescence, although in this figure, and in other experiments, Δ51 VSV GFP appears brightest. As expected, fluorescence from RFP expressing viruses was fainter, although still easily detectable. This particular RFP (mFRP1) is an engineered monomeric version of the protein (104). mRFP1 was chosen for cloning into VSV because it matures substantially faster than previously characterized red fluorescent proteins, even though fluorescence is known to be reduced. The fast maturation time was crucial because a rapidly cytopathic virus such as VSV would likely kill cells before the slower maturing reporter proteins had a chance to fluoresce.

Δ51 VSV GFPLuc was also confirmed to express the firefly luciferase reporter gene, which bioluminesces upon addition of the substrate Luciferin. Luciferase assays revealed that 10^6 Vero cells infected with this virus expressed more than 10^{10} Relative Light Units (RLU) of luciferase above background (data not shown).

Characterization of mouse tumour cell lines in vitro

Previous work in our lab has shown that CT26 murine (Balb/c) colon adenocarcinoma cells are highly susceptible to both WT and AV1 VSV, with IFN pretreatment affording no protection (27). Because one of the goals of the current research was to develop new syngeneic mouse tumour models in which to test VSV, we compared the in vitro VSV sensitivity of several such tumour cell lines, along with CT26 cells. The B16F10, EMT6 and 4T1 tumour cell lines were chosen because they were easily obtainable from the American Type Tissue Collection, and had been reasonably well characterized. B16F10 is a highly metastatic melanoma in C57BL6 mice (108), while both EMT6 and 4T1 are derived from breast tumours in Balb/c mice

(109, 110). MT1A2, which was readily available from a colleague (C. Addison), is a breast tumour cell line derived from FVBN transgenic Polyoma Middle T antigen-expressing mice (111).

Figure 7A illustrates the viability (metabolic activity) of these cells lines 24 hours after infection with between 0.001 and 100 PFU/cell of WT or Δ51 VSV GFP. All cell lines are quite susceptible to high MOI infection (10-100 PFU/cell) with both viruses, however at lower MOIs, distinct differences become apparent. 4T1 and MT1A2 cells seem to be somewhat less susceptible to WT VSV GFP at very low MOIs compared with the other cell lines tested. In comparing infection with Δ51 and WT VSV GFP, it appears that CT26 and B16F10 cells are similarly susceptible to both viruses, while EMT6, 4T1, and MT1A2 cells are significantly less susceptible to Δ51 VSV GFP infection at low MOIs.

Because some of the cell lines seemed less susceptible to low MOI VSV infection, we wanted to see if these cells were actually resistant to virus spread, or if spread was just delayed. We thus infected the same panel of cell lines with WT and Δ51 VSV GFP at 0.01 PFU/cell and assessed viability by flow cytometry after 3 days (Figure 7B). As discussed in *Materials and Methods*, and illustrated in Figure 3, we categorized cells as "healthy" or not based on forward versus side scatter gating. Figure 7B illustrates that both CT26 and B16F10 cells are completely susceptible to low MOI infection with both Δ51 VSV GFP and WT VSV GFP, as was suggested by metabolic assay after 24 hours. Some uninfected cell lines exhibited death from overcrowding after 3 days in culture.

The longer period of infection in this experiment revealed differential sensitivity of 4T1, EMT6, and MT1A2 cells to VSV (Figure 7B). Healthy cell gating shows

Figure 7. Characterization of VSV susceptibility and IFN sensitivity of mouse tumour cell lines.

A: Viability of various mouse tumour cell lines 24 hours after infection with WT or Δ51 VSV GFP with Mulitplicities of Infection (MOI) from 0.001 to 100 PFU/cell. Viability of triplicate samples was assessed by a metabolic MTS assay as described in *Materials and Methods*.
B: Viabilty of various tumour cell lines 3 days after infection with WT or Δ51 VSV GFP at 0.01 PFU/cell assessed by flow cytometry. Because many cells were so fragmented that they had lost GFP and Propidium iodide expression, viability was assessed in duplicate samples by gating healthy cells according to forward and side scatter, as detailed in Figure 3.
C: The sensitivity of various mouse tumour cell lines to the antiviral effects of exogenous Interferon was assayed. Cells were plated at 70% confluence in media supplemented with or without 100 U/ml Universal IFNα. The next day, cells were infected with WT VSV GFP or Δ51 VSV GFP at 0.1 PFU/cell. After 14 hours, cell supernatants were harvested and titred on Vero cells in duplicate.

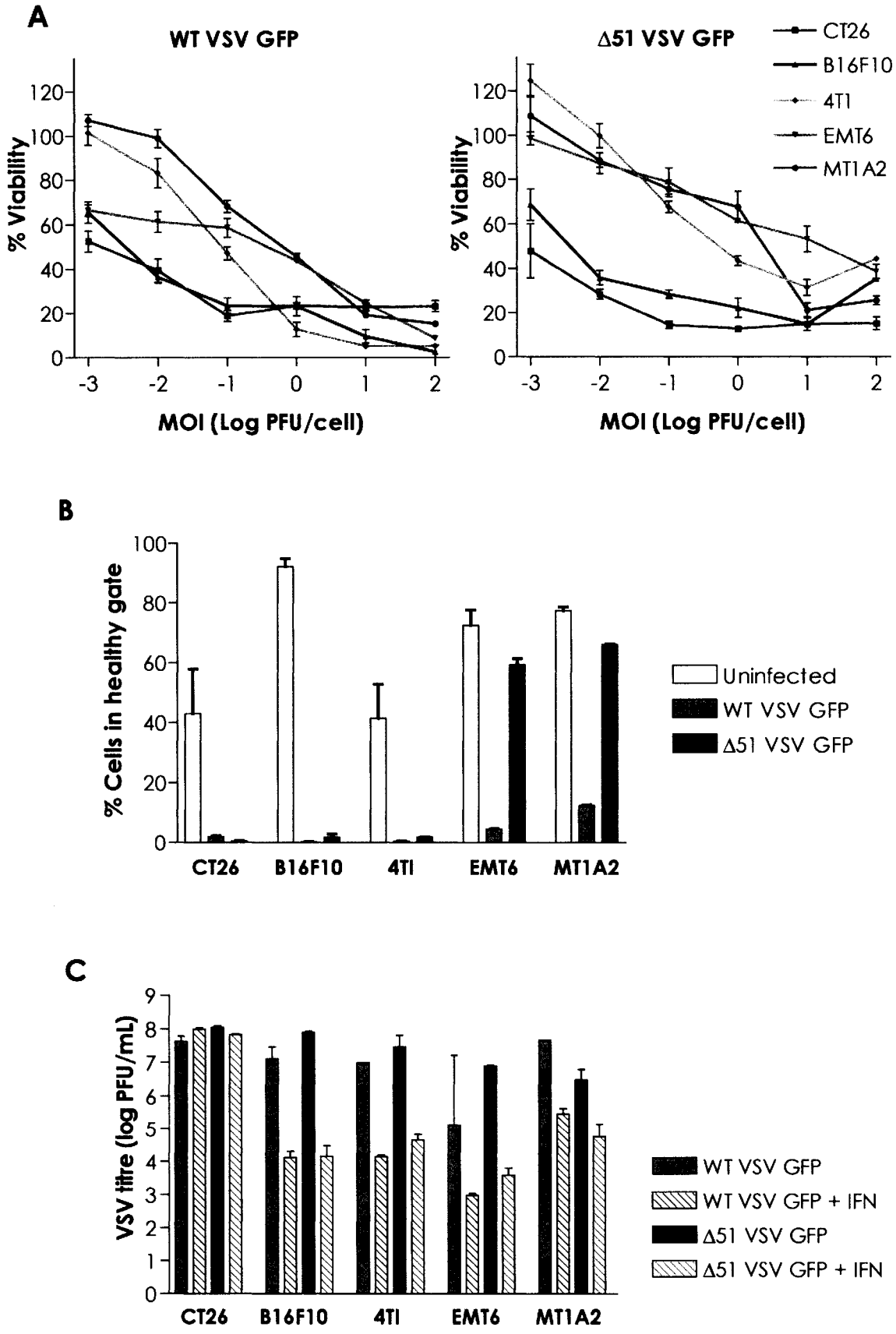
A
WT VSV GFP
Δ51 VSV GFP
CT26
B16F10
4T1
EMT6
MT1A2
% Viability
MOI (Log PFU/cell)
B
% Cells in healthy gate
Uninfected
WT VSV GFP
Δ51 VSV GFP
CT26
B16F10
4TI
EMT6
MT1A2
C
VSV titre (log PFU/mL)
WT VSV GFP
WT VSV GFP + IFN
Δ51 VSV GFP
Δ51 VSV GFP + IFN
CT26
B16F10
4TI
EMT6
MT1A2

that 4T1 cells are very susceptible to low MOI infection with both WT and Δ51 VSV GFP, while EMT6 and MT1A2 are much less susceptible to Δ51 than WT. During the course of this experiment, cells were examined for GFP expression by microscopy: the pattern of GFP expression was consistent with the healthy cell gating data, suggesting that cells were killed by productive infection with viruses (data not shown). GFP expression by flow cytometry was not presented because by this late time point, many of the cells were so disintegrated that they lost GFP expression. Thus, this experiment highlighted the reduced ability of Δ51 VSV GFP to spread within EMT6 and MT1A2 cells.

It was also important to characterize the sensitivity of these cell lines to exogenous IFN, because in an in vivo setting, even if tumour cells themselves cannot produce IFN in response to VSV infection, normal murine cells could. Figure 7C illustrates the amount of virus produced 14 hours after infection with either WT VSV GFP or Δ51 VSV GFP (MOI = 0.1), both with and without exogenous IFNα pretreatment. This figure illustrates that without IFN, at an early time point after infection, all cell lines produce fairly high titres of both viruses. This is consistent with the susceptibility of all cell lines to high MOI infection with both viruses (Figure 7A). In this experiment, most of the virus produced is from one or two cycles of infection, and thus defects in spread may not be apparent. Exogenous IFN had some effect on the amount of virus produced by all cell lines except CT26.

In general, Figure 7 suggests that B16F10 and 4T1 cells can respond to IFN, yet they likely cannot produce it, as evidenced by their susceptibility to low MOI infection with Δ51 VSV GFP, a virus which is known to induce IFN production in capable cells (27). A possible explanation for the EMT6 and MT1A2 data is that

these cells are susceptible to incoming VSV (both WT and Δ51), but as IFN (or possibly some other factor) is produced by the Δ51 infected cells, the spread of the this virus is prevented. As in other cell lines (27), WT VSV would prevent the production of IFN and thus allow its own spread.

Visualization of VSV GFP in tumours

As mentioned in the *Introduction*, multiple intranasal (IN) doses of AV1 or AV2 VSV can cure 100% of mice in a metastatic CT26 model (27). In this model, tumour cells are injected intravenously (IV), and lodge and form tumours primarily in the lungs. When these mice are treated with virus IV instead of IN, complete cures seem to be more difficult to obtain (D. Stojdl, unpublished results). Thus it might be useful to get an idea of the efficiency with which IV-administered VSV targets CT26 lung tumours. As shown in Figure 8A, Δ51 VSV GFP seems to target these lung tumours very efficiently, with all tumour nodules appearing brightly fluorescent just 24 hours after IV injection. Furthermore, virus appears only in the tumours and not in surrounding normal lung tissue. The last panel of Figure 8A illustrates a set of lungs with just three tumours, each of which have been efficiently targeted by VSV. This panel more convincingly shows the lack of fluorescence in normal lung tissue. Perfusion of mice to remove blood confirmed that the high blood supply of normal lung tissue was not quenching fluorescence (Appendix I). In these experiments, fluorescence was not observed in any other organs (data not shown).

Research in our lab has shown that IV-administered AV1 and AV2 VSV are also effective treatments for subcutaneous CT26 tumours, however complete cures seem to require multiple doses of virus (27). Analysis of GFP in this model revealed substantial fluorescence, with however, significant variability between specimens.

Figure 8. Imaging VSV GFP in tumour bearing mice in situ.

A: CT26 lung tumour model: Balb/c mice were seeded IV with $3x10^5$ CT26 cells, resulting in formation of lung tumours within two weeks. The first two panels illustrate one set of lungs from a mouse 24 hours after treatment with $3x10^8$ PFU Δ51 VSV GFP. The last panel illustrates a tumour 24 hours after IV treatment with $1x10^9$ PFU Δ51 VSV GFP.

B: CT26 subcutaneous tumour model: Balb/c mice were injected subcutaneously in the left flank with $3x10^5$ CT26 cells. After easily palpable tumours had formed, mice were treated with virus intravenously. The first panel represents a tumour 13 hours after treatment with $1x10^9$ PFU WT VSV GFP. The middle panel illustrates a tumour 24 hours after treatment with $3x10^8$ PFU Δ51 VSV GFP. The last panel illustrates a tumour 4 days after treatment with $5x10^8$ PFU Δ51 VSV GFP.

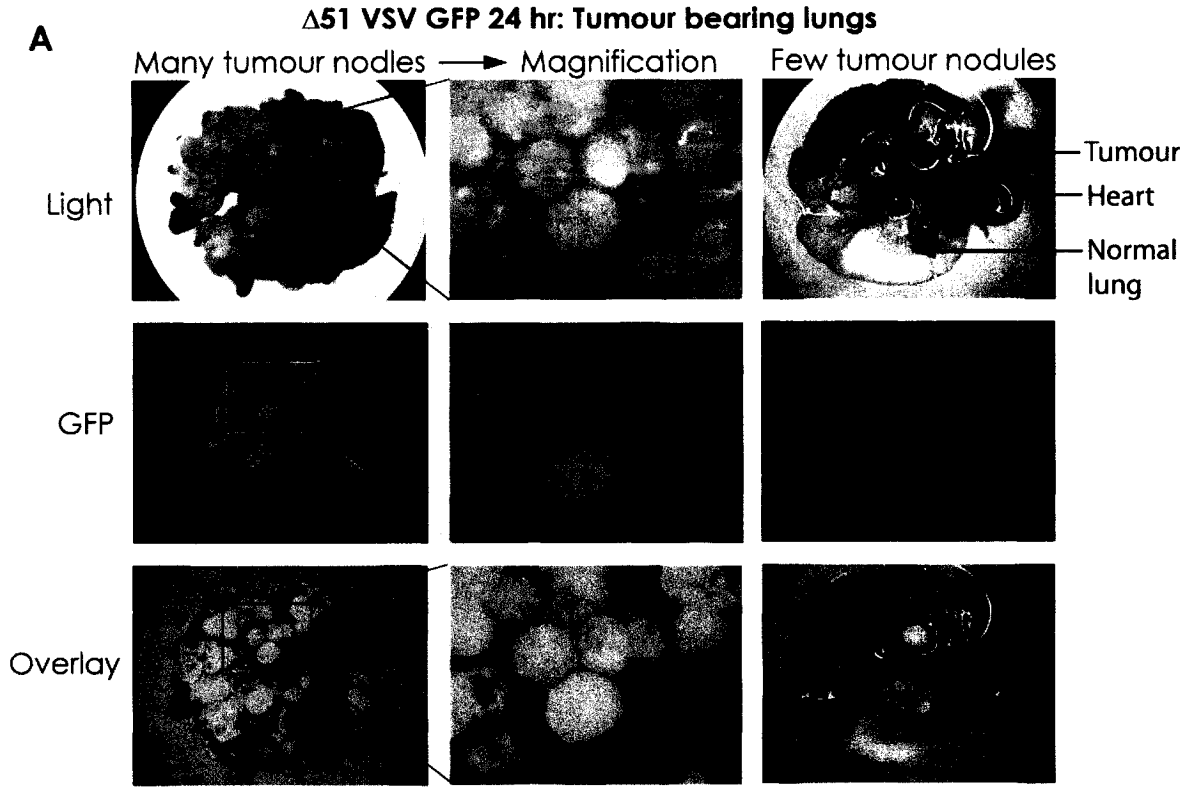
A
Δ51 VSV GFP 24 hr: Tumour bearing lungs
Many tumour nodles
Magnification
Few tumour nodules
Light
GFP
Overlay
Tumour
Heart
Normal lung

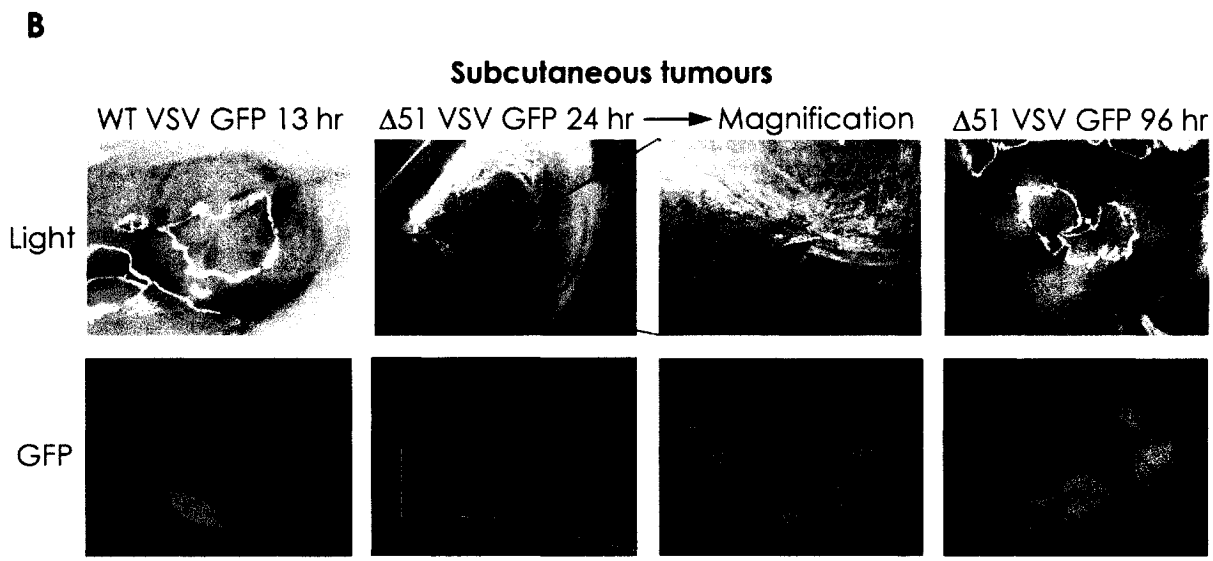
B
Subcutaneous tumours
WT VSV GFP 13 hr
Δ51 VSV GFP 24 hr
Magnification
Δ51 VSV GFP 96 hr
Light
GFP

Examples of subcutaneous tumours at different time points after treatment with WT or Δ51 VSV GFP are shown in Figure 8B. We did not observe differences in the fluorescence of tumours treated with these two viruses. However we have tried to address this issue with more sensitive methods described later.

The first panel of Figure 8B shows a tumour just 13 hours after treatment with WT VSV GFP. This picture illustrates a phenomenon observed quite commonly with both WT and Δ51 VSV GFP: Rather than virus being equally distributed around the whole tumour, the vast majority of virus was found concentrated in one area. Based only on these observations, it is difficult to say if this is due to the preferential delivery or spread of virus in certain areas of the tumour, or even if the effect is simply part of a random phenomenon without physiological significance.

The second panel of Figure 8B illustrates a tumour 24 hours after infection with Δ51 VSV GFP; this is as an example in which virus is quite evenly distributed in small foci. As shown in the magnification, these small patches of GFP often appear to be associated with distinct, branching tumour blood vessels, which appear darker in the fluorescent image due to quenching of GFP by hemoglobin. The last panel shows a tumour four days after treatment with Δ51 VSV GFP. By this time point, fluorescence has spread to cover most of the tumour surface. This technique of whole tumour imaging provides a picture mainly of the tumour surface. However in experiments discussed later, we have investigated the distribution of virus inside such tumours.

Co-injection of GFP and RFP VSV illustrates individual foci of infection

The extensive fluorescence of lung tumours after VSV GFP administration led to the question of whether this was due to the very rapid spread of a small amount

of virus, or delivery of a large amount. We reasoned that co-delivery of GFP and RFP expressing VSVs would allow us to assess delivery by visualization of individual three dimensional "plaques" of virus, which would be either red *or* green. Thus, if large areas of infection were found to be only red *or* green, we could assume that this was due to the spread of a single particle of virus, whereas a uniform mixture of both colours would indicate co-delivery and spread of many particles of virus. Such an experiment could also shed light on the reason for the irregular distribution of virus found in many subcutaneous tumours. This experiment was attempted before the rescue of Δ51 VSV RFP, so the WT RFP and GFP viruses were used.

Balb/c mice bearing both CT26 subcutaneous tumours and lung tumours were injected IV with a mixture of $5x10^8$ PFU of both WT VSV GFP and WT VSV RFP ($1x10^9$ PFU total). Mice were euthanized very early after injection (11-16 hours), so that viral plaques could be seen before extensive spread had blurred them. As shown in Figure 9A, individual viral plaques were indeed visible. There were likely hundreds of individual virus particles delivered just to the surface of every nodule of tumour (see middle panel), suggesting that the delivery of virus to these lung tumours is very efficient. The right hand panel of Figure 9A illustrates a lower dose of virus ($2x10^7$ PFU each) after 24 hours. Although only one mouse was treated with this dose, the results suggest that by lowering the dose by 1/25, there appear to be many tumour nodules that remain untargeted by VSV, at least on the surface.

Figure 9B illustrates several subcutaneous tumours after co-injection of GFP and RFP viruses. As observed previously, delivery was somewhat variable, with some tumours being fairly evenly covered with virus, while others either had substantially less virus, or it seemed to be unevenly distributed. The middle panel, for example,

Figure 9. Individual foci of VSV visualized by co-injection of GFP and RFP expressing viruses.

Balb/c mice were seeded with $3x10^5$ CT26 cells IV, and 3 days later, subcutaneous tumours were initiated via subcutaneous injection of $3x10^5$ CT26 cells in the left flank of the same mice. Ten days later, mice were treated with virus intravenously as indicated, and sacrificed for analysis of GFP and RFP expression as indicated. **A** illustrates lung tumours, while **B** illustrates subcutaneous tumours.

A

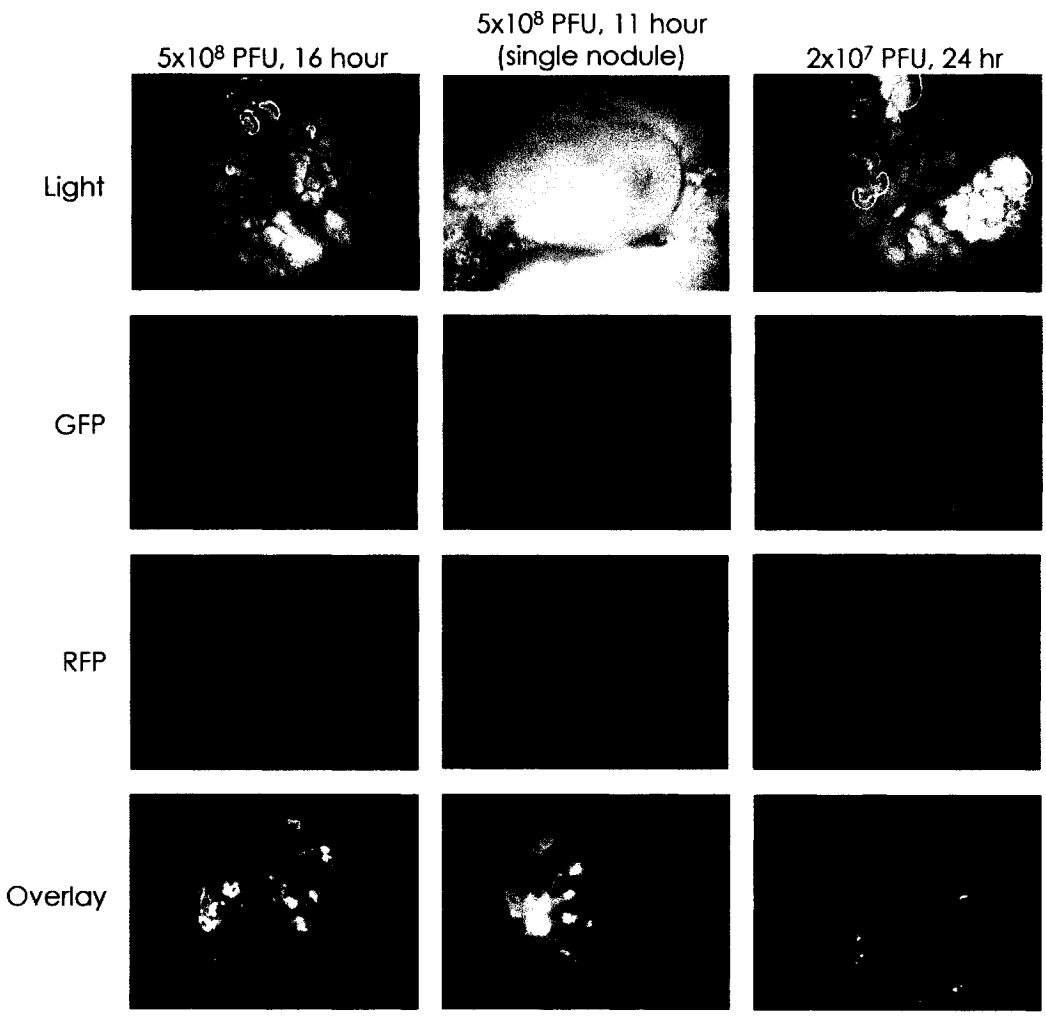
5x10^8 PFU, 16 hour
5x10^8 PFU, 11 hour (single nodule)
2x10^7 PFU, 24 hr
Light
GFP
RFP
Overlay

B

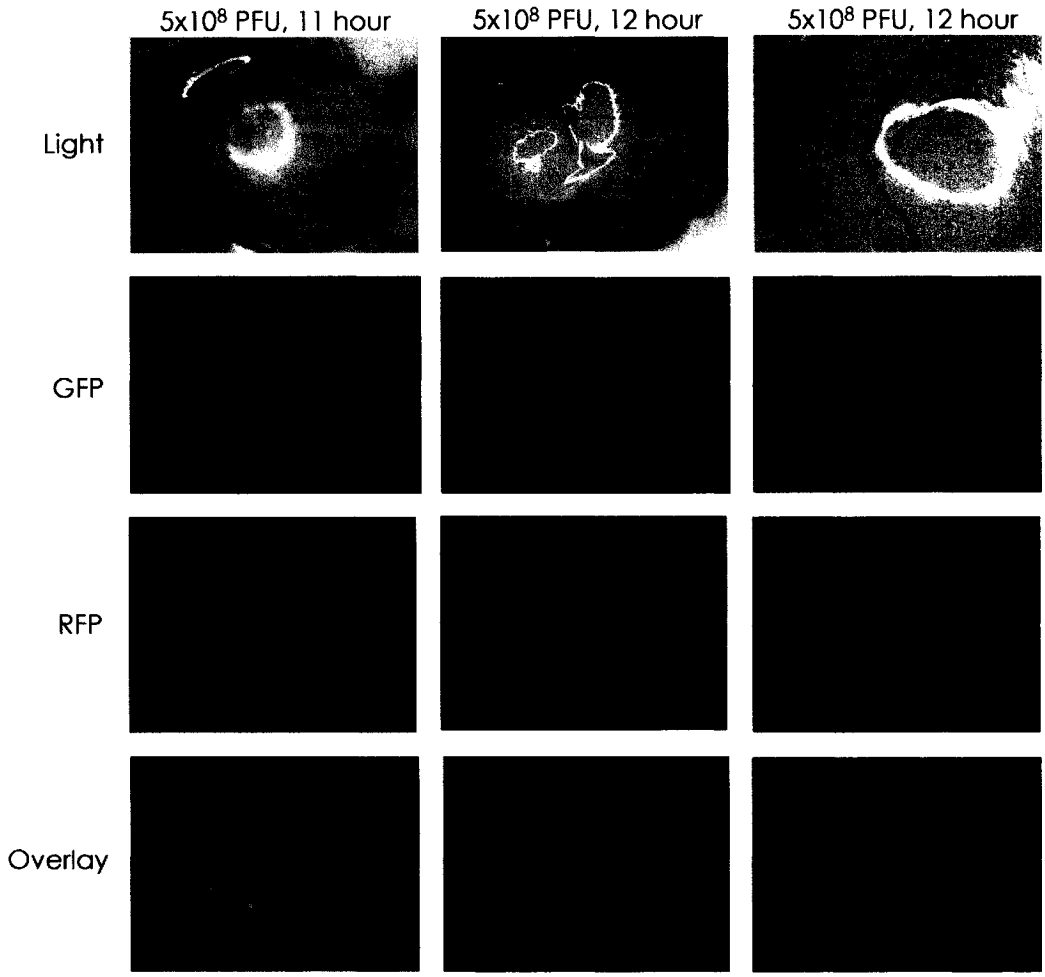
5x10^8 PFU, 11 hour
5x10^8 PFU, 12 hour
5x10^8 PFU, 12 hour
Light
GFP
RFP
Overlay

confirms that certain areas of the tumour (perhaps the interface between normal and tumour tissue) are more efficiently targeted than other areas. Since the most fluorescent areas of the tumour were both red and green, this suggests that many particles of virus were preferentially delivered to this area, rather than random delivery followed by preferential replication.

In these experiments with WT VSV at early time points, we sometimes observed fluorescence in other organs. For example, in the right hand panel of Figure 9A, there is obvious fluorescence in what could be a major vessel. As described in the next section, in some mice, we also saw fluorescence in the liver, the spleen, and in certain areas of the neck.

G-less WT VSV GFP illustrates delivery without spread

As diagrammed in Figure 6A, we had access to a WT M-containing VSV expressing GFP but lacking the coding region for the G protein. This virus can only be propagated on cells artificially expressing G; in other cells, the virus enters as usual, transcribes its genes, and replicates its genome, but it cannot bud because it does not make any G protein. Injection of mice with this virus would allow us to definitively visualize delivered virus without any spread, although it was difficult to obtain enough of this virus to do many experiments.

The results, shown in Figure 10A, were somewhat unexpected: compared with both lung and subcutaneous tumours, more G-less virus seemed to be found in the liver and spleen, and even more was evident in lymph nodes in both the neck and retro-peritoneal cavity. This experiment has been carried out with both tumour bearing and non-tumour bearing mice to exclude the possibility that small metastases might account for the presence of virus in apparently normal organs.

Figure 10. G-less WT VSV GFP illustrates delivery of virus without spread.

A: CT26 tumour-bearing or non-tumour-bearing mice were treated IV with $2x10^8$ infectious units of G-less VSV GFP and imaged for GFP expression after 10-11 hours. The retroperitoneal lymph node picture is from a non-tumour bearing animal, while the rest of the pictures are from the same animal bearing both lung and subcutaneous CT26 tumours.
B: Some animals treated with replicating WT VSV GFP also displayed fluorescence in normal organs such as the lymph nodes and liver. Pictures are from separate animals treated with $5x10^8$ PFU IV after 12-13 hours.

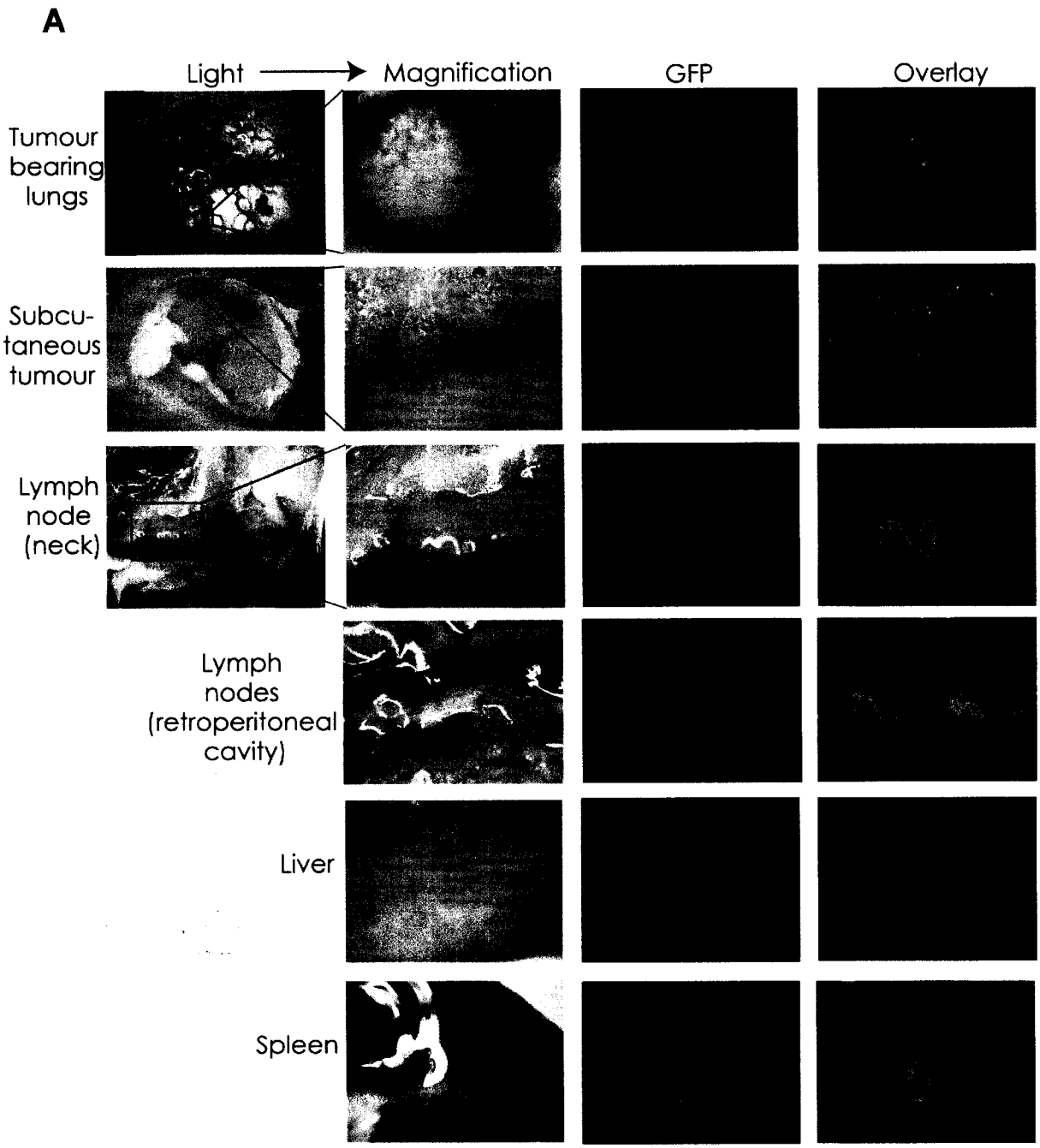
A
Light
Magnification
GFP
Overlay
Tumour bearing lungs
Subcu-taneous tumour
Lymph node (neck)
Lymph nodes (retroperitoneal cavity)
Liver
Spleen

B

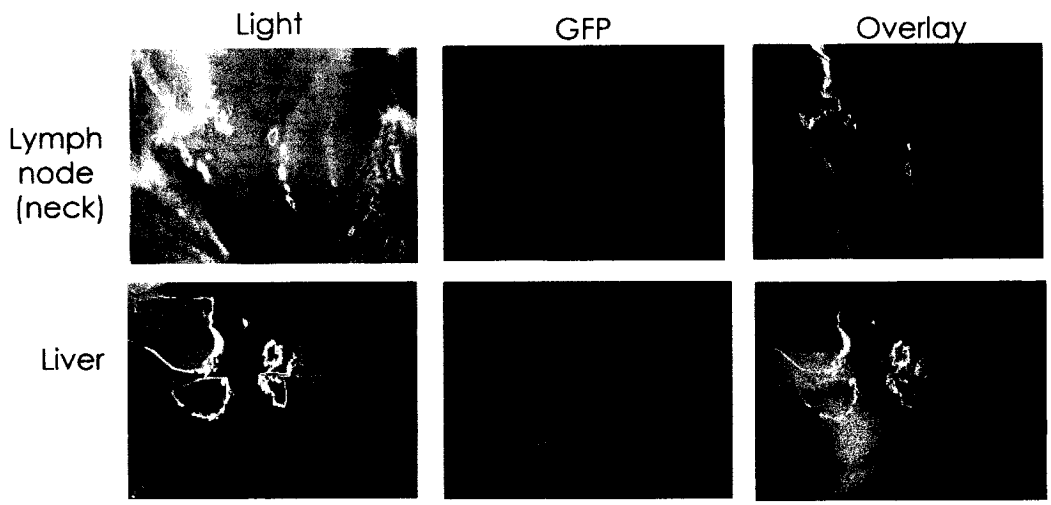

It was also interesting that all of the virus delivered to the subcutaneous tumour shown in Figure 10A was found near the interface between the tumour and the normal capsule surrounding it (see magnification). This is consistent with some previous observations that foci of replicating VSV GFP were brightest at the tumour / normal interface (for example, see Figure 8B, first panel and Figure 9B second panel).

As mentioned above, we did occasionally observe WT VSV GFP fluorescence in normal tissues, which made the results with the G-less virus less surprising. Some examples are shown in Figure 10B. Although we have not carried out a detailed analysis of GFP expression in normal mouse tissues infected with WT VSV GFP or Δ51 VSV GFP, we have performed a more rigorous plaque titration-based biodistribution assay with the IFN inducing mutant VSV, as described in the next section.

Kinetic biodistribution of AV1 VSV in tumour bearing mice reveals extensive replication of virus in subcutaneous tumours despite poor delivery

As mentioned above, we wanted to quantify the delivery and spread of mutant VSV in tumours compared to normal tissues. Thus, a kinetic biodistribution experiment was undertaken in which subcutaneous CT26 tumour bearing mice were treated intravenously with 10^9 PFU of AV1 VSV. After various time points from 5 minutes to 6 days after infection, pairs of mice were euthanized, perfused, and tumours and major organs were frozen for later homogenization and VSV quantitation by plaque titration.

As illustrated in Figure 11, the highest virus titre immediately after injection was found in the liver (7.2 +/- 0.5 $\log_{10}$ PFU/g), followed by the spleen (5.5 +/- 0.13), while tumour titres were much lower (3.0 +/- 1.1). By 24 hours following injection, tumour

Figure 11. Kinetic biodistribution of AV1 VSV in mice shows that intravenous delivery to tumours is poor, although replication is rapid, extensive, and selective.

CT26 subcutaneous tumour-bearing mice were intravenously injected with 10^9 PFU of AV1 VSV. Pairs of mice were sacrificed and perfused with PBS after 5 minutes, 3, 8, 24, 72, or 144 hours. Organs were frozen and later homogenized and titred on Vero cells. When no virus was detected, data was analyzed by calculating the maximum amount of virus that could have been present in the sample without being detected by our method (about 100 PFU/g). Thus, the Y axis is cut off below 100 PFU/g. Points represent the mean of two values, with standard error.

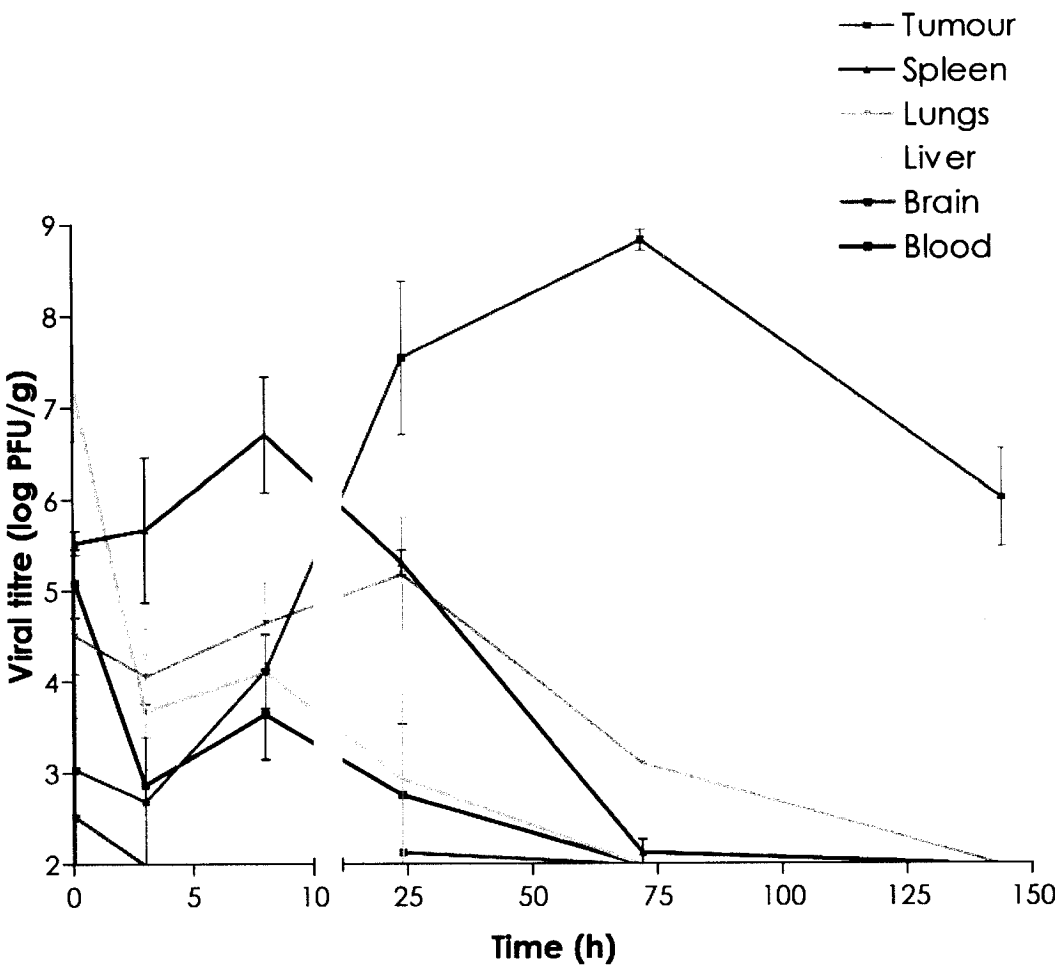
Tumour
Spleen
Lungs
Liver
Brain
Blood
Viral titre (log PFU/g)
9
8
7
6
5
4
3
2
0
5
10
25
50
75
100
125
150
Time (h)

titres had dramatically increased by over 4 logs, while liver titres had decreased by the same amount. This suggests that AV1 VSV probably does not productively infect the liver, while Figure 10B indicates that WT VSV GFP does at least in some instances. Tumour titres continued to increase up to 3 days after infection while virus in normal tissue was undetectable at this time point except for in one lung sample.

Viral tumour titre increases with increasing IV dose

In order to more thoroughly investigate the IV delivery of virus to CT26 subcutaneous tumours, different doses of Δ51 VSV GFP (from 10^3 to 10^9 PFU) were administered to mice, and the tumours were titred after 24 hours. This experiment was expected to provide data about the minimum effective virus dose, as well as any possible level at which virus replication in tumours might be saturated.

As shown in Figure 12, tumour titres increased in a roughly linear pattern as the virus dose was increased from 10^6 to 10^9 PFU. At both 10^5 PFU and 10^4 PFU, only one of 3 tumours had detectable virus. Thus, if there is a minimum effective tumour targeting dose, it is probably near 10^6 PFU. However, one cannot exclude the possibility that lower doses might target tumours at such low efficiency that virus replication would not be detected by 24 hours after infection. The tumour titre difference between 10^9 and 10^8 PFU is significant ($P = 0.04$), however the differences between other single log steps are not, possibly due to increased variation at lower doses. Thus, no saturating dose of VSV was detected.

Tumour VSV levels are comparable in both slow infusion and bolus IV injection protocols

One of the broad goals of the current project was to carry out detailed preclinical testing of oncolytic virus therapy before going into human trials. We thus

Figure 12. Viral tumour titre increases with increasing IV dose.

CT26 subcutaneous tumour-bearing mice were intravenously injected with Δ51 VSV GFP at 10^9 PFU, or serial ten fold dilutions down to 10^3 PFU. After 24 hours, mice were sacrificed, and tumours were frozen and later homogenized and titred on Vero cells, with a limit of detection of about 100 PFU/g (indicated by the dashed line). Each tumour is shown as an individual point, with bar representing the mean. Relevant statistical determinations are discussed in the text.

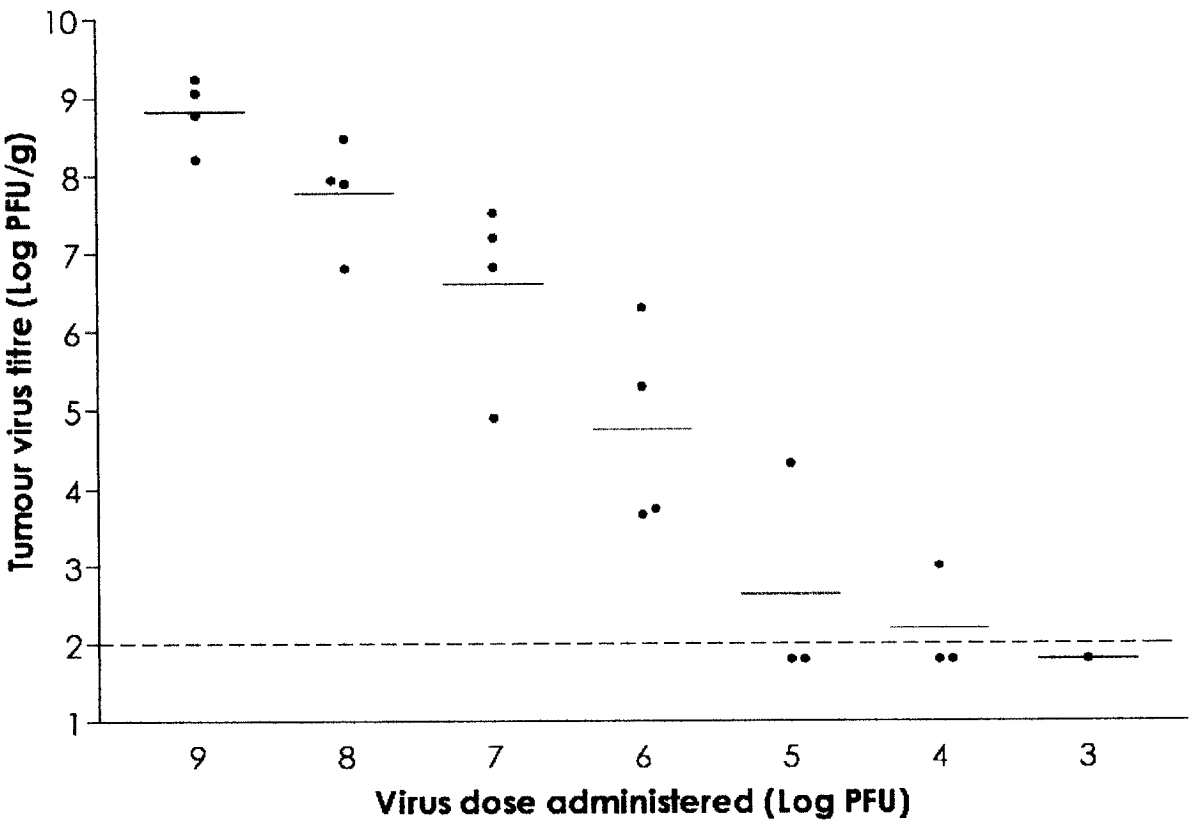
10
9
8
7
6
5
4
3
2
1
Tumour virus titre (Log PFU/g)
9
8
7
6
5
4
3
Virus dose administered (Log PFU)

decided to use our CT26 mouse model to investigate an observation made with oncolytic Newcastle Disease Virus (PV701) in Phase I clinical trials (112). Although these trials were not designed to assess efficacy, the authors noted that more tumour responses were observed when NDV was administered in a slow infusion (over 3 hours) as opposed to a bolus IV injection (10 minutes). There are several possible explanations for this phenomenon, as noted in the *Discussion*. One possible explanation is that a slower infusion results in more uniform delivery of virus to tumours, thus resulting in increased replication and tumour killing. Figure 13 illustrates the luciferase activity present in subcutaneous CT26 tumours 18 hours after administration of Δ51 VSV GFPLuc into the tail vein either by a bolus injection of a few seconds, or via a slow infusion of 12 minutes. There was no significant difference in mean luciferase activity between the two groups, however the slower infusion may result in more consistent delivery.

Investigation of VSV replication in tumours during multiple versus single dosing regimens

As mentioned in the Introduction, 6 doses of AV2 VSV, administered IV every other day, can cure 5/8 mice of subcutaneous CT26 tumours, while a single dose results in only partial response followed by renewed tumour growth (27). There are several reasons why multiple doses may be better than a single dose: 1) more total virus is administered, 2) virus administered at different time points targets different parts of the tumour, or 3) multiple dosing augments indirect tumour killing mechanisms. In order to begin to investigate these possibilities, two different reporter viruses were administered at different time points so that their replication could be tracked independently. In this experiment, mice were treated with a virus

Figure 13. Tumour VSV levels are comparable in both slow infusion and bolus IV injection protocols.

CT26 subcutaneous tumour-bearing mice were intravenously injected with $5x10^8$ PFU Δ51 VSV GFPLuc in a bolus of a few seconds, or a slow infusion of 12 minutes. Tumours were homogenized and luciferase activity was assayed as described in *Materials and Methods*. Each tumour is shown as an individual point, with bar representing the mean.

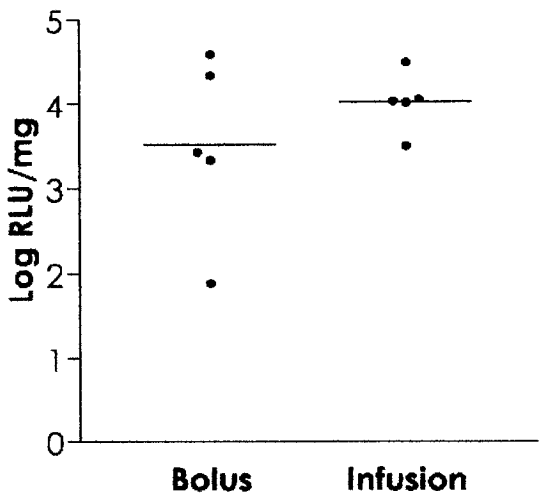
5
4
3
2
1
0
Log RLU/mg
Bolus
Infusion

not expressing luciferase (Δ51 VSV RFP or AV1 VSV), or dilution buffer control, followed by treatment with Δ51 VSV GFPLuc after some time interval. Twenty-four hours after the last dose of virus, mice were euthanized and tumours were homogenized and assayed for luciferase activity.

As shown in Figure 14A, administration of a primary IV dose of virus 48 hours before a second IV dose of Δ51 VSV GFPLuc reduced the luciferase activity by 2.7 logs compared to PBS (P=0.01). When the interval was less than this (24 hours) the difference was not significant, while intervals more than this showed even greater inhibition. These results were very interesting given the above noted observation that multiple IV dosing at 48 hour intervals is much more efficacious than single dosing. If very little of the second dose of virus is getting to the tumour, this would suggest that the increased efficacy may come from either targeting a very small number of new tumour sites, or from indirect virus induced anti-tumour effects.

Thus, although this experiment was initiated to investigate the mechanism of increased efficacy of multiple doses, it stimulated new questions about the reason for decreased replication of VSV in tumours 48 hours after a primary dose. Antiviral responses provoked by the first virus (innate or possibly acquired) could inhibit replication of the second virus. This effect might be due to systemic virus induced factors in the serum, such as cytokines or early IgM antibodies, or it could be a local effect, possibly dependent upon replication of the first dose of virus in the tumour. The effect might also be independent of host antiviral responses, for example, if the second dose of virus is delivered only to areas of the tumour that have already been killed by the first dose of virus. These issues are examined in more detail in the *Discussion*.

Figure 14. Investigation of virus replication in tumours during multiple versus single dosing regimens.

A: CT26 subcutaneous tumour-bearing mice were intravenously injected with $5x10^8$ PFU of a non-Luciferase expressing virus (either Δ51 VSV GFP or AV1 VSV), by intravenous or intranasal route, as indicated. Control mice were injected with PBS IV. Between 24 and 96 hours later (as indicated), mice were challenged with $5x10^8$ PFU Δ51 VSV GFP by IV route. 24 hours after the last dose of virus, mice were euthanized and tumours were assayed for luciferase activity as described in *Materials and Methods*. Each tumour is shown as an individual point, with bar representing the mean. Relevant statistical determinations are discussed in the text.
B: As above, except that the second dose of virus ($5x10^8$ PFU Δ51 VSV GFPLuc) was administered by direct injection into the tumour (IT) rather than IV. As above, luciferase activity was determined 24 hours after the last dose. Each tumour is shown as an individual point, with bar representing the mean. Relevant statistical determinations are discussed in the text.

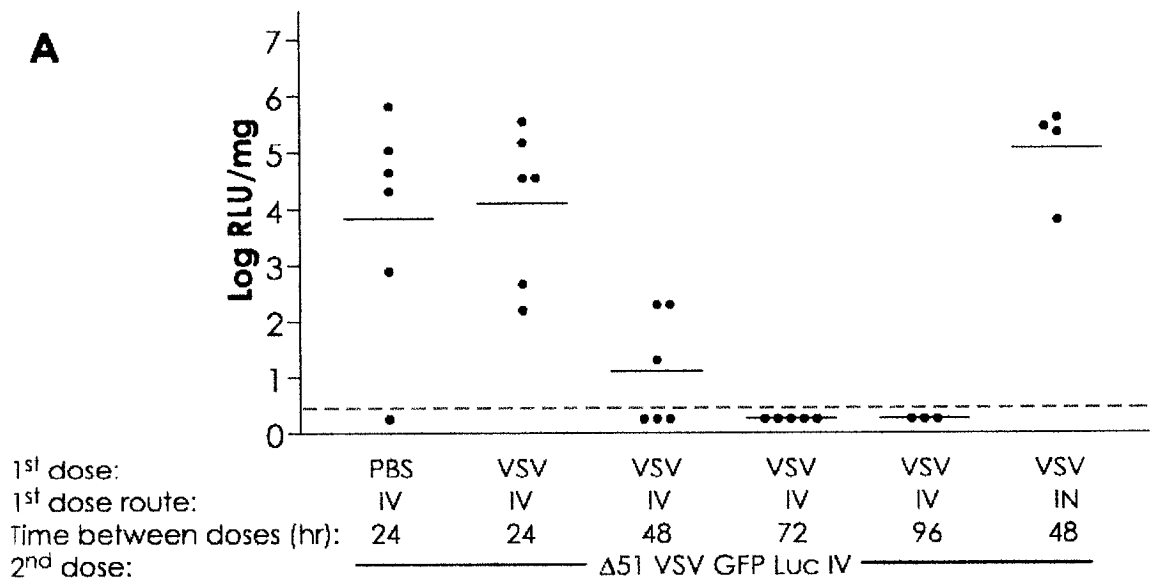
A
Log RLU/mg
0
1
2
3
4
5
6
7
1st dose: PBS VSV VSV VSV VSV VSV
1st dose route: IV IV IV IV IV IN
Time between doses (hr): 24 24 48 72 96 48
2nd dose: Δ51 VSV GFP Luc IV

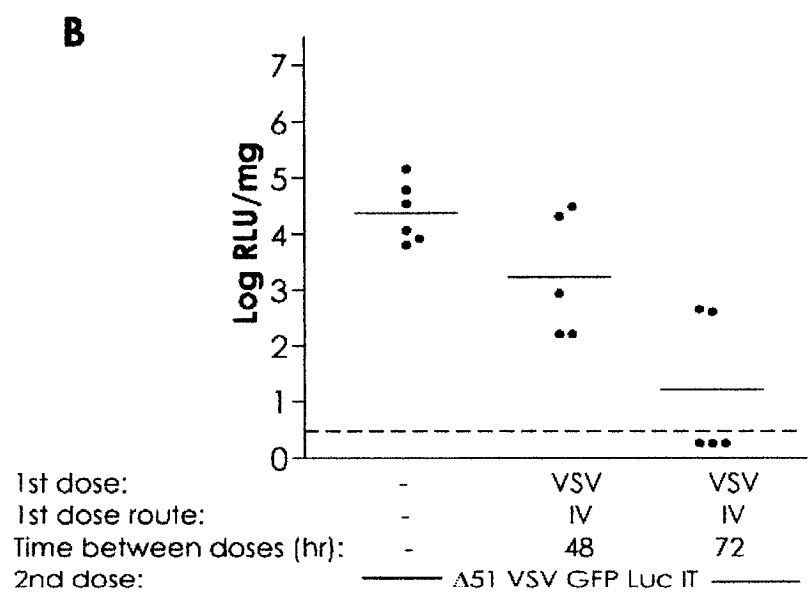
B
Log RLU/mg
0
1
2
3
4
5
6
7
1st dose: - VSV VSV
1st dose route: - IV IV
Time between doses (hr): - 48 72
2nd dose: Δ51 VSV GFP Luc IT

To begin to investigate the conditions under which this multiple dose inhibition effect occurs, several modified multiple dosing experiments were designed. In the first experiment, the first dose of virus was administered intranasally (IN) rather than IV, followed 48 hours later by Δ51 VSV GFPLuc IV. As show in Figure 14A, there was no significant difference between the luciferase activity recovered from tumours after an IN priming dose versus PBS IV. Thus, if a general host antiviral response is responsible for this effect, it is a host response that is not induced by intranasally administered VSV after 48 hours. In the second experiment, the first dose was administered IV, but this time the second dose was administered intratumourally (IT), either after 48 or 72 hours. As shown in Figure 14B, there was some decrease in luciferase activity due to IT injected virus 48 hours after an IV dose, however this result was not quite significant (P=0.05). When the time interval was 72 hours, the result was significant (P=0.0004). It is reasonable to assume that if there is a specific block in the IV delivery of virus, IT administration might be able to bypass this block. These results suggest that at 48 hours, part of the second dose block could be in IV delivery, but at 72 hours, there is also a block independent of IV delivery. A totally separate line of investigation, discussed below, has provided some new clues about this phenomenon.

VSV replicates preferentially in the tumour rim, while inducing extensive apoptosis in the core

A major goal of the project undertaken was to investigate the distribution of virus in tumours, and the progression of tumour cell killing. Imaging of whole tumours treated with fluorescent protein-expressing viruses (Figures 8 and 9) revealed the distribution of virus only on the surface of tumours. As a more rigorous way to

investigate virus distribution throughout tumours, we performed anti-VSV immunofluorescence on thin tumour sections. Because we were also interested in characterizing VSV-induced tumour cell killing, we simultaneously performed a TUNEL assay to detect the double stranded DNA breaks that are a hallmark of apoptotic cell death (113).

Figure 15 shows examples of an untreated subcutaneous tumour, and tumours treated IV with Δ51 VSV RFP for two or five days. All fields of view illustrate the edge of the tumour and part of the centre. In the two-day treated tumour, viral antigen appears to be concentrated specifically at the interface between dense tumour tissue and surrounding normal tissue, with little to no virus found in the centre of the tumour. In the five-day treated tumour, again, virus was concentrated at the tumour rim, with however, more spread into the centre.

The most interesting observation was the presence of extensive TUNEL staining inside the tumours of both two and five day treated animals. Control tumours displayed occasional bright TUNEL stained cells, with a small patch of more concentrated staining in the centre (not shown), while VSV treated tumours were uniformly apoptotic. It is especially interesting that the vast majority of apoptotic cells in the 2 day treated tumour were not expressing viral antigen. This indicates that these cells may be subject to an indirect mechanism of virus-induced killing.

VSV induces bystander tumour cell killing

Although the TUNEL staining results were intriguing, it is conventional to confirm an apoptotic phenotype using more than one marker before making conclusions. A hallmark of apoptosis is the cleavage of pro-caspase 3 into an

Figure 15. Visualization of VSV and TUNEL staining in subcutaneous tumours.

CT26 subcutaneous tumour-bearing mice were intravenously injected with $5x10^8$ PFU Δ51 VSV RFP, and sacrificed after 2 or 5 days. Frozen tumours were sectioned and anti-VSV immunofluoresence was performed (Cy3-red) followed by TUNEL staining (FITC-green), with Hoescht-counterstained nuclei (blue). This experiment was repeated with a different set of tumours with similar results (data not shown). Original magnification 10x.

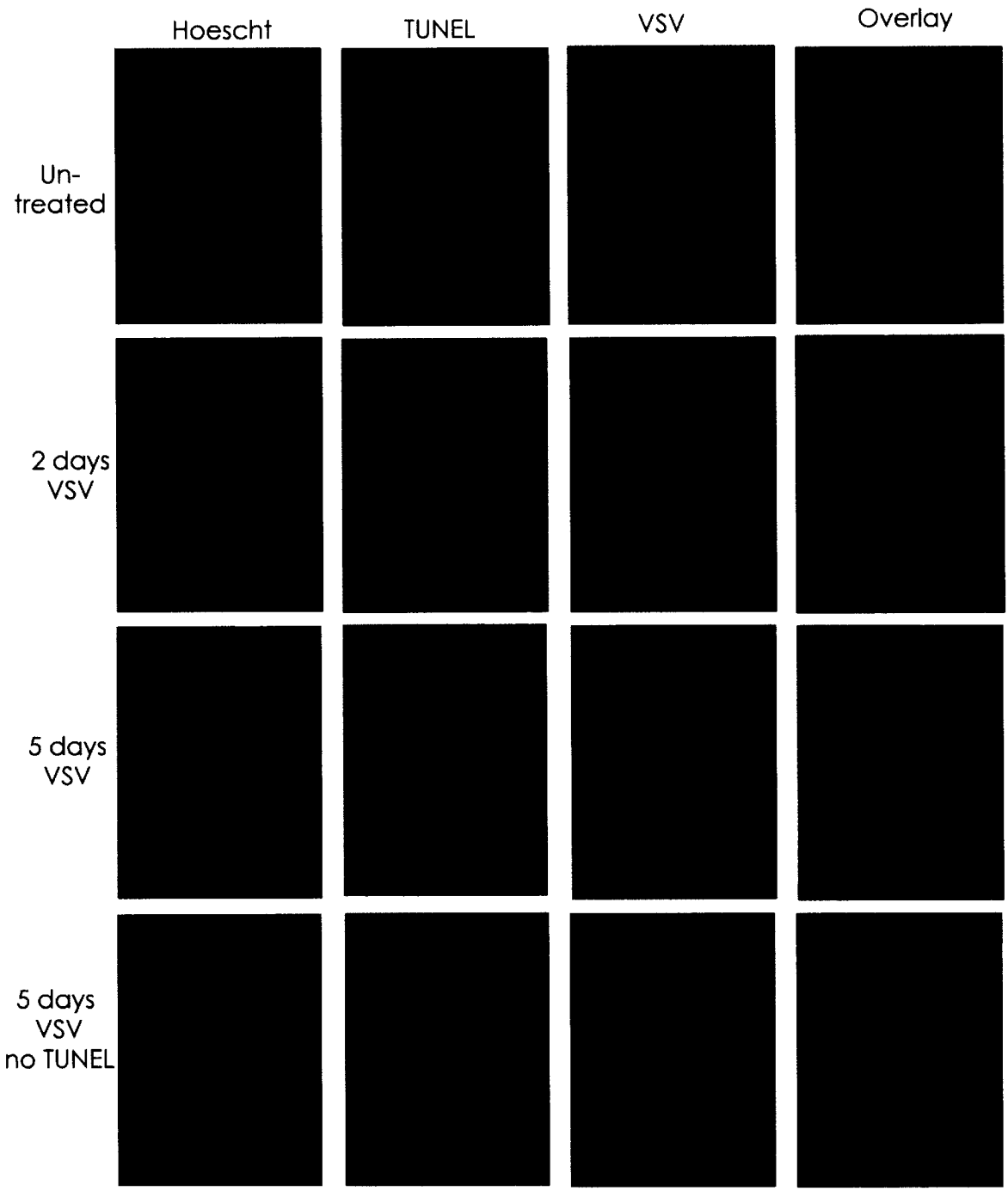
Hoescht
TUNEL
VSV
Overlay
Un-
treated
2 days
VSV
5 days
VSV
5 days
VSV
no TUNEL

active protease, which then cleaves a large number of substrates responsible for inducing cell death and characteristic apoptotic changes, including the double stranded DNA breaks detected by the TUNEL assay (114). Thus, an antibody that specifically binds only to the activated form of caspase 3 was obtained and used to perform Horseradish peroxidase based immunohistochemistry (IHC) on a panel of treated and untreated tumours. In this method, a brown precipitate marks positively stained cells, while all nuclei are counterstained blue with hematoxylin.

Figure 16 illustrates representative examples of Hematoxylin and Eosin (H&E) morphology staining, as well as IHC for VSV and active caspase 3, on tumours treated with Δ51 VSV GFP for two days (Figure 16B) or five days (Figure 16C) compared with untreated tumours (Figure 16A). Untreated tumours were predominantly healthy, displaying minimal active caspase 3 staining. However pockets of reactivity were evident in the centre of large untreated tumours, and this staining correlated with fragmented and pyknotic nuclei revealed by H&E (Figure 16A, left hand magnification).

Tumours treated with VSV for two days showed virus often concentrated on the tumour rim (or tumour / normal interface) with predominant active caspase 3 staining throughout the tumour core. Magnifications of VSV positive areas revealed disintegration of cellular structures, along with patchy active capsase 3 staining (Figure 16B, right hand magnification). Areas of the tumour core that were highly positive for active caspase 3, yet negative for VSV, displayed marked nuclear condensation and development of large spaces between cells (Figure 16B, left hand magnification). A tumour treated for five days displayed very uniform active caspase 3 staining throughout the tumour core (Figure 16C). In this example VSV is

Figure 16. VSV induces bystander tumour cell killing.

CT26 subcutaneous tumour-bearing mice were intravenously injected with $5x10^8$ PFU of IFN inducing VSV mutants (either AV1 VSV, or recombinant reporter gene expressing Δ51 VSVs). Two or five days later, mice were euthanized, and frozen tumour sections were immunohistochemically stained for VSV and active caspase 3, along with untreated tumours. Examples of this staining, as well as hematoxylin and eosin (H&E) morphology staining are illustrated. **A** is a tumour from an untreated mouse, **B** is from a mouse treated with Δ51 VSV GFP for two days, and **C** is from a mouse treated with the same virus for five days. Size bars (1mm) indicate magnification of whole tumours, while inset panels were originally magnified at 20x. Panels **D** and **E** show quantification of VSV and active caspase 3 stained area, respectively, as described in *Materials and Methods* and Figure 5. Each tumour is shown as an individual point, with bar representing the mean. Relevant statistical determinations are discussed in the text.

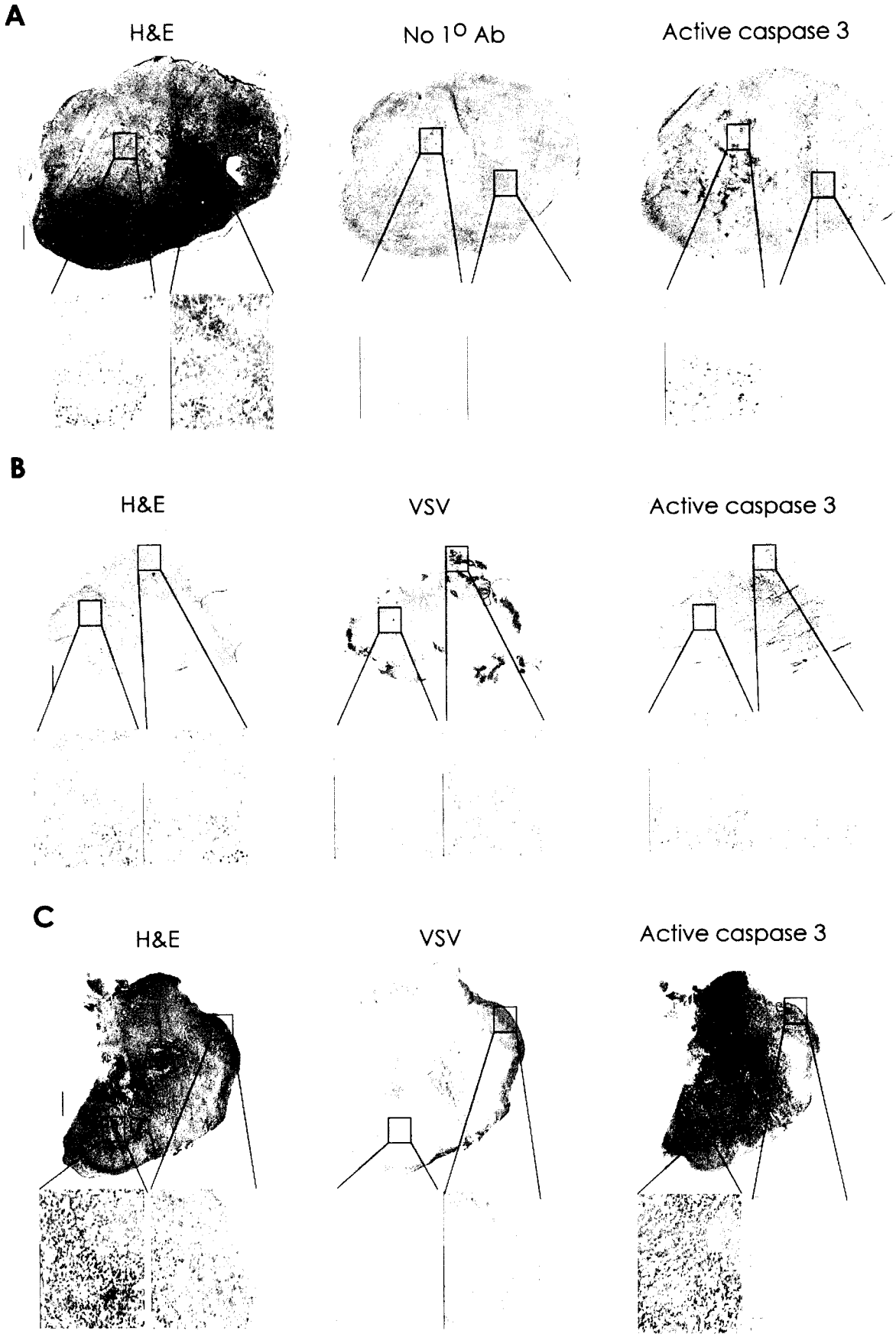
A
H&E
No 1° Ab
Active caspase 3
B
H&E
VSV
Active caspase 3
C
H&E
VSV
Active caspase 3

D

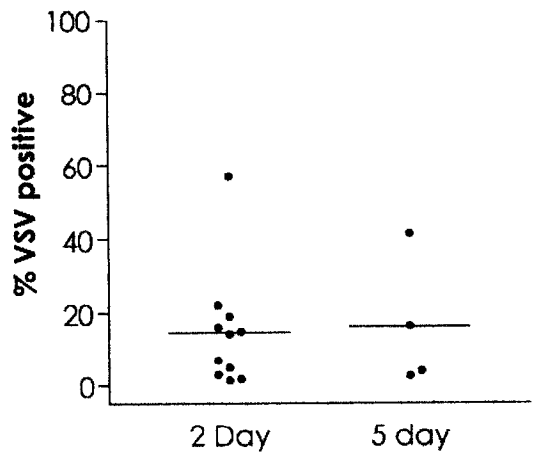
100
80
60
40
20
0
% VSV positive
2 Day
5 day

E

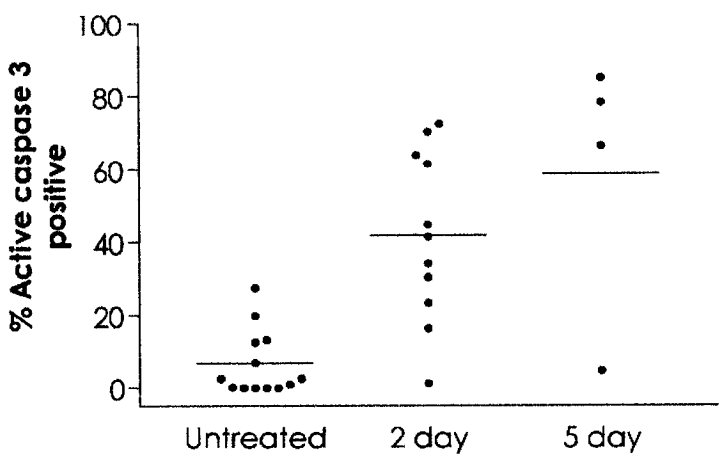
100
80
60
40
20
0
% Active caspase 3 positive
Untreated
2 day
5 day

found predominantly at the tumour rim, however in other examples there appears to be more virus in the centre, as was seen with TUNEL staining (Figure 15).

After staining a large number of both treated and untreated tumours, some variability was observed in the active caspase 3 staining pattern, so results were quantified to determine significance. As detailed in Figure 5, and in other research papers (106), we use Adobe Photoshop to define a positive brown-staining threshold on scans of whole tumour sections, and used this to quantify the percentage of positive stained area. This quantification method revealed that while untreated tumours displayed an average of 6.7 +/- 2.5 % active caspase 3 staining, tumours treated with VSV displayed 42 +/- 7% staining after 2 days, and 59 +/- 18 % after 5 days (Figure 16E). Interestingly, tumours treated with VSV for 2 days displayed only 15 +/- 5% staining for VSV (Figure 16D), indicating that on average, there is far more apoptosis in VSV treated tumours than actual VSV staining. Thus, quantification of VSV staining and active caspase 3 staining supports the observations of individual tumours which suggested some sort of VSV induced bystander killing effect. Images of all tumours used for this quantification are provided in Appendices II, III and IV. Further research on a limited number of samples after different treatments (WT VSV IV, Δ51 VSV IT, or in nude mice) is presented in Appendices V, VI, and VII.

VSV induces subcutaneous tumour vascular shut-down

There are many plausible mechanisms by which treatment with VSV could induce bystander killing of tumour cells, including induction of cytotoxic cytokines, or cell mediated components of the innate or acquired immune system. Furthermore, activation of any of these mechanisms might not act on tumour cells

themselves, but could act on the supporting tumour structure, including blood vessels. We chose to begin by examining the effects of VSV on tumour vascular perfusion and hypoxia because this investigation could also provide information about the lack of intravenous delivery of VSV to tumours 48 hours after a prior dose (Figure 14).

Fluorescent carboxylate-modified polystyrene microspheres with 0.1 um diameter (approximately the same size as VSV virions) were used to measure tumour perfusion. These highly stable microspheres can be injected intravenously into animals, and flow easily through even small capillaries, but do not readily leak out (115). Although these fluorescent microspheres have a short half-life in the blood, they can be used to image tumour blood flow and perfusion if tissues are examined soon after injection (115).

In order to simultaneously detect hypoxia in tumours, we obtained the chemical pimonidazole-HCl (Hypoxyprobe, Chemicon). Under low oxygen conditions, Hypoxyprobe chemically conjugates to proteins, forming new antigens that can then be detected in tissue sections by immunohistochemistry (116). Hypoxyprobe metabolism requires cellular enzymes, however, so only viable hypoxic cells will stain strongly with Hypoxyprobe. Previous studies have shown that Hypoxyprobe staining typically surrounds necrotic regions in tumours (116).

In order to test the hypothesis that VSV induces a tumour vascular shutdown, we treated groups of CT26 subcutaneous tumour bearing mice with either PBS or AV1 VSV ($5x10^8$ PFU IV), and two days later we administered Hypoxyprobe (intraperitoneally) and then fluorescent microspheres (intravenously) before sacrificing the mice and freezing the tumours for sectioning. Fluorescent

microspheres were detected in thin tumour sections using a high resolution fluorescent scanner. Immunohistochemistry for VSV, active caspase 3, and hypoxyprobe was performed on serial sections to relate blood flow, hypoxia, apoptosis, and VSV staining at a regional level.

Figure 17A illustrates the distribution of fluorescent microspheres in VSV-treated versus PBS-treated tumours. Four of the six PBS-treated tumours contain an even distribution of microspheres throughout most of the tumour, while two of the tumours have significant regions without perfusion. In contrast, five of the six VSV treated tumours lacked microsphere perfusion throughout most of the tumour core, with regions on the rim still retaining some blood flow. Thus, although some tumour to tumour variability was observed, these results suggest that treatment with VSV may be associated with a loss of blood flow to the tumour core.

Detailed examples of PBS-treated and VSV-treated tumours are presented in Figures 17B and C respectively. The untreated tumour contains minimal hypoxia and active caspase 3 staining, although a small region of hypoxia was found which seems to correlate with a lack of perfusion, as shown in the magnification. In the treated tumour, VSV is present in a few places mainly on the tumour rim, while most of the tumour core is non-perfused, active caspase 3 positive, and surrounded by hypoxyprobe staining. As shown in magnification ii of this panel, the extreme rim of the tumour is neither apoptotic, nor hypoxic, but just inside this rim, hypoxia staining outlines apoptosis, as would be expected based on the metabolic requirement of hypoxia staining. Interestingly, this magnification shows that a blood vessel which still perfused (by microspheres) creates an island of healthy tumour

Figure 17. VSV induces subcutaneous tumour vascular shut-down.

CT26 subcutaneous tumour-bearing mice were intravenously injected with $5x10^8$ PFU AV1 VSV or PBS and 48 hours later, animals were treated with Hypoxyprobe (intraperitoneally) to assess hypoxia and fluorescent microspheres (intravenously) to assess tumour perfusion. Further details are provided in the text and in *Materials and Methods*. **A** illustrates distribution of microspheres in all tumours. Size bars (1mm) indicate magnifications of whole tumours. **B** and **C** show detailed examples of tumours treated with PBS and VSV respectively, including Hematoxylin and Eosin (H&E) morphology staining, microsphere distribution, active caspase 3, hypoxia, and VSV immunohistochemistry.

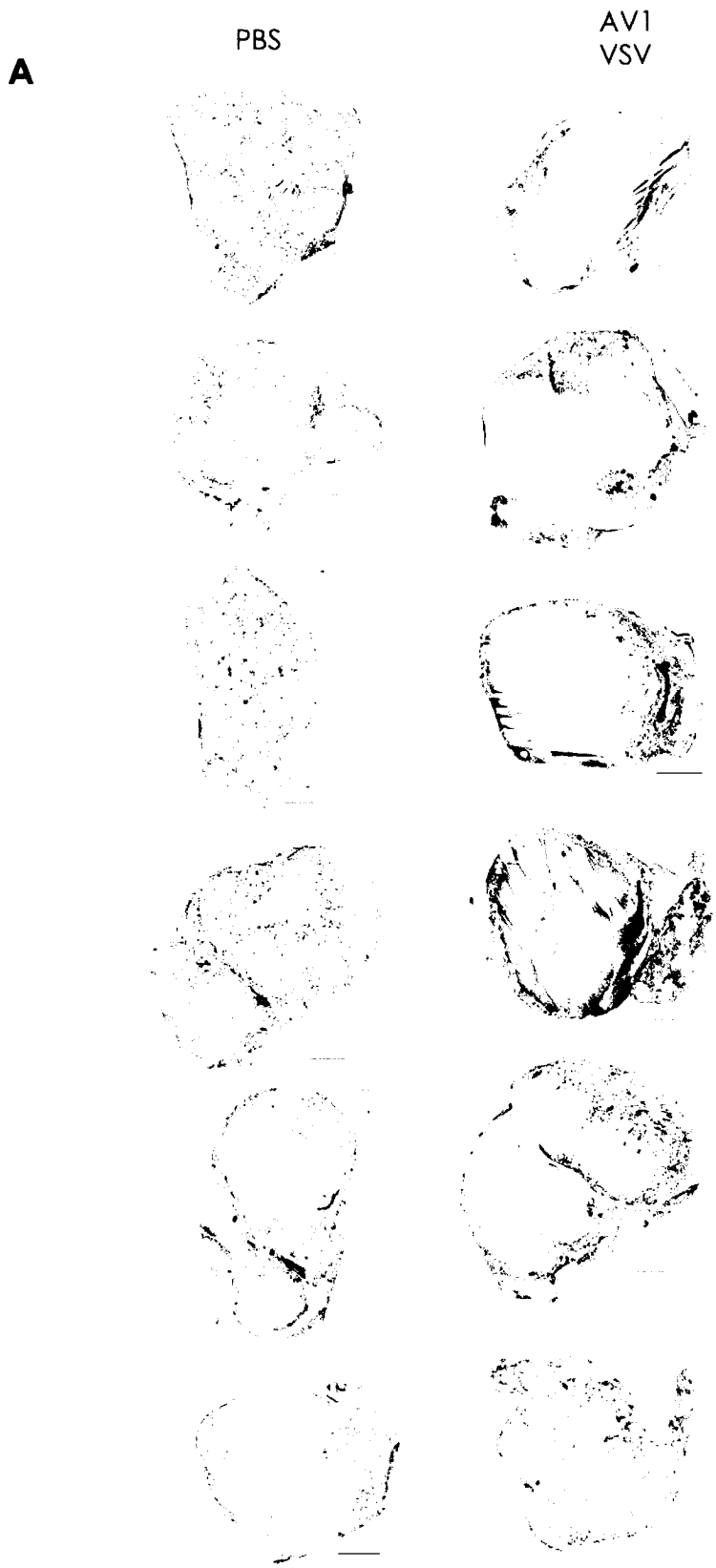
A
PBS
AV1
VSV

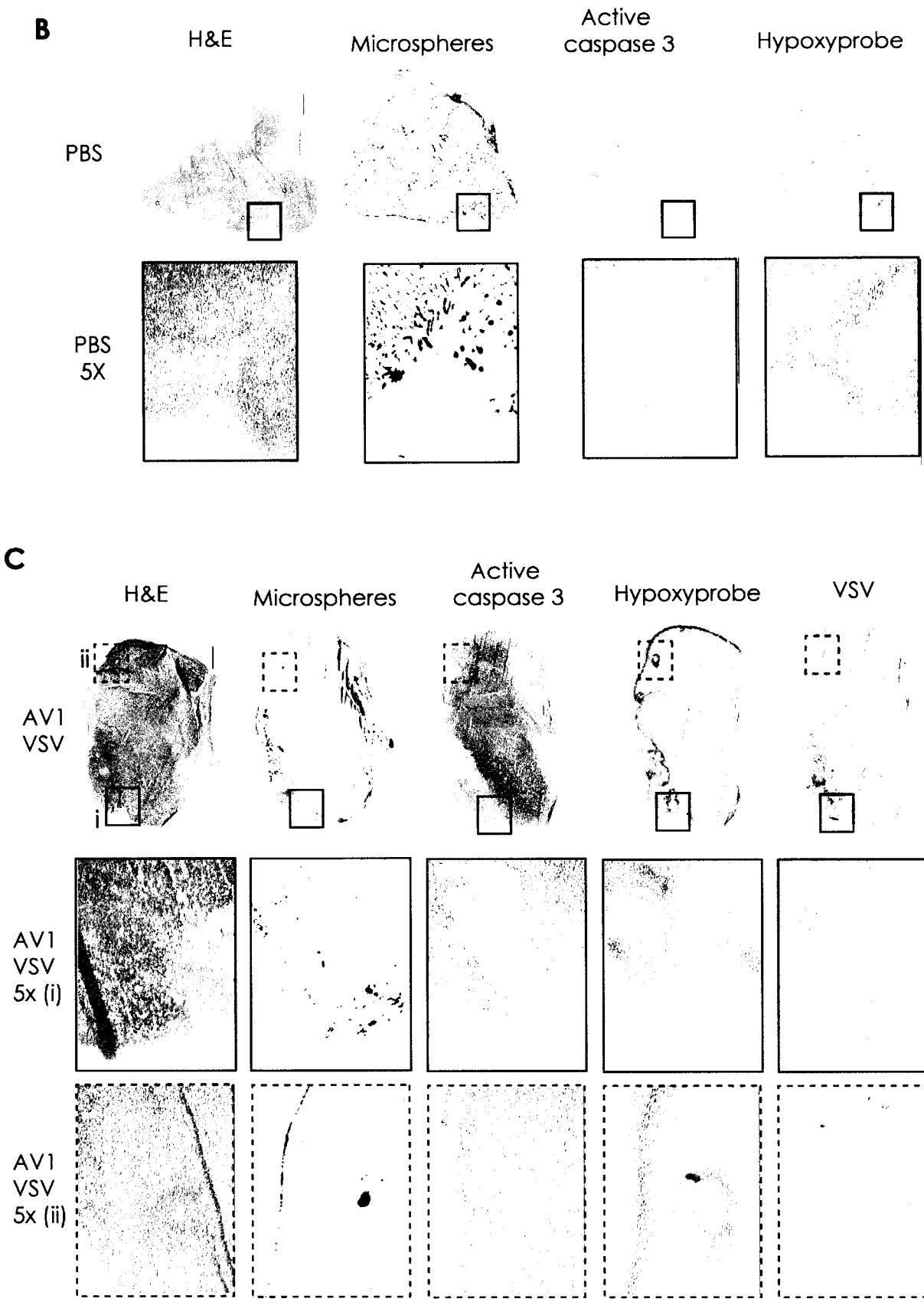
B
H&E
Microspheres
Active caspase 3
Hypoxyprobe
PBS
PBS 5X
C
H&E
Microspheres
Active caspase 3
Hypoxyprobe
VSV
AV1 VSV
ii
i
AV1 VSV 5x (i)
AV1 VSV 5x (ii)

tissue within the apoptotic core.

Complete pictures of active caspase 3, hypoxia, VSV and microsphere distribution in all tumours in this experiment are presented in Appendix VIII. Although active caspase 3 staining usually corresponded well with hypoxia and lack of perfusion, one of the six tumours displayed a lack of perfusion without significant active caspase 3 staining, while another displayed significant active caspase 3 staining without a lack of perfusion. Thus, although the results are intriguing, more samples need to be analyzed to draw conclusions about the relationships between apoptosis, perfusion, and hypoxia, as well as the impact of these parameters on subsequent delivery of second and third doses of VSV. An important experiment that has not been completed yet is an analysis of tumour perfusion, hypoxia, and apoptosis at earlier time points after treatment (results of two tumours 15 hours after VSV treatment are shown in Appendix IX). Completion of these experiments could tell us if tumour vascular shut-off precedes the induction of apoptosis, or follows it, or if there is any relationship between the two observations at all. In addition, it might prove fruitful to begin examining other mechanisms of bystander cell killing, as discussed further in the *Discussion*.

B16F10 subcutaneous tumours are more susceptible to VSV delivered intratumourally than intravenously

As mentioned in the Introduction, one of the goals of the current research was to develop new syngeneic mouse tumour models in which to test the oncolytic activity of VSV. In Figure 7, VSV susceptibility and IFN sensitivity were analyzed in several mouse tumour cell lines. While we have only begun to test these cell lines in vivo, we have made some interesting observations. For example, it appears that IT

delivered VSV is able to replicate much better in subcutaneous B16F10 tumours than IV delivered virus. Figure 18 illustrates VSV immunohistochemistry of four such tumours treated with IFN inducing VSVs IT, versus four tumours treated IV. All four IT treated tumours demonstrated significant areas of VSV replication, while VSV staining in IV treated tumours was limited to rare clusters of a few cells. Preliminary data indicates that replication of VSV within subcutaneous EMT6 tumours may also be much better when virus is administered IT (Appendix X). In the future, it will be interesting to correlate the VSV and IFN sensitivity of all of these cell lines in vitro with virus replication in vivo after different routes of administration.

Figure 18. VSV replicates more in B16F10 subcutaneous tumours when virus is administered intratumourally instead of intravenously.

B16F10 subcutaneous tumour-bearing mice were treated intratumourally or intravenously with $5x10^8$ PFU of VSV (either Δ51 VSV RFP or Δ51 VSV GFPLuc). After two days, tumours were sectioned and immunohistochemically stained for VSV. Size bars (1mm) indicate magnification of whole tumours.

VSV
intratumoural

VSV
intravenous

Discussion

At the beginning of this project, we knew that IFN-inducing mutants of VSV replicated selectively in tumour cells in vitro, and were attenuated in mice in vivo (27). Furthermore, these viruses could be administered systemically to both nude mice and immune competent mice, resulting in significant durable cancer cures (27). However, we also knew that there were certain limitations to VSV therapy. For example, a single high intravenous dose of AV2 VSV could slow CT26 subcutaneous tumour growth in immune competent mice, but could not completely cure any animals (although multiple doses could) (27). This suggested that VSV could reach a tumour and begin to exert some effect, yet fail to eradicate the tumour for some reason. In vitro studies suggest that CT26 cells are virtually defenseless in the face of a spreading VSV infection, even in the presence of exogenous IFN (Figure 7), so we knew that there must be other barriers to VSV in vivo.

Thus, the hypothesis of this project was that VSV would selectively replicate inside murine tumours in vivo, yet certain barriers must be limiting the spread of the virus. We knew that acquired immunity would probably clear virus from animals within weeks, but with the massive 1000 fold virus amplification possible inside every cell, this should be plenty of time, unless delivery to tumours is extremely poor and / or there are other barriers to virus spread. With this general hypothesis in mind, we employed some classic techniques as well as more novel methods to characterize the intravenous delivery of VSV in tumour bearing mice, and subsequent spread and tumour killing over time.

VSV replicates rapidly in subcutaneous tumours despite inefficient intravenous delivery

Several lines of evidence point to the relatively inefficient intravenous delivery of VSV to subcutaneous tumours. Firstly, the kinetic plaque assay-based biodistribution of AV1 VSV indicates that of the 10^9 PFU intravenously injected, only about 100 PFU was detectable in (~0.1g) subcutaneous CT26 tumours after 5 minutes (Figure 11). In contrast, more than 10^7 PFU/g was detectable in the liver at this time point, with intermediate titres found in the spleen and lungs ($5x10^5$ PFU/g and $5x10^4$ PFU/g respectively). Despite the apparently dismal initial tumour titre, tumour selective replication was rapid and sustained: by 24 hours, tumour titres had increased by more than 4 logs and had reached $5x10^8$ PFU/g by 72 hours, while virus was only detected in one lung sample at this time point.

A more detailed discussion of the biodistribution results will be provided after examining other evidence supporting the inefficient intravenous delivery of VSV to subcutaneous tumours. One such piece of evidence is the in situ imaging of replication defective G-less WT VSV GFP in tumour bearing mice (Figure 10A). While dozens of single green cells can be seen in this representative picture of the liver, a similar magnification of a subcutaneous tumour from the same mouse reveals just a handful of infected cells. Furthermore, although the distribution of fluorescence was quite uniform over the whole liver, virus in the subcutaneous tumour was only found at the interface between the tumour and its fatty capsule, as shown in the magnification. Thus, although this data is certainly not quantitative, it is consistent with the biodistribution results indicating poor delivery of VSV to subcutaneous tumours compared to the liver.

Another indication of virus delivery is provided by immunohisotchemical staining for VSV in tumour sections soon after intravenous infection. Although we did not attempt a thorough survey of VSV delivery by this method, several tumours infected with either Δ51 VSV GFP or AV1 VSV for between 7 and 15 hours are presented in Appendix XI. These figures show that only a very small percentage of the tumour is infected by virus soon after injection. In these sections, we can fairly easily count the number of plaques: In order from top to bottom, the tumours have 5-10, 20-30, 10-20, and 70-100 foci of infection. If we use these values as upper and lower limits of virus delivery, and assuming about 1000 5um sections from a tumour of 5mm diameter, that amounts to between $5x10^3$ and 10^5 total PFU delivered to tumours. This is more than the 100 PFU per tumour estimated from the kinetic plaque-assay based biodistibution data (Figure 9). However, the plaque assay method probably underestimate actual delivery, because particles that have already entered cells will not be titratable once the virion disassembles. In any case, both of these estimates are certainly consistent with a very small fraction of the input intravenous virus dose initiating replication in subcutaneous tumours.

Why is intravenous virus delivery to subcutaneous tumour so inefficient?

As discussed above, several independent lines of evidence point to the inefficiency with which VSV is delivered to subcutaneous tumour by the intravenous route. The critical question is, why? A meaningful answer requires some discussion of the physiology of a large bolus of virus injected into the blood stream and the factors that determine where in the body it ends up. In general, material injected into the tail vein will be routed into the large posterior vena cava, which empties into the heart (117). The heart pumps this blood to the lungs, where gas exchange

occurs in the small capillaries, followed by transit back to the heart. The heart will then pump this oxygenated blood throughout the body, to the subcutaneous tumour as well as other organs.

In order to infect the tumour, the virus must leave the bloodstream. While all blood vessels are readily permeably to small plasma proteins such as albumin (diameter ~7nm), permeability to larger particles such as VSV (180 X 75 nm) is tightly restricted. As discussed by Hobbs and colleagues (118), normal vessels have interendothelial junctions of about 7 nm, with rare channels of 50-70nm called caveolae, and possibly slightly larger channels called vesiclo-vacuolar organelles in some types of vessels. Endothelial cells in the liver, on the other hand have frequent fenestations of 100 to 175 nm which readily allow extravasation of virus-sized particles (118). Since all venous blood from the gastrointestinal tract flows through the liver before going back to the heart, this provides a vast surface area for large particles to leak out of the blood. Furthermore, these permeable venous channels in the liver (called sinusoids) contain large numbers of specialized resident macrophages called Kupffer cells, which have an enormous phagocytic capacity for particulate matter such as viruses (119). The spleen and bone marrow also contain leaky sinusoids which allow extravasation of relatively large particles. Fluid and particles that leak out of the blood and escape phagocytosis enter lymph vessels, which filter into lymph nodes before returning the to the heart where lymph and blood recombine (117).

This model can explain both the short half-life of VSV in the blood, and rapid accumulation in the liver revealed by the kinetic biodistribution data (Figure 11). Although most of the initial virus dose was not detected at the earliest time point

(probably due to virus entry into cells or inactivation), others have performed acute biodistribution studies with radioactively labeled VSV in which the majority of input virus can be accounted for (120). This data shows that just 3 minutes after intravenous injection, radioactivity in the blood had dropped by more than 10 fold, and after 20 minutes, 70% of the radioactivity could be recovered from the liver (120). Similar biodistribution results were obtained with intravenously injected NDV (120), HSV (121), Type 3 Reovirus (122), Frog Virus 3 (123), Simian Immunodeficiency Virus (124), and Type 5 Adenovirus (125, 126) as well as inert plastic virus-sized particles (127) and liposomes (128).

The precise mechanism by which viruses are taken up by Kupffer cells is not entirely clear (129). There may be some receptor dependent infection of macrophages, but the simple particulate nature of viruses also seems to result in non-specific phagocytosis (119, 123). Furthermore, there is evidence that very low levels of "natural" antibodies to viruses exist even in naïve animals (130, 131), and binding of this natural IgM could target viruses for more efficient phagocytosis. Kupffer cells are generally thought to be quite resistant to virus infection (123), and indeed, the biodistribution results do not suggest any productive replication of AV1 VSV in the liver. However, we have observed GFP expression in the liver after systemic injection with both replicating and non-replicating WT VSV GFP (Figure 10). While Figure 10b shows an example in which WT VSV GFP seems to have spread throughout the liver, this was not uniformly observed. There is evidence that Kupffer cells can be saturated with virus, and that after this point, virus will be able to spread to other cell types in the liver (132). Thus, the variability in GFP expression found in the liver after infection with WT VSV GFP might result from infection of Kupffer cells, or

it might result from dosing near the Kupffer cell saturation phagocytic threshold level, such that virus is released throughout the liver to infect other cells. Further experiments are needed to systematically compare the biodistribution of WT and IFN inducing mutants of VSV.

Despite the propensity of the liver to rapidly clear the vast majority of particulate matter from the blood stream, VSV and other particles obviously do reach tissues and tumours to some degree. In fact, compared to most non-sinusoidal endothelium (ie. all tissues except the liver, spleen and bone marrow), tumour vasculature has been characterized as being quite permeable to macromolecules, as reviewed previously (133). For example, subcutaneous tumours were found to leak about five times more ferretin (~11 nm diameter) than surrounding normal tissue (134). Studies of larger particles are more relevant to the current research. For example, intravenous injection of liposomes or latex beads of 100-2,000 nm diameter revealed that several different types of tumours grown subcutaneously in nude mice all have vascular pores between 380 and 780 nm in diameter, while vascular pores in surrounding normal tissue were estimated to have diameters less than 100 nm because no particle extravasation was observed (118). The increased vascular leakiness of tumours is probably related to the chaotic manner in which tumours induce blood vessels to grow within and around them (133). In particular, tumours secrete Vascular Endothelial Growth Factor (VEGF), which both promotes blood vessel growth and leakiness (135).

Although subcutaneous tumours tend to have increased permeability to macromolecules compared with surrounding normal tissue, they also have substantially higher pressure, due to defective lymphatic drainage (133). For

example, a survey of diverse solid human neoplasms found that interstitial tumour pressures above 15 mm Hg were common, compared to a maximum of 3 mm Hg for normal skin and breast tissue (4). This high pressure is thought to severely limit the diffusion of particles into the tumour, but if particles do enter the tumour, impaired lymphatic drainage may cause them to accumulate (133). Thus, the physiological factors that enhance or inhibit intravenous delivery of macromolecular particles such as viruses to tumours are quite complex. On the one hand, tumour blood vessel leakiness and poor lymphatic drainage may promote delivery and accumulation, while factors that could limit delivery include rapid blood clearance by the liver, and high tumour interstitial pressure.

Besides unfavourable biodistribution of intravenously administered viruses, another potential difficulty in delivery is inactivation in the blood. As mentioned above, low levels of natural antibodies to viruses, including VSV, have been documented (130, 131), and these antibodies could lead to complement mediated inactivation of virus in the blood (131). Furthermore, in vitro studies with Type 5 Adenovirus have suggested that in the bloodstream of human patients, more than 90% of virus may be sequestered by erythrocytes (126). Although low levels of natural antibodies to VSV have been documented (130), a therapeutic dose of VSV is not substantially inactivated by whole blood (R. Marius, unpublished data).

Studies with the G-less WT VSV GFP indicated a massive concentration of GFP in lymph nodes in both tumour bearing and non-tumour bearing animals (Figure 10A). It was intriguing that such an amount of virus could accumulate in small lymph nodes without any spread of the virus. This suggested that either VSV was very efficiently delivered to some cells in lymph nodes, or perhaps antigen

presenting cells infected in the periphery homed to lymph nodes to present antigen after infection. Research by others has shown that dendritic cells in vitro take up VSV and present viral antigens to T cells (136). When these dendritic cells are injected back into mice, they home to the spleen and probably to lymph nodes, and release small amounts of infectious virus (136).

We can only speculate as to the possible role of high level lymph node infection on viral oncolysis. Although virus appears to be extremely concentrated in lymph nodes, the potential effect of sequestering virus (away from the tumour) is probably insignificant compared to sequestration by the liver, simply due to the comparatively small lymph node mass. In fact, replication in lymph nodes could be a highly desirable oncolytic virus property, because lymph nodes are extremely common sites of metastases (131). Efficient trafficking of VSV to lymph nodes likely initiates a potent anti-VSV specific acquired immune response, which would act to limit spread of the virus in tumours. However, a potent anti-VSV immune response could also indirectly contribute to the induction of an anti-tumour immune response, for example, by increasing trafficking of lymphocytes to VSV infected tumours.

Heterogeneous delivery of VSV to subcutaneous tumours

Besides the inefficient delivery of VSV to tumours in general, results presented herein suggest that VSV is also frequently distributed heterogeneously to tumours, although this evidence by definition must be descriptive. A typical example is illustrated by whole tumour surface GFP imaging (Figure 8B first panel). In this example, the surface of the subcutaneous tumour contains a few small spots of GFP near the edges of the tumour, with the vast majority of fluorescence concentrated in a single large focus. Co-delivery of GFP and RFP expressing viruses (Figure 9B)

suggests that large foci of infection such as this may originate from preferential delivery of many particles of virus to a small location in the tumour, rather than preferential viral spread of a single particle of virus at this location. As an example, the middle panel of Figure 9B illustrates quite clearly a tumour in which many individual plaques of both GFP and RFP viruses are concentrated in a small area at the interface between the tumour and normal muscle tissue, with much of the tumour remaining apparently free of virus. Another example is provided by fluorescent imaging of the replication defective G-less WT VSV GFP in tumours: the only fluorescence that could be found in this subcutaneous tumour is at the interface between the tumour and its surrounding capsule of fatty tissue (Figure 10A).

Immunofluoresence (Figure 15) and immunohistochemistry (Figure 16 and Appendix II) are consistent with preferential delivery at the tumour / normal interface. However these tumours were examined two days after intravenous infection, so interpretations concerning delivery are complicated by spread and possible clearance of the virus. Tumour sections from earlier time points after infection (7-15 hours) are illustrated in Appendix XI. In the first tumour (7 hours), between 5 and 10 single infected cells (or clusters of a few cells) are all seen within a small region of the tumour close to the surface, with the remaining tumour staining negative for VSV. In the second tumour (10 hours), most of the 20-30 plaques are localized at the interface between dense tumour tissue and surrounding connective tissue, or within the tumour in close proximity to connective tissue that divides the tumour into distinct compartments. The third tumour (15 hours), has between 10 and 20 foci of infection sequestered within two areas of the tumour, both close to

the tumour / normal interface. The last tumour represents an exception to this pattern: approximately a third of the tumour area contains a very even distribution of foci of infection. Thus, during the course of this project, we often (but not always) observed that VSV seemed to be delivered preferentially near the borders between tumour and normal tissue.

The pattern of virus delivery seen in most tumours is very similar to patterns of tumour blood vessel leakiness observed by others (137). Dvorak and colleagues studied the vascular leakage of several different tracers (with diameters of 3, 12, 17 and ~50 nm) in five different types of subcutaneous tumours using several techniques (137). The smallest tracer (3nm) could easily leak from all vessels (both tumour and normal). However the 12-50 nm particles only leaked from tumour vessels, and in all five tumours studied, leakage was confined to very specific areas of the tumour, namely "vessels at the tumor-host interface" and "vessels in the connective tissue surrounding and separating individual tumour nodules" (137). Thus, one could speculate that the same physiological factors that determine vascular leakage to inert macromolecular tracers may also have some role in determining where VSV can leave the blood stream to initiate tumour infection.

While the relationships between tumour morphology and intravenous virus delivery have not been investigated for most oncolytic viruses under development, one exception is Adenovirus, which is a non-enveloped DNA virus with similar virion dimensions as VSV (138). Preferential adenoviral infection of the tumour periphery, similar to our observations, was described in subcutaneous cervical cancer xenografts in nude mice (139). Other studies have highlighted the role of the tumour Extracellular Matrix (ECM) in intravenous adenovirus delivery. The ECM is a

three dimensional lattice of fibres, linker proteins, and space-filling glycosaminoglycans that is responsible for maintaining the structure of both normal organs and solid tumours (140). ECM can be quite different in tumours versus normal tissue, in particular regarding the basement membrane that supports endothelial cells. While normal endothelium has a continuous basement membrane, this ECM component is often discontinuous in tumour blood vessels (140). It has been suggested that the nature of the basement membrane plays a role in the delivery of Type 5/35 Adenovirus to xenograft liver metastases in mice via portal venous infusion. This virus was able to target only 8% of 3,000 metastases examined, and the few targeted tumour nodules seemed to have a visibly thinner basement membrane separating blood vessels from tumour cells (141). Very recently, the same group expanded their results by examining the relationship between morphology, vascularization, basement membrane distribution, and adenovirus transduction in four different types of liver metastases (142). In this study, it was found that IV administered adenovirus could only infect tumour cells if they were in direct contact with blood vessels lacking a continuous basement membrane.

A pertinent study of the treatment of rat liver metastases using WT VSV administered via the hepatic artery was recently published (143). One day after injection, VSV was found to be distributed evenly throughout tumour nodules, in contrast to our results suggesting preferential targeting to the tumour / host interface. The liver tumour metastases examined in this study were smaller than the typical subcutaneous tumours we have examined, so this could play a role in the different observations. However, it is well known that vasculature can vary substantially among different tumours, and in the same tumour when it is

transplanted or seeded in different organs (118). Along this line, surface GFP imaging of CT26 lung tumour metastases suggested superior intravenous delivery of VSV to these nodules (Figure 8A and 9A). We did not pursue detailed studies in this model because of variability in tumour burden, but, if these tumours are indeed targeted by VSV more efficiently than subcutaneous tumours, it would be interesting to know if this is related to differences in surrounding normal tissue, tumour size, or perhaps even proximity to the heart.

In discussing mechanisms of intravenous virus delivery to tumours, it should also be noted that a virus may have ways to enter a tumour that an inert tracer does not: for example, we do not know if VSV can cross the endothelial barrier in vivo by replicating in endothelial cells. It is known, however, that WT non recombinant VSV can productively infect polarized endothelial cell monolayers in tissue culture (144) and fresh umbilical cord vein explants (145). To add another possibility, we could consider the role of "mosaic" tumour blood vessels, in which tumour cells and endothelial cells combine to form a continuous vessel (146). Finally, we also need to examine the possibility that VSV could traffic to tumours by infecting or binding to lymphocytes, which have active mechanisms of squeezing through blood vessels (147). A goal of future research will be to determine exactly which cells are the first targets of intravenously delivered VSV.

Investigation of the relationship between intravenous VSV dose and tumour titres after 24 hours

A study of the relationship between intravenous dose of VSV and subcutaneous tumour virus titres after 24 hours (Figure 12) was pursued with several possible outcomes in mind. Firstly, we hoped to determine if there was a minimum

dose of virus that could consistently reach tumours and initiate replication. This determination could provide us with indirect information concerning the amount of virus that is probably delivered to tumours from a typical therapeutic dose. Secondly, detailed studies with a non-replicating adenovirus had indicated a non-linear IV dose versus transgene expression profile, which was experimentally associated with saturation of adenovirus uptake by liver Kupffer cells, leading to increased transduction of target cells beyond the saturating dose (132). This experiment could also indicate if the same phenomenon might be occurring with VSV. Lastly because we had observed a heterogeneous distribution of VSV within subcutaneous tumours, with apparently large amounts of virus co-delivered to discrete sites, it was also possible that increasing the virus dose past a certain point would not actually increase tumour titres because most of the extra virus would go to small areas of the tumour which might be already saturated with virus.

As shown in Figure 10, doses between 10^6 and 10^9 PFU resulted in consistent delivery of virus to tumours, with increasing doses giving increased tumour titres. Although a dose as low as 10^4 PFU could initiate detectable replication in one of three tumours , the lowest dose able to consistently target tumours was 10^6 PFU, resulting 24 hours later in a mean titre of $5x10^4$ PFU/g. If we were to assume that delivery of 10^6 PFU (the lowest consistent dose) results in about 10 PFU reaching the tumour and initiating replication, then we could also estimate that a typical therapeutic dose of 10^9 PFU should result in delivery of about 1000 fold more virus than a dose of 10^6 PFU, ie. 10^4 PFU. This estimate assumes a linear dose versus tumour titre relationship, which is not inconsistent with the data. Therapeutic delivery of about 10^4 PFU of virus is consistent with estimates described previously in

this report. However, we cannot be sure that a minimal amount of virus delivered at lower doses could not initiate replication in a tumour which is still too low to be detected 24 hours later. Thus, this experiment could not provide us with a reliable estimate of the minimum IV dose of VSV that could initiate amplification within subcutaneous tumours.

Although substantial tumour-to-tumour variability was observed in this experiment, the amount of virus found in tumours after 24 hours did tend to increase proportionally with increasing IV dose. In particular, the difference between the 10^8 and 10^9 PFU dose group is significant ($P<0.05$). Thus, we must conclude that although delivery of VSV may be heterogeneous, it is not so localized that increasing the dose does not increase tumour titres. Furthermore, we did not observe a threshold dose beyond which virus replication increased dramatically compared to previous incrememental dose increases. With adenovirus, this liver saturation threshold occurred beyond 10^{10} PFU, and required fairly precise observations to detect (132), so we certainly cannot rule out the possibility of Kupffer cell saturation by VSV.

Replication of VSV in tumours is equivalent in intravenous bolus and slow infusion protocols

One goal of the current project was to use information gleaned from VSV delivery and spread studies to design better clinical cancer treatment protocols, which might eventually be adopted in clinical trials. From the other direction, we wanted to correlate observations about the relationship between cancer treatment efficacy and virus treatment protocol, with studies of virus delivery and spread. The latter experimental angle spurred two related studies of VSV delivery and spread.

Firstly, we investigated how virus gene expression in tumours was related to the duration of intravenous virus injection (bolus versus slow infusion), and secondly, we investigated virus gene expression during multiple versus single dosing protocols.

The work relating to intravenous infusion time was originally prompted by observations made with oncolytic Newcastle Disease Virus (PV701) in Phase I clinical trials (112). Specifically, greater tumour responses were observed when NDV was administered in a slow infusion (over 3 hours) as opposed to a bolus IV injection (10 minutes). We hypothesized that administering virus over a longer period of time might result in a better distribution of virus throughout the tumour, because tumour vascular perfusion and permeability are known to vary significantly within individual tumour vessels over time. For example, quantification of vascular permeability to albumin in a single 0.2 mm^2 region of subcutaneous tumour showed that permeability easily varied by two to five fold from hour to hour (148). In a more descriptive study, perfused tumour blood vessels were labeled by intravenous injection of different coloured tracers spaced 15 minutes apart (149). Blood vessels were often observed to be perfused by only one tracer, indicating temporary occlusion of blood flow within short time intervals. Since the half life of intravenously injected virus in the blood is on the order of minutes, we postulated that temporarily non-perfused / non-permeable blood vessels might not be accessible to virus, but prolonging the duration of infusion could increase the amount of time in which virus is present in the blood and thus increase the chance of virus being able to reach more areas of the tumour.

Alternatively, a slower infusion of virus might result in increased efficacy by avoiding hyperactivation of a systemic innate immune response which could

dampen virus spread. Indeed, the original reason for adopting the slow infusion NDV protocol was the acute toxicity of a bolus injection (112). On a completely different vein, we also imagined how slow infusion of virus could actually decrease delivery to tumours, if it allowed a potential sink such as the liver to take up more virus. As shown in Figure 13, there was no significant difference in the luciferase activity detected in homogenized subcutaneous CT26 tumours 18 hours after administration of Δ51 VSV GFPLuc in a bolus, versus 12 minute infusion protocol. However, there may be less variability within the results for slow infusion compared to bolus, and this in itself might lead to more consistent efficacy. In the future, it would be worthwhile to compare these two protocols in terms of longer term tumour growth response. It would also be interesting to compare the distribution of virus in tumours after administration by either bolus or slow infusion.

Investigation of the mechanism by which multiple IV doses of VSV results in increased cancer treatment efficacy

Related to the experiment described above is the phenomenon of increased efficacy via multiple systemic doses of VSV. Specifically, work by D. Stojdl in our lab has shown that 6 IV doses of $5x10^8$ PFU of AV2 VSV (administered Monday, Wednesday, and Friday for two weeks) could completely cure 5/8 immune competent mice of subcutaneous CT26 tumours, while a single dose could significantly slow tumour growth, but no durable cures were observed (27).

Again, there are several possible explanations for this phenomenon. Firstly, in the multiple dosing protocol, more total virus is administered, and the difference between $5x10^8$ PFU and $3x10^9$ PFU might be enough to cross a threshold, resulting in delivery of enough virus to be able to eradicate a tumour. Secondly, for the same

reasons discussed in the previous section (temporal heterogeneity of tumour perfusion and vascular permeability), delivery of virus at different time points might target new areas of the tumour that were not targeted by previous doses. It has been suggested that tumours are compartmentalized into separate units by connective tissue, through which virus may not be able to spread (150). If fractionated dosing is better able to target all of the compartments of a tumour, that could explain the increased efficacy of multiple doses. The importance of dose fractionation is supported by studies with intratumourally administered oncolytic Adenovirus and Measles virus, showing that multiple low dose injections of virus results in better efficacy then administering the same total dose in a single injection (150, 151). Thirdly, delivery of multiple doses of virus could stimulate indirect tumour killing mechanisms.

Experiments presented in Figure 14 indicate that in a typical multiple dosing regimen (doses every 48 hours), the second dose of virus does not replicate substantially in tumours, and doses administered more than 48 hours after the first injection replicate even less. Given the dramatically increased efficacy of a 48 hour interval multiple dosing regimen, these results were intriguing. If very little of the second dose of virus is initiating replication in the tumour, this would suggest that the increased efficacy may come from either targeting a very small number of new tumour sites, or from indirect virus induced anti-tumour effects. These possibilities will be discussed further after the examination of other experiments.

With respect to the multiple dosing data, we were interested, on a more mechanistic level, in the reason for the 48 hour second dose inhibition. Although an acquired immune response can begin by two days after infection, it is generally

thought to require 4-5 days to begin clearing infection (152), but the innate immune system could certainly be playing a role. Another option is that all of the possible sites of virus replication in the tumour are already saturated by this point, leaving no "fertile ground" for replication of the second virus. Alternatively, the tumour physiology or vasculature may be altered on a local level such that virus delivery or spread are inhibited.

In order to begin to explore these possibilities, we carried out several modified multiple dosing experiments. We found that when the first dose of virus is intranasal rather than intravenous, replication of the second (IV) dose in the tumour is no different than in PBS treated controls (Figure 14A). Intranasal administration of virus is known to elicit systemic innate and acquired immune responses (153), however it evidently does not prevent tumour infection. It is possibility that intranasal administration of virus fails to trigger the production of some systemic factor (which is produced upon IV infection) that is responsible for this effect. Another possibility is that intranasal infection does not efficiently result in targeting of virus to tumours, and virus replication in the tumour is required for this effect. Future studies will be required to address the differences between IV and IN virus administration.

Another clue as to the mechanism of multiple dose inhibition was provided by the observation that this effect is not as severe when the second dose of virus is administered intratumourally rather than intravenously (Figure 14B). This observation is consistent with the block in IV second dose replication being at least partly at the level of delivery (since spread initiated via intratumoural injection is less severely affected). It is also possible, however, that intratumoural injection of virus results in its

distribution to "infectable" sites of tumour, while intravenous delivery targets sites that are not "infectable". For example, we have observed that intravenously administered virus seems to be preferentially delivered to the tumour rim. Thus, one might suggest the second IV dose of virus cannot replicate in tumours because most of the rim is already infected, while the intratumourally administered virus can replicate in the uninfected core. This possibility is complicated by immunohistochemical observations of tumours. As we will discuss in the next section, intravenous administration of VSV seems to induce apoptosis in the tumour core, indicating that this area of the tumour might not be fertile ground for virus replication. Furthermore, we have observed that intratumoral administration of virus does not necessarily target the tumour core more than the rim (Appendix VI). In the multiple dosing experiment, we also observed that when the interval between doses was 72 hours as opposed to 48 hours, there was a significant block in the replication of intratumourally delivered virus. Thus there may be different mechanisms of virus inhibition operating at different times after the first dose.

As discussed more fully below, further experiments revealed a block in blood flow to tumours 48 hours after an intravenous dose of VSV, and obviously this could be playing some role in preventing delivery of virus. Thus, we will postpone a more thorough discussion of the multiple dosing data until then.

VSV induces bystander tumour cell killing

One of the goals of the current project was to investigate the spread and tumour killing activity of VSV, with the idea in mind that physiological barriers or innate responses to virus could be limiting the ability of VSV to spread throughout subcutaneous tumours. To begin exploring these ideas, we performed anti-VSV

immunofluoresence (Figure 15) and immunohistchemistry (Figure 16 and Appendix II-IV) on thin sections of tumours after intravenous treatment with IFN-inducing VSV mutants. We found that two days after VSV treatment, obvious spread of virus had occurred, with a tendency for virus to concentrate near the tumour periphery. Interestingly, when we examined these same tumours for apoptotic cell markers, including TUNEL and active caspase 3, we found that the tumour cores which were surrounded by VSV staining were usually highly apoptotic. Quantification of these results revealed that tumours treated with VSV for two days stained positive for VSV in 15+/- 5% of the area of the section, while active caspase 3 staining was present in 42+/- 7% of the section. Untreated tumours had an average of 6.7 +/- 2.5 % active caspase 3 staining. Although we did not have as many samples to analyze after five days of VSV treatment, these tumours were also characterized by extensive apoptosis.

It could be argued that these apoptotic VSV-negative cells in the tumour core could represent a late-stage VSV infection in which the antigens have been so degraded that they cannot be detected by our polyclonal antibody. This possibility seems unlikely. The VSV-negative active caspase 3-positive cells have intact condensed nuclei, while the VSV-positive active caspase 3-positive cells have largely lost all cellular architecture (Figures 16 B and C). It is difficult to imagine that this disintegrated cellular morphology could precede the condensed yet intact nucleus morphology. Furthermore, results discussed above suggest that VSV is delivered preferentially to the tumour rim, not the core.

The other possibility is that infection with VSV can induce tumour cell killing in a way that does not required direct infection of tumour cells. In other words, VSV

induces bystander tumour killing. This could occur if cells of the innate or acquired immune system were stimulated by virus to directly kill uninfected tumour cells, or to secrete toxic tumour-killing cytokines or other toxic effector molecules. Bystander tumour cell killing could also be induced indirectly, by acting on cells supporting the tumour such as endothelial cells. Another possibility is the direct infection of endothelial cells or other host cells supporting the tumour.

Before discussing the possible mechanisms of bystander cell killing in more detail, it should be noted that this phenomenon has not been observed by others studying VSV therapy in different tumour models. For example, injection of non recombinant WT VSV directly into subcutaneous xenograft tumours in nude mice was reported to result in TUNEL staining only in areas containing VSV antigen at several time points after infection (89). Another group noted the co-localization of necrotic tumour tissues (defined by hematoxylin and eosin morphology staining) with VSV antigen in rat hepatic metastases one day after infusion of WT VSV via the hepatic artery (154). In neither study were the observations formally quantified.

While our observations (Figure 12 and 13) were made with IFN inducing mutants of VSV administered intravenously in immune competent mice, we have begun to investigate whether or not this phenomenon occurs in different conditions, namely 1) in nude mice 2) intratumoural virus injection and 3) when the virus is WT as opposed to IFN inducing. Preliminary results presented in Appendices V-VII indicate that some amount of bystander cell killing seems to occur in all of these conditions, although we will have to analyze more samples to be able to make conclusions.

What are potential mechanisms for VSV induced bystander tumour cell killing?

With respect to potential mechanisms of bystander cell killing, published studies of other viruses would suggest several. For example, bystander tumour cell killing has been observed with nonlytic strains of NDV, and it was suggested that macrophages may be responsible for this effect (155, 156). Macrophages are phagocytic cells that can engulf pathogens, infected cells, and apoptotic cells, and present antigens to stimulate acquired immunity (157). Activated macrophages also secrete a variety of cytotoxic products and cytokines (157). Shirrmacher and colleagues studied the anti-tumour effects of a strain of NDV that infects mouse and human cells without lysing them, and produces only non-infectious progeny viruses in these cells. They observed that even when just a small proportion of tumour cells were infected with this virus in nude mice, substantial anti-tumour effects were observed, beyond that which could be accounted for by simple destruction of infected cells (155). They found that macrophages stimulated by this strain of NDV in vitro could lyse tumour cells, and transfer of NDV-stimulated macrophages into tumour-bearing mice could induce significant anti-tumour effects (156). Subsequent studies showed that both active and UV inactivated non-lytic NDV could increase macrophage cell surface expression of Tumor Necrosis Factor α Related Apoptosis Inducing Ligand (TRAIL) (158). Neutralization of TRAIL blocked the ability of NDV stimulated macrophages to kill tumour cells in vitro.

Interestingly, Reovirus and Measles virus, which are both currently under investigation as oncolytic agents, also induce infected cells to produce TRAIL, resulting in apoptosis of uninfected tumour cells in vitro (159, 160). While non-lytic NDV-mediated bystander killing was associated with TRAIL, an oncolytic strain of

NDV may also induce bystander tumour cell killing, but in this case, the culprit appears to be Tumour Necrosis Factor α (TNFα). Although these studies were only done in vitro, it was shown that oncolytic NDV could cause normal human blood mononuclear cells and rat splenocytes to secrete TNFα, resulting in indirect tumour cell killing (161). Along these lines, it is known that AV1 and AV2 VSV (but not WT VSV) can upregulate TRAIL mRNA in some infected cells (27). It has also been shown that WT VSV does not induce TNFα production by monocytes in vitro, but there is no data about AV1 or AV2 (162). Studies of other viruses in immunodeficient mouse cancer models have suggested that bystander effects could be mediated by Natural Killer cells for Sindbis virus (163), and neutrophils for Measles virus (164).

Another approach to finding candidate bystander effect-mediators is to look for cytokines or other factors known to be toxic to CT26 cells. In vitro studies have shown that CT26 cells are quite resistant TNFα and IFNγ, yet in combination these cytokines can reduce cell viability to just over 40%, and induce an apoptotic morphology (165). In several instances, exogenous TNFα was shown to exert significant responses against CT26 tumours in mice (166, 167). Interestingly, this result has been correlated with effects on the tumour vasculature, not effects on CT26 cells themselves. For example, flavone acetic acid, a synthetic TNFα inducer, was shown to dramatically reduce CT26 subcutaneous tumour blood flow just one hour after intraperitoneal administration (168). This vascular shutdown was still apparent 2 days after injection, and the effect could be completely blocked by pretreatment with neutralizing antibodies against TNFα (168).

Some evidence suggests that Type I IFN may also be able to induce host-mediated killing of CT26 tumours in vivo. We have shown that CT26 cells are

resistant to the antiviral effects of IFN (Figure 7C), while others have shown that CT26 cells are also highly resistant to the anti-proliferative effects of IFNα/β in vitro (169). However, several studies have shown that Type I IFN, or synthetic IFN inducers, can mediate significant anti-tumour effects in vivo (170-172). In one instance this was correlated with apoptosis of endothelial cells (171).

Several studies have characterized the anti-vascular effects of Type I IFN in other tumours models (173-176). For example, Dvorak and Gresser found that exogenous IFN treatment could significantly inhibit the growth of two IFN resistant tumour cell lines in immune competent mice, and regressing tumours (five days after treatment) showed massive necrosis and histological evidence of acute deprivation of blood flow without any inflammation (177). A single day after IFN treatment, tumours displayed graded areas of necrosis, thus allowing the specific inspection of blood vessels in regions of the tumour before they became necrotic. Examination of more than 1,000 blood vessels by electron microscope revealed that tumours treated with IFN for one day had almost twice as many damaged blood vessels as control tumours. Endothelial cell injury was followed by plasma and then erythrocyte leakage from blood vessels, followed by reduced blood flow and tissue perfusion, leading to coagulative necrosis (177). No pathological abnormalities were observed in normal tissue during IFN therapy; it was suggested that high proliferative index of tumour endothelial cells, coupled with their already marginal functionality, contributed to their disproportional sensitivity to IFN.

Thus, there is no shortage of plausible mechanisms by which VSV could induce bystander killing of CT26 tumour cells, although we have only discussed innate anti-tumour effects. Although many oncolytic viruses, including HSV (109)

and VSV (27), are known to stimulate acquired anti-tumour immune responses in immune competent mouse models, this type of response is generally thought to require 4-5 days to establish (152). Since the VSV-mediated bystander killing effect is very robust just two days after infection, we have concentrated on possible effects of the innate immune system rather than acquired immune mechanisms. Of course, a thorough histological time course comparing VSV spread and tumour killing ability in immune competent and immunodeficient mouse models will need to be carried out to confirm these assumptions. Collaborators (K. Parato and A. Power) are currently investigating the effects on acquired immunity on VSV oncolysis in detail.

VSV reduces tumour perfusion

As discussed above, there is no shortage of plausible pathways through which VSV could induce bystander tumour cell apoptosis. We chose, however, to investigate tumour hypoxia and perfusion first for several reasons. Firstly, VSV seems to induce massive, uniform apoptosis throughout the tumour core, rather than a patchy, heterogeneous apoptosis. This particular pattern seems more consistent with vascular collapse than cytokine mediated killing. Furthermore, the potential block in intravenous delivery of virus 48 hours after a prior dose could possibly be explained by a tumour vascular shutdown. Lastly, there were several plausible physiological pathways that could explain how VSV could induce a tumour vascular shutdown, as discussed above.

As shown in Figure 17 (and Appendix VIII), four of six untreated subcutaneous CT26 tumours were thoroughly perfused by 100 nm fluorescent bead, while two of the six tumours had significant regions without blood flow. Tumours treated with VSV for two days demonstrated severe lack of perfusion in five of the six tumours

examined. Hypoxprobe staining correlated with the perfusion analysis: non-perfused tumours displayed intense staining only at the perfused tumour rim, with only very faint staining in the core, likely indicating metabolic inactivity in this region (hypoxyprobe adduct formation requires active cellular metabolism). Perfused tumours either showed minimal hypoxia staining, or in the untreated tumours with non-perfused regions, hypoxia staining outlined these necrotic zones. The active caspase 3 staining pattern did not correlate as tightly with perfusion and hypoxia: we observed one VSV treated tumour that showed significant active caspase 3 staining, yet remained well perfused, while another tumour lacked perfusion but did not significantly stain for active caspase 3. Thus, although we can with some confidence associate VSV treatment with loss of tumour blood flow, we cannot necessarily say that this effect is related to active caspase 3 staining, without performing further experiments.

This experiment was prompted by questions about the mechanism of bystander tumour killing (Figure 16), and the mechanism of 48 hour multiple dose inhibition (Figure 14). Does this experiment actually provide any insight into these questions? With respect to the multiple dose inhibition, the answer is maybe. Certainly, lack of tumour blood flow could account for lack of delivery of virus into the area without blood flow, but in general, tumours were still perfused at the rim. Furthermore, our results suggest that intravenous administration of VSV often, but not always results in virus delivery near the tumour periphery. Thus, if we want to use the tumour perfusion data to explain the multiple dose inhibition data, we must assume that the area in which VSV would normally be delivered at least somewhat overlaps with the area in which tumour blood flow is blocked. This is not impossible to

imagine: In several tumours, only a very thin portion of the tumour rim is perfused (although less dense surrounding normal tissue is well perfused). Furthermore, at least in some of the tumours, VSV is already present in much of the rim of the tumour that is accessible to blood flow. Thus, a lack of blood flow to most of the tumour, coupled with direct VSV killing in much of the rest of the tumour, could account for the observed significant inhibition in second dose virus gene expression when administered IV 48 hours or more after a prior dose.

Critically, we will need to examine tumours 24 hours after administration of VSV. If the hypothesis that vascular shutdown blocks delivery of VSV is correct, we would predict that tumour vasculature would still be functional 24 hours after VSV treatment, because we did not observe significant inhibition of intravenous delivery of a second dose of virus at this time point. We have examined two tumours for vascular perfusion at earlier time points after VSV treatment, and one of the two does seem to show an intermediate patchy tumour perfusion (Appendix IX), however we will have to analyze more samples to make any conclusions.

Another question is, does this experiment tell us anything about the mechanism of VSV induced bystander tumour killing? Again, the answer can only be maybe. Any sort of massive induction of tumour cell apoptosis could also be responsible for inducing concurrent apoptosis in endothelial cells, which results in vascular collapse that is associated with tumour apoptosis, but not the cause of it. Since, we did observe some tumours in which active caspase 3 staining and tumour perfusion did not correlate, it is possible that two separate virus induced effects are responsible for inducing apoptosis and vascular shutdown. Again, we will need to analyze more tumours from an early time course after VSV treatment to try to

determine the sequence with which these pathophysiological changed occur, and the correlations between them.

Another complicated result which needs to be addressed is the observation of successful intratumoural delivery of virus two days after intravenous injection of a first dose. In order for this to be possible, we must assume that VSV can at least initiate some gene expression in a tumour that appears to be highly apoptotic in the core, and undergoing prior direct killing by VSV in much of the tumour rim. Since productive IT delivery *is* significantly inhibited after 72 hours, one might suggest that at this time point, tumour cell killing has reached a point at which virus gene expression is not supported. With respect to this inconsistency, metabolic activity in the apoptotic core is not supported by the pattern of hypoxia staining. Detectable hypoxyprobe adduct formation is known to require active metabolism, so necrotic areas of a tumour are generally surrounded by intense hypoxia stain, as we have observed two days after VSV treatment. However, an alternative explanation for the pattern of hypoxia staining surrounding the apoptotic core is that the intraperitoneally administered Hypoxyprobe does not sufficiently perfuse into the tumour core. Future experiments could help to clarify these issues. For example, a thorough immunohistochemical study of tumours treated intravenously with one VSV, and then intratumourally with a different VSV, could show us where the intratumoural dose of virus replicates in this particular situation. In vitro, it might be useful to induce apoptosis of CT26 cells and assess their ability to undergo productive VSV infection at various points after triggering cell death.

Indications of oncolytic activity in other murine cancer models

One objective of this project, which is still only in preliminary stages, is the investigation of VSV oncolysis in other murine tumour models. As shown in Figure 7, we obtained several model cell lines, and tested them for in vitro sensitivity to WT VSV GFP and Δ51 VSV GFP, and also for sensitivity to the antiviral effects of IFN. Interestingly, all of the new tumour cell lines showed some sensitivity to IFN, as opposed to CT26 cells, which were completely unaffected. Although both viruses could productively infect all cell lines acutely (Figure 7C), Δ51 VSV GFP was less able to spread in some of the cells at low MOI (Figure 7A and B).

Intravenous injection of Δ51 VSV RFP or GFPLuc into C57Bl6 mice bearing B16F10 subcutaneous tumours resulted in minimal viral replication in tumours, as revealed by immunohistochemistry (Figure 18). Interestingly, in 4/4 tumours treated with virus intratumourally, substantially more VSV staining was evident. We have not been able to investigate the reason for this difference, although several possibilities come to mind. Namely, intravenous injection of virus could result in increased production of IFN, which might inhibit the spread of virus in these IFN sensitive tumours. Alternatively, VSV biodistribution might be altered in C57Bl6 mice, such that the liver is a better sink for IV injected VSV than in Balb/C mice. Another possibility is that the vasculature induced by B16 tumours in C57Bl6 mice is somehow not conducive to intravenous delivery of virus. Future experiments will aim to test some of these possibilities by placing B16 tumours in nude Balb/c mice, or by obtaining IFN resistant C57Bl6 tumours to see if they can be better targeted by IV route. Although we were not able to investigate the other tumour models in detail, some preliminary results are presented in Appendix X.

Conclusions and future directions

The overarching hypothesis of this project was that a single IV dose of VSV cannot completely cure mice of CT26 subcutaneous tumours because innate or physiological barriers limit the delivery of VSV, or subsequent spread and tumour killing ability. We have shown that IV delivery indeed probably represents a significant limitation to therapeutic efficacy. Furthermore, whole surface tumour imaging and immunohistochemical observations suggest that delivery of VSV to tumours is not uniform; rather virus often appears to be preferentially targeted to the tumour rim.

It would be useful in the future to use other approaches to examine the delivery of VSV to subcutaneous tumours. For example, to get a better idea of the number of tumour cells initially targeted by virus, one could treat mice with the non-replicating WT VSV GFP, enzymatically disperse tumours, and then quantify the number of GFP positive cells by flow cytometry. Furthermore, one could simultaneously label endothelial cells with an antibody to determine if these are the first cells targeted by VSV, or if VSV can pass directly through the endothelium to infect tumour cells . It will also be interesting to investigate delivery of virus to CT26 lung metastases. If indeed virus is delivered better to these tumours, that could provide us with some insight into what is controlling the delivery of VSV.

With respect to the observed heterogeneous spatial delivery of VSV to subcutaneous tumours, several important experiments come to mind. Firstly, if vascular leakiness is actually a crucial factor in determining where VSV initiates replication in tumours, then perhaps we could co-localize sites of VSV delivery with sites of vascular leakage to macromolecular tracers, such as fluorescent

microspheres. Another approach would be to perform more detailed immunohistochemical studies of tumours, staining for components of the extracellular matrix, or other tumour stromal structures.

Another area of future research could be in improving the delivery of VSV to subcutaneous or other tumours. If vascular leakiness does indeed play a role, then perhaps increasing tumour vascular permeability would improve the delivery of VSV. Along these lines, it was reported that local induction of tumour hyperthermia could improve intravenous delivery of oncolytic Vaccinia virus to subcutaneous tumours by more than 100 fold (178). This virus is several times larger than VSV, so vascular leakiness may be even more important for the intravenous delivery of this virus.

Another goal of the current research was to characterize the spread of VSV within tumours, and any possible barriers to that spread. It was found that viral titres increase dramatically in tumours over time, but immunohistochemical studies showed that VSV remained mostly near the tumour rim, while apoptosis was induced in the tumour core. This bystander effect could limit the spread of virus to the tumour core, but it could also contribute to increased overall tumour cell killing. A more thorough examination of tumour sections at later time points after VSV therapy, perhaps with the aid of a professional pathologist, might be able to provide some clues as to factors that could limit the spread of VSV within tumours.

Other researchers have suggested that the normal tumour stroma may limit the spread of oncolytic viruses. For example, intratumourally injected wild type adenovirus was found to persist within highly susceptible subcutaneous tumours in immunodeficient mice for more than 100 days without eliminating the tumour (179). Histological examination of these static tumours revealed that virus was present in a

"patchy and uneven distribution", with most of the virus "wedged between necrotic tumour tissue and the connective tissue component of the tumour" (179). As such, uninfected viable tumour tissue was observed to be separated from infected areas of the tumour by normal connective tissue (179). Although the 100 day virus persistence would probably not happen in immune competent animals, the barriers to virus spread identified may still be relevant. Normal tumour stromal cells would not be expected to be permissive to VSV infection after the induction of protective systemic IFN, thus it would be interesting to investigate the role of the normal tumour stroma in the spread of VSV. One approach that may prove fruitful is the placement of MT1A2 tumours into readily available GFP transgenic FVBN mice (180). Treatment of these animals with an RFP expressing virus could permit the identification of clear relationships between host tissue and virus spread.

Another goal of the current research was to determine why multiple dosing seems to be required for generating complete cures in the subcutaneous CT26 model. While we did not answer this question, we did find that in the dosing regimen employed, doses after the first likely result in only minimal direct virus mediated killing. Thus, either a minimal amount of virus replication is required for the effect of multiple dose-mediated curing, or alternatively, multiple dosing stimulates some indirect anti-tumour effect. The latter possibility fits with the observation that a single dose of VSV induces significant bystander tumour cell killing. While we have not examined the acquired immune response to virus in these acute experiments, it is certainly also possible that multiple dosing stimulates anti-tumour immunity in a way that single dosing does not, and perhaps this is what leads to durable cancer

cures. Experiments comparing multiple dosing in immune deficient and immune competent mice could also shed some light on this phenomenon.

With respect to the mechanism of multiple dose inhibition, it would be interesting to see if lack of perfusion correlates with lack of virus delivery by simultaneously assessing delivery of the second dose of virus and blood flow tracers. Besides this, it would certainly be useful to perform other multiple dosing experiments, for example using UV inactivated or G-less virus, a lower dose of virus, completely different viruses, and intratumourally administered first dose of virus.

Further research will also need to be done to clarify the role of tumour blood flow in VSV induced bystander tumour killing, as discussed above. However other approaches to this phenomenon are certainly warranted. For example, we could use antibodies to deplete mice of some of the candidate bystander effect mediators discussed above (ie TNFα and Type I IFN).

References

1. 2004. Canadian Cancer Statistics 2004. Canadian Cancer Society.
2. Alison, M.R., Sarraf, C.E. 1997. Introduction to cancer. *In* Understanding Cancer : From Basic Science to Clinical Practice. Cambridge University Press, New York. 1-36.
3. Alison, M.S., Sarraf, C.E. 1997. Cancer Treatment. *In* Understanding Cancer : From Basic Science to Clinical Practice. Cambridge University Press, New York. 205-227.
4. Jain, R.K. 2001. Delivery of molecular medicine to solid tumors: lessons from in vivo imaging of gene expression and function. *J Control Release* 74:7-25.
5. Sinkovics, J., and J. Horvath. 1993. New developments in the virus therapy of cancer: a historical review. *Intervirology* 36:193-214.
6. Lindenmann, J., Klein, P.A. 1967. Immunological Aspects of Viral Oncolysis. *Recent Results in Cancer Research* 9.
7. Levaditi, C., Haber, P. 1937. Recherches sur le virus de la peste aviare pathogene pour la souris. Ses affinites pour les neoplasmes. *Revue d'immunologie* 3.
8. Cassel, W.A., and R.E. Garrett. 1965. Newcastle Disease Virus as an Antineoplastic Agent. *Cancer* 18:863-868.
9. Cassel, W.A., and R.E. Garrett. 1966. Tumor immunity after viral oncolysis. *J Bacteriol* 92:792.
10. Sinkovics, J.G., and C.D. Howe. 1969. Superinfection of tumors with viruses. *Experientia* 25:733-734.
11. Hakkinen, I., and P. Halonen. 1971. Induction of tumor immunity in mice with antigens prepared from influenza and vesicular stomatitis virus grown in suspension culture of Ehrlich ascites cells. *J Natl Cancer Inst* 46:1161-1167.
12. Southam, C.M., and A.E. Moore. 1952. Clinical studies of viruses as antineoplastic agents with particular reference to Egypt 101 virus. *Cancer* 5:1025-1034.
13. Cassel, W.A., and D.R. Murray. 1992. A ten-year follow-up on stage II malignant melanoma patients treated postsurgically with Newcastle disease virus oncolysate. *Med Oncol Tumor Pharmacother* 9:169-171.
14. Okuno, Y., T. Asada, K. Yamanishi, T. Otsuka, M. Takahashi, T. Tanioka, H. Aoyama, O. Fukui, K. Matsumoto, F. Uemura, and A. Wada. 1978. Studies on the use of mumps virus for treatment of human cancer. *Biken J* 21:37-49.
15. Kenney, S., and J.S. Pagano. 1994. Viruses as oncolytic agents: a new age for "therapeutic" viruses? *J Natl Cancer Inst* 86:1185-1186.
16. Nelson, N.J. 1999. Scientific interest in Newcastle disease virus is reviving. *J Natl Cancer Inst* 91:1708-1710.
17. Martuza, R.L., A. Malick, J.M. Markert, K.L. Ruffner, and D.M. Coen. 1991. Experimental therapy of human glioma by means of a genetically engineered virus mutant. *Science* 252:854-856.
18. Bischoff, J.R., D.H. Kirn, A. Williams, C. Heise, S. Horn, M. Muna, L. Ng, J.A. Nye, A. Sampson-Johannes, A. Fattaey, and F. McCormick. 1996. An adenovirus mutant that replicates selectively in p53-deficient human tumor cells. *Science* 274:373-376.

19. McCart, J.A., J.M. Ward, J. Lee, Y. Hu, H.R. Alexander, S.K. Libutti, B. Moss, and D.L. Bartlett. 2001. Systemic cancer therapy with a tumor-selective vaccinia virus mutant lacking thymidine kinase and vaccinia growth factor genes. *Cancer Res* 61:8751-8757.
20. Bergmann, M., I. Romirer, M. Sachet, R. Fleischhacker, A. Garcia-Sastre, P. Palese, K. Wolff, H. Pehamberger, R. Jakesz, and T. Muster. 2001. A genetically engineered influenza A virus with ras-dependent oncolytic properties. *Cancer Res* 61:8188-8193.
21. Randazzo, B.P., S. Kesari, R.M. Gesser, D. Alsop, J.C. Ford, S.M. Brown, A. Maclean, and N.W. Fraser. 1995. Treatment of experimental intracranial murine melanoma with a neuroattenuated herpes simplex virus 1 mutant. *Virology* 211:94-101.
22. Lorence, R.M., K.W. Reichard, B.B. Katubig, H.M. Reyes, A. Phuangsab, B.R. Mitchell, C.J. Cascino, R.J. Walter, and M.E. Peeples. 1994. Complete regression of human neuroblastoma xenografts in athymic mice after local Newcastle disease virus therapy. *J Natl Cancer Inst* 86:1228-1233.
23. Lorence, R.M., B.B. Katubig, K.W. Reichard, H.M. Reyes, A. Phuangsab, M.D. Sassetti, R.J. Walter, and M.E. Peeples. 1994. Complete regression of human fibrosarcoma xenografts after local Newcastle disease virus therapy. *Cancer Res* 54:6017-6021.
24. Strong, J.E., M.C. Coffey, D. Tang, P. Sabinin, and P.W. Lee. 1998. The molecular basis of viral oncolysis: usurpation of the Ras signaling pathway by reovirus. *Embo J* 17:3351-3362.
25. Coffey, M.C., J.E. Strong, P.A. Forsyth, and P.W. Lee. 1998. Reovirus therapy of tumors with activated Ras pathway. *Science* 282:1332-1334.
26. Stojdl, D.F., B. Lichty, S. Knowles, R. Marius, H. Atkins, N. Sonenberg, and J.C. Bell. 2000. Exploiting tumor-specific defects in the interferon pathway with a previously unknown oncolytic virus. *Nat Med* 6:821-825.
27. Stojdl, D.F., B.D. Lichty, B.R. tenOever, J.M. Paterson, A.T. Power, S. Knowles, R. Marius, J. Reynard, L. Poliquin, H. Atkins, E.G. Brown, R.K. Durbin, J.E. Durbin, J. Hiscott, and J.C. Bell. 2003. VSV strains with defects in their ability to shutdown innate immunity are potent systemic anti-cancer agents. *Cancer Cell* 4:263-275.
28. Wagner, R.W.a.J.K.R. 1996. Rhabdoviridae: The viruses and their replication. *In* Fields Virology. B.N. Fields, Knipe, D.M., Howley, P.M. et al., editor. Raven Publishers, Philadelphia. 1121-1132.
29. Qanungo, K.R., D. Shaji, M. Mathur, and A.K. Banerjee. 2004. Two RNA polymerase complexes from vesicular stomatitis virus-infected cells that carry out transcription and replication of genome RNA. *Proc Natl Acad Sci U S A* 101:5952-5957.
30. Ahmed, M., M.O. McKenzie, S. Puckett, M. Hojnacki, L. Poliquin, and D.S. Lyles. 2003. Ability of the matrix protein of vesicular stomatitis virus to suppress beta interferon gene expression is genetically correlated with the inhibition of host RNA and protein synthesis. *J Virol* 77:4646-4657.
31. Lyles, D.S., M.O. McKenzie, M. Ahmed, and S.C. Woolwine. 1996. Potency of wild-type and temperature-sensitive vesicular stomatitis virus matrix protein in the inhibition of host-directed gene expression. *Virology* 225:172-180.

32. Howatson, A.F. 1970. Vesicular stomatitis and related viruses. *Adv Virus Res* 16:195-256.
33. Letchworth, G.J., L.L. Rodriguez, and J. Del cbarrera. 1999. Vesicular stomatitis. *Vet J* 157:239-260.
34. Rodriguez, L.L. 2002. Emergence and re-emergence of vesicular stomatitis in the United States. *Virus Res* 85:211-219.
35. Mead, D.G., F.B. Ramberg, D.G. Besselsen, and C.J. Mare. 2000. Transmission of vesicular stomatitis virus from infected to noninfected black flies co-feeding on nonviremic deer mice. *Science* 287:485-487.
36. Mead, D.G., E.W. Gray, R. Noblet, M.D. Murphy, E.W. Howerth, and D.E. Stallknecht. 2004. Biological transmission of vesicular stomatitis virus (New Jersey serotype) by Simulium vittatum (Diptera: Simuliidae) to domestic swine (Sus scrofa). *J Med Entomol* 41:78-82.
37. Isaacs, A., and J. Lindenmann. 1957. Virus interference. I. The interferon. *Proc R Soc Lond B Biol Sci* 147:258-267.
38. Foster, G.R., and N.B. Finter. 1998. Are all type I human interferons equivalent? *J Viral Hepat* 5:143-152.
39. Roberts, R.M., L. Liu, Q. Guo, D. Leaman, and J. Bixby. 1998. The evolution of the type I interferons. *J Interferon Cytokine Res* 18:805-816.
40. van den Broek, M.F., U. Muller, S. Huang, R.M. Zinkernagel, and M. Aguet. 1995. Immune defence in mice lacking type I and/or type II interferon receptors. *Immunol Rev* 148:5-18.
41. Stewart, W.E. 1981. The interferon system. Springer-Verlag, New York. 493 pp.
42. Sato, M., N. Hata, M. Asagiri, T. Nakaya, T. Taniguchi, and N. Tanaka. 1998. Positive feedback regulation of type I IFN genes by the IFN-inducible transcription factor IRF-7. *FEBS Lett* 441:106-110.
43. Sato, M., H. Suemori, N. Hata, M. Asagiri, K. Ogasawara, K. Nakao, T. Nakaya, M. Katsuki, S. Noguchi, N. Tanaka, and T. Taniguchi. 2000. Distinct and essential roles of transcription factors IRF-3 and IRF-7 in response to viruses for IFN-alpha/beta gene induction. *Immunity* 13:539-548.
44. Marie, I., J.E. Durbin, and D.E. Levy. 1998. Differential viral induction of distinct interferon-alpha genes by positive feedback through interferon regulatory factor-7. *Embo J* 17:6660-6669.
45. de Veer, M.J., M. Holko, M. Frevel, E. Walker, S. Der, J.M. Paranjape, R.H. Silverman, and B.R. Williams. 2001. Functional classification of interferon-stimulated genes identified using microarrays. *J Leukoc Biol* 69:912-920.
46. Espert, L., G. Degols, C. Gongora, D. Blondel, B.R. Williams, R.H. Silverman, and N. Mechti. 2003. ISG20, a new interferon-induced RNase specific for single-stranded RNA, defines an alternative antiviral pathway against RNA genomic viruses. *J Biol Chem* 278:16151-16158.
47. Hui, D.J., C.R. Bhasker, W.C. Merrick, and G.C. Sen. 2003. Viral stress-inducible protein p56 inhibits translation by blocking the interaction of eIF3 with the ternary complex eIF2.GTP.Met-tRNAi. *J Biol Chem* 278:39477-39482.
48. Stojdl, D.F., N. Abraham, S. Knowles, R. Marius, A. Brasey, B.D. Lichty, E.G. Brown, N. Sonenberg, and J.C. Bell. 2000. The murine double-stranded RNA-dependent protein kinase PKR is required for resistance to vesicular stomatitis virus. *J Virol* 74:9580-9585.

49. Zhou, A., J. Paranjape, T.L. Brown, H. Nie, S. Naik, B. Dong, A. Chang, B. Trapp, R. Fairchild, C. Colmenares, and R.H. Silverman. 1997. Interferon action and apoptosis are defective in mice devoid of 2',5'-oligoadenylate-dependent RNase L. *Embo J* 16:6355-6363.
50. Nakaya, T., M. Sato, N. Hata, M. Asagiri, H. Suemori, S. Noguchi, N. Tanaka, and T. Taniguchi. 2001. Gene induction pathways mediated by distinct IRFs during viral infection. *Biochem Biophys Res Commun* 283:1150-1156.
51. Grandvaux, N., M.J. Servant, B. tenOever, G.C. Sen, S. Balachandran, G.N. Barber, R. Lin, and J. Hiscott. 2002. Transcriptional profiling of interferon regulatory factor 3 target genes: direct involvement in the regulation of interferon-stimulated genes. *J Virol* 76:5532-5539.
52. Hata, N., M. Sato, A. Takaoka, M. Asagiri, N. Tanaka, and T. Taniguchi. 2001. Constitutive IFN-alpha/beta signal for efficient IFN-alpha/beta gene induction by virus. *Biochem Biophys Res Commun* 285:518-525.
53. Izaguirre, A., B.J. Barnes, S. Amrute, W.S. Yeow, N. Megjugorac, J. Dai, D. Feng, E. Chung, P.M. Pitha, and P. Fitzgerald-Bocarsly. 2003. Comparative analysis of IRF and IFN-alpha expression in human plasmacytoid and monocyte-derived dendritic cells. *J Leukoc Biol* 74:1125-1138.
54. Barchet, W., M. Cella, B. Odermatt, C. Asselin-Paturel, M. Colonna, and U. Kalinke. 2002. Virus-induced interferon alpha production by a dendritic cell subset in the absence of feedback signaling in vivo. *J Exp Med* 195:507-516.
55. Levy, D.E., I. Marie, and A. Prakash. 2003. Ringing the interferon alarm: differential regulation of gene expression at the interface between innate and adaptive immunity. *Curr Opin Immunol* 15:52-58.
56. Fitzgerald, K.A., S.M. McWhirter, K.L. Faia, D.C. Rowe, E. Latz, D.T. Golenbock, A.J. Coyle, S.M. Liao, and T. Maniatis. 2003. IKKepsilon and TBK1 are essential components of the IRF3 signaling pathway. *Nat Immunol* 4:491-496.
57. Sharma, S., B.R. tenOever, N. Grandvaux, G.P. Zhou, R. Lin, and J. Hiscott. 2003. Triggering the interferon antiviral response through an IKK-related pathway. *Science* 300:1148-1151.
58. Hemmi, H., O. Takeuchi, S. Sato, M. Yamamoto, T. Kaisho, H. Sanjo, T. Kawai, K. Hoshino, K. Takeda, and S. Akira. 2004. The Roles of Two IkappaB Kinase-related Kinases in Lipopolysaccharide and Double Stranded RNA Signaling and Viral Infection. *J Exp Med* 199:1641-1650.
59. Diebold, S.S., T. Kaisho, H. Hemmi, S. Akira, and C. Reis e Sousa. 2004. Innate antiviral responses by means of TLR7-mediated recognition of single-stranded RNA. *Science* 303:1529-1531.
60. Heil, F., H. Hemmi, H. Hochrein, F. Ampenberger, C. Kirschning, S. Akira, G. Lipford, H. Wagner, and S. Bauer. 2004. Species-specific recognition of single-stranded RNA via toll-like receptor 7 and 8. *Science* 303:1526-1529.
61. Lund, J.M., L. Alexopoulou, A. Sato, M. Karow, N.C. Adams, N.W. Gale, A. Iwasaki, and R.A. Flavell. 2004. Recognition of single-stranded RNA viruses by Toll-like receptor 7. *Proc Natl Acad Sci U S A* 101:5598-5603.
62. Edelmann, K.H., S. Richardson-Burns, L. Alexopoulou, K.L. Tyler, R.A. Flavell, and M.B. Oldstone. 2004. Does Toll-like receptor 3 play a biological role in virus infections? *Virology* 322:231-238.
63. Francoeur, A.M., T. Lam, and C.P. Stanners. 1980. PIF, a highly sensitive plaque assay for the induction of interferon. *Virology* 105:526-536.

64. Marcus, P.I., L.L. Rodriguez, and M.J. Sekellick. 1998. Interferon induction as a quasispecies marker of vesicular stomatitis virus populations. *J Virol* 72:542-549.
65. Marcus, P.I., and M.J. Sekellick. 1994. Interferon induction: regulation by both virus and cell. *Hokkaido Igaku Zasshi* 69:1320-1331.
66. Muller, I., P. Kropf, J.A. Louis, and G. Milon. 1994. Expansion of gamma interferon-producing CD8+ T cells following secondary infection of mice immune to Leishmania major. *Infect Immun* 62:2575-2581.
67. Williams, B.R.G., Fish, E.N. 1985. Interferon and viruses: in vitro studies. *In* Interferons, their impact in biology and medicine. J. Taylor-Papadimitriou, editor. Oxford University Press, Oxford. 40-60.
68. Stanwick, T.L., R.F. Schinazi, D.E. Campbell, and A.J. Nahmias. 1981. Combined antiviral effect of interferon and acyclovir on herpes simplex virus types 1 and 2. *Antimicrob Agents Chemother* 19:672-674.
69. Chawla-Sarkar, M., D.J. Lindner, Y.F. Liu, B.R. Williams, G.C. Sen, R.H. Silverman, and E.C. Borden. 2003. Apoptosis and interferons: role of interferon-stimulated genes as mediators of apoptosis. *Apoptosis* 8:237-249.
70. Gresser, I., C. Bourali, J.P. Levy, D. Fontaine-Brouty-Boye, and M.T. Thomas. 1969. Increased survival in mice inoculated with tumor cells and treated with interferon preparations. *Proc Natl Acad Sci U S A* 63:51-57.
71. Ruddon, R.W. 1995. Tumor immunology: Immunologic approaches to the diagnosis and treatment of cancer. *In* Cancer biology. Oxford University Press, New York. 442-475.
72. Gresser, I., F. Belardelli, C. Maury, M.T. Maunoury, and M.G. Tovey. 1983. Injection of mice with antibody to interferon enhances the growth of transplantable murine tumors. *J Exp Med* 158:2095-2107.
73. Picaud, S., B. Bardot, E. De Maeyer, and I. Seif. 2002. Enhanced tumor development in mice lacking a functional type I interferon receptor. *J Interferon Cytokine Res* 22:457-462.
74. Kaido, T., M.T. Bandu, C. Maury, M. Ferrantini, F. Belardelli, and I. Gresser. 1995. IFN-alpha 1 gene transfection completely abolishes the tumorigenicity of murine B16 melanoma cells in allogeneic DBA/2 mice and decreases their tumorigenicity in syngeneic C57BL/6 mice. *Int J Cancer* 60:221-229.
75. Colamonici, O.R., B. Porterfield, P. Domanski, R.K. Handa, S. Flex, C.E. Samuel, R. Pine, and M.O. Diaz. 1994. Ligand-independent anti-oncogenic activity of the alpha subunit of the type I interferon receptor. *J Biol Chem* 269:27275-27279.
76. Duguay, D., F. Mercier, J. Stagg, D. Martineau, J. Bramson, M. Servant, R. Lin, J. Galipeau, and J. Hiscott. 2002. In vivo interferon regulatory factor 3 tumor suppressor activity in B16 melanoma tumors. *Cancer Res* 62:5148-5152.
77. Yim, J.H., S.J. Wu, M.J. Casey, J.A. Norton, and G.M. Doherty. 1997. IFN regulatory factor-1 gene transfer into an aggressive, nonimmunogenic sarcoma suppresses the malignant phenotype and enhances immunogenicity in syngeneic mice. *J Immunol* 158:1284-1292.
78. Willman, C.L., C.E. Sever, M.G. Pallavicini, H. Harada, N. Tanaka, M.L. Slovak, H. Yamamoto, K. Harada, T.C. Meeker, A.F. List, and et al. 1993. Deletion of IRF-1, mapping to chromosome 5q31.1, in human leukemia and preleukemic myelodysplasia. *Science* 259:968-971.

79. Diaz, M.O., C.M. Rubin, A. Harden, S. Ziemin, R.A. Larson, M.M. Le Beau, and J.D. Rowley. 1990. Deletions of interferon genes in acute lymphoblastic leukemia. *N Engl J Med* 322:77-82.
80. Ambrus, J.L., Sr., W. Dembinski, J.L. Ambrus, Jr., D.E. Sykes, S. Akhter, M.N. Kulaylat, A. Islam, and K.C. Chadha. 2003. Free interferon-alpha/beta receptors in the circulation of patients with adenocarcinoma. *Cancer* 98:2730-2733.
81. Meurs, E.F., J. Galabru, G.N. Barber, M.G. Katze, and A.G. Hovanessian. 1993. Tumor suppressor function of the interferon-induced double-stranded RNA-activated protein kinase. *Proc Natl Acad Sci U S A* 90:232-236.
82. Barber, G.N., S. Thompson, T.G. Lee, T. Strom, R. Jagus, A. Darveau, and M.G. Katze. 1994. The 58-kilodalton inhibitor of the interferon-induced double-stranded RNA-activated protein kinase is a tetratricopeptide repeat protein with oncogenic properties. *Proc Natl Acad Sci U S A* 91:4278-4282.
83. Hii, S.I., L. Hardy, T. Crough, E.J. Payne, K. Grimmett, D. Gill, and N.A. McMillan. 2004. Loss of PKR activity in chronic lymphocytic leukemia. *Int J Cancer* 109:329-335.
84. Wong, L.H., K.G. Krauer, I. Hatzinisiriou, M.J. Estcourt, P. Hersey, N.D. Tam, S. Edmondson, R.J. Devenish, and S.J. Ralph. 1997. Interferon-resistant human melanoma cells are deficient in ISGF3 components, STAT1, STAT2, and p48-ISGF3gamma. *J Biol Chem* 272:28779-28785.
85. Carpten, J., N. Nupponen, S. Isaacs, R. Sood, C. Robbins, J. Xu, M. Faruque, T. Moses, C. Ewing, E. Gillanders, P. Hu, P. Bujnovszky, I. Makalowska, A. Baffoe-Bonnie, D. Faith, J. Smith, D. Stephan, K. Wiley, M. Brownstein, D. Gildea, B. Kelly, R. Jenkins, G. Hostetter, M. Matikainen, J. Schleutker, K. Klinger, T. Connors, Y. Xiang, Z. Wang, A. De Marzo, N. Papadopoulos, O.P. Kallioniemi, R. Burk, D. Meyers, H. Gronberg, P. Meltzer, R. Silverman, J. Bailey-Wilson, P. Walsh, W. Isaacs, and J. Trent. 2002. Germline mutations in the ribonuclease L gene in families showing linkage with HPC1. *Nat Genet* 30:181-184.
86. Ding, Y., L. Wang, L.K. Su, J.A. Frey, R. Shao, K.K. Hunt, and D.H. Yan. 2004. Antitumor activity of IFIX, a novel interferon-inducible HIN-200 gene, in breast cancer. *Oncogene* 23:4556-4566.
87. Takaoka, A., S. Hayakawa, H. Yanai, D. Stoiber, H. Negishi, H. Kikuchi, S. Sasaki, K. Imai, T. Shibue, K. Honda, and T. Taniguchi. 2003. Integration of interferon-alpha/beta signalling to p53 responses in tumour suppression and antiviral defence. *Nature* 424:516-523.
88. Balachandran, S., and G.N. Barber. 2000. Vesicular stomatitis virus (VSV) therapy of tumors. *IUBMB Life* 50:135-138.
89. Balachandran, S., M. Porosnicu, and G.N. Barber. 2001. Oncolytic activity of vesicular stomatitis virus is effective against tumors exhibiting aberrant p53, Ras, or myc function and involves the induction of apoptosis. *J Virol* 75:3474-3479.
90. Lawson, N.D., E.A. Stillman, M.A. Whitt, and J.K. Rose. 1995. Recombinant vesicular stomatitis viruses from DNA. *Proc Natl Acad Sci U S A* 92:4477-4481.
91. Fernandez, M., M. Porosnicu, D. Markovic, and G.N. Barber. 2002. Genetically engineered vesicular stomatitis virus in gene therapy: application for treatment of malignant disease. *J Virol* 76:895-904.

92. Okada, H., and N. Kuwashima. 2002. Gene therapy and biologic therapy with interleukin-4. *Curr Gene Ther* 2:437-450.
93. Fillat, C., M. Carrio, A. Cascante, and B. Sangro. 2003. Suicide gene therapy mediated by the Herpes Simplex virus thymidine kinase gene/Ganciclovir system: fifteen years of application. *Curr Gene Ther* 3:13-26.
94. Porosnicu, M., A. Mian, and G.N. Barber. 2003. The oncolytic effect of recombinant vesicular stomatitis virus is enhanced by expression of the fusion cytosine deaminase/uracil phosphoribosyltransferase suicide gene. *Cancer Res* 63:8366-8376.
95. Ebert, O., K. Shinozaki, C. Kournioti, M.S. Park, A. Garcia-Sastre, and S.L. Woo. 2004. Syncytia induction enhances the oncolytic potential of vesicular stomatitis virus in virotherapy for cancer. *Cancer Res* 64:3265-3270.
96. Francoeur, A.M., L. Poliquin, and C.P. Stanners. 1987. The isolation of interferon-inducing mutants of vesicular stomatitis virus with altered viral P function for the inhibition of total protein synthesis. *Virology* 160:236-245.
97. Farmilo, A.J., and C.P. Stanners. 1972. Mutant of vesicular stomatitis virus which allows deoxyribonucleic acid synthesis and division in cells synthesizing viral ribonucleic acid. *J Virol* 10:605-613.
98. Desforges, M., J. Charron, S. Berard, S. Beausoleil, D.F. Stojdl, G. Despars, B. Laverdiere, J.C. Bell, P.J. Talbot, C.P. Stanners, and L. Poliquin. 2001. Different host-cell shutoff strategies related to the matrix protein lead to persistence of vesicular stomatitis virus mutants on fibroblast cells. *Virus Res* 76:87-102.
99. Terstegen, L., P. Gatsios, S. Ludwig, S. Pleschka, W. Jahnen-Dechent, P.C. Heinrich, and L. Graeve. 2001. The vesicular stomatitis virus matrix protein inhibits glycoprotein 130-dependent STAT activation. *J Immunol* 167:5209-5216.
100. Ferran, M.C., and J.M. Lucas-Lenard. 1997. The vesicular stomatitis virus matrix protein inhibits transcription from the human beta interferon promoter. *J Virol* 71:371-377.
101. von Kobbe, C., J.M. van Deursen, J.P. Rodrigues, D. Sitterlin, A. Bachi, X. Wu, M. Wilm, M. Carmo-Fonseca, and E. Izaurralde. 2000. Vesicular stomatitis virus matrix protein inhibits host cell gene expression by targeting the nucleoporin Nup98. *Mol Cell* 6:1243-1252.
102. Obuchi, M., M. Fernandez, and G.N. Barber. 2003. Development of recombinant vesicular stomatitis viruses that exploit defects in host defense to augment specific oncolytic activity. *J Virol* 77:8843-8856.
103. Schnell, M.J., L. Buonocore, M.A. Whitt, and J.K. Rose. 1996. The minimal conserved transcription stop-start signal promotes stable expression of a foreign gene in vesicular stomatitis virus. *J Virol* 70:2318-2323.
104. Campbell, R.E., O. Tour, A.E. Palmer, P.A. Steinbach, G.S. Baird, D.A. Zacharias, and R.Y. Tsien. 2002. A monomeric red fluorescent protein. *Proc Natl Acad Sci U S A* 99:7877-7882.
105. Keirnan, J.A. 1999. Histological staining in one or two colours. *In* Histological & histochemical methods : theory and practice. Pergamon Press, Oxford, England.
106. Lehr, H.A., C.M. van der Loos, P. Teeling, and A.M. Gown. 1999. Complete chromogen separation and analysis in double immunohistochemical stains using Photoshop-based image analysis. *J Histochem Cytochem* 47:119-126.

107. Emeny, J.M., and M.J. Morgan. 1979. Regulation of the interferon system: evidence that Vero cells have a genetic defect in interferon production. *J Gen Virol* 43:247-252.
108. Shrayer, D., H. Bogaars, V.J. Hearing, A. Maizel, and H. Wanebo. 1995. Further characterization of a clinically relevant model of melanoma metastasis and an effective vaccine. *Cancer Immunol Immunother* 40:277-282.
109. Thomas, D.L., and N.W. Fraser. 2003. HSV-1 therapy of primary tumors reduces the number of metastases in an immune-competent model of metastatic breast cancer. *Mol Ther* 8:543-551.
110. Edwards, P., J.C. Cendan, D.B. Topping, L.L. Moldawer, S. MacKay, E. Copeland, and D.S. Lind. 1996. Tumor cell nitric oxide inhibits cell growth in vitro, but stimulates tumorigenesis and experimental lung metastasis in vivo. *J Surg Res* 63:49-52.
111. Addison, C.L., T. Braciak, R. Ralston, W.J. Muller, J. Gauldie, and F.L. Graham. 1995. Intratumoral injection of an adenovirus expressing interleukin 2 induces regression and immunity in a murine breast cancer model. *Proc Natl Acad Sci U S A* 92:8522-8526.
112. Lorence, R.M., A.L. Pecora, P.P. Major, S.J. Hotte, S.A. Laurie, M.S. Roberts, W.S. Groene, and M.K. Bamat. 2003. Overview of phase I studies of intravenous administration of PV701, an oncolytic virus. *Curr Opin Mol Ther* 5:618-624.
113. Stadelmann, C., and H. Lassmann. 2000. Detection of apoptosis in tissue sections. *Cell Tissue Res* 301:19-31.
114. Porter, A.G., and R.U. Janicke. 1999. Emerging roles of caspase-3 in apoptosis. *Cell Death Differ* 6:99-104.
115. Springer, M.L., T.K. Ip, and H.M. Blau. 2000. Angiogenesis monitored by perfusion with a space-filling microbead suspension. *Mol Ther* 1:82-87.
116. Pogue, B.W., K.D. Paulsen, J.A. O'Hara, C.M. Wilmot, and H.M. Swartz. 2001. Estimation of oxygen distribution in RIF-1 tumors by diffusion model-based interpretation of pimonidazole hypoxia and eppendorf measurements. *Radiat Res* 155:15-25.
117. Churchland, P. 1996. Circulation and gas exchange. *In* Biology. N.A. Campbell, editor. The Benjamin / Cummings Publishing Company, Inc.
118. Hobbs, S.K., W.L. Monsky, F. Yuan, W.G. Roberts, L. Griffith, V.P. Torchilin, and R.K. Jain. 1998. Regulation of transport pathways in tumor vessels: role of tumor type and microenvironment. *Proc Natl Acad Sci U S A* 95:4607-4612.
119. Kirn, A., J.P. Gut, and J.L. Gendrault. 1982. Interaction of viruses with sinusoidal cells. *Prog Liver Dis* 7:377-392.
120. Brunner, K.T., D. Hurez, C.R. Mc, and B. Benacerraf. 1960. Blood clearance of P32-labeled vesicular stomatitis and Newcastle disease viruses by the reticuloendothelial system in mice. *J Immunol* 85:99-105.
121. Schellingerhout, D., A. Bogdanov, Jr., E. Marecos, M. Spear, X. Breakefield, and R. Weissleder. 1998. Mapping the in vivo distribution of herpes simplex virions. *Hum Gene Ther* 9:1543-1549.
122. Verdin, E.M., S.P. Lynn, B.N. Fields, and E. Maratos-Flier. 1988. Uptake of reovirus serotype 1 by the lungs from the bloodstream is mediated by the viral hemagglutinin. *J Virol* 62:545-551.

123. Steffan, A.M. 1997. [Hepatic macrophages and virus]. *Pathol Biol (Paris)* 45:169-183.
124. Zhang, L., P.J. Dailey, A. Gettie, J. Blanchard, and D.D. Ho. 2002. The liver is a major organ for clearing simian immunodeficiency virus in rhesus monkeys. *J Virol* 76:5271-5273.
125. Alemany, R., K. Suzuki, and D.T. Curiel. 2000. Blood clearance rates of adenovirus type 5 in mice. *J Gen Virol* 81:2605-2609.
126. Green, N.K., C.W. Herbert, S.J. Hale, A.B. Hale, V. Mautner, R. Harkins, T. Hermiston, K. Ulbrich, K.D. Fisher, and L.W. Seymour. 2004. Extended plasma circulation time and decreased toxicity of polymer-coated adenovirus. *Gene Ther*.
127. Ogawara, K., K. Furumoto, Y. Takakura, M. Hashida, K. Higaki, and T. Kimura. 2001. Surface hydrophobicity of particles is not necessarily the most important determinant in their in vivo disposition after intravenous administration in rats. *J Control Release* 77:191-198.
128. Papahadjopoulos, D., and A. Gabizon. 1987. Targeting of liposomes to tumor cells in vivo. *Ann N Y Acad Sci* 507:64-74.
129. Green, N.K., and L.W. Seymour. 2002. Adenoviral vectors: systemic delivery and tumor targeting. *Cancer Gene Ther* 9:1036-1042.
130. Ochsenbein, A.F., T. Fehr, C. Lutz, M. Suter, F. Brombacher, H. Hengartner, and R.M. Zinkernagel. 1999. Control of early viral and bacterial distribution and disease by natural antibodies. *Science* 286:2156-2159.
131. Wakimoto, H., K. Ikeda, T. Abe, T. Ichikawa, F.H. Hochberg, R.A. Ezekowitz, M.S. Pasternack, and E.A. Chiocca. 2002. The complement response against an oncolytic virus is species-specific in its activation pathways. *Mol Ther* 5:275-282.
132. Tao, N., G.P. Gao, M. Parr, J. Johnston, T. Baradet, J.M. Wilson, J. Barsoum, and S.E. Fawell. 2001. Sequestration of adenoviral vector by Kupffer cells leads to a nonlinear dose response of transduction in liver. *Mol Ther* 3:28-35.
133. McDonald, D.M., and P. Baluk. 2002. Significance of blood vessel leakiness in cancer. *Cancer Res* 62:5381-5385.
134. Kohn, S., J.A. Nagy, H.F. Dvorak, and A.M. Dvorak. 1992. Pathways of macromolecular tracer transport across venules and small veins. Structural basis for the hyperpermeability of tumor blood vessels. *Lab Invest* 67:596-607.
135. Jain, R.K. 2002. Tumor angiogenesis and accessibility: role of vascular endothelial growth factor. *Semin Oncol* 29:3-9.
136. Ludewig, B., K.J. Maloy, C. Lopez-Macias, B. Odermatt, H. Hengartner, and R.M. Zinkernagel. 2000. Induction of optimal anti-viral neutralizing B cell responses by dendritic cells requires transport and release of virus particles in secondary lymphoid organs. *Eur J Immunol* 30:185-196.
137. Dvorak, H.F., J.A. Nagy, J.T. Dvorak, and A.M. Dvorak. 1988. Identification and characterization of the blood vessels of solid tumors that are leaky to circulating macromolecules. *Am J Pathol* 133:95-109.
138. Vile, R., D. Ando, and D. Kirn. 2002. The oncolytic virotherapy treatment platform for cancer: unique biological and biosafety points to consider. *Cancer Gene Ther* 9:1062-1067.

139. Heise, C.C., A.M. Williams, S. Xue, M. Propst, and D.H. Kirn. 1999. Intravenous administration of ONYX-015, a selectively replicating adenovirus, induces antitumoral efficacy. *Cancer Res* 59:2623-2628.
140. Ruddon, R.W. 1995. Alterations of cellular differentiation in cancer. *In* Cancer biology. Oxford University Press, New York. 141-230.
141. Shayakhmetov, D.M., Z.Y. Li, S. Ni, and A. Lieber. 2002. Targeting of adenovirus vectors to tumor cells does not enable efficient transduction of breast cancer metastases. *Cancer Res* 62:1063-1068.
142. Li, Z.Y., S. Ni, X. Yang, N. Kiviat, and A. Lieber. 2004. Xenograft models for liver metastasis: Relationship between tumor morphology and adenovirus vector transduction. *Mol Ther* 9:650-657.
143. Shinozaki, K., O. Ebert, C. Kournioti, Y.S. Tai, and S.L. Woo. 2004. Oncolysis of multifocal hepatocellular carcinoma in the rat liver by hepatic artery infusion of vesicular stomatitis virus. *Mol Ther* 9:368-376.
144. Lombardi, T., R. Montesano, and L. Orci. 1985. Polarized plasma membrane domains in cultured endothelial cells. *Exp Cell Res* 161:242-246.
145. Zaczynska, E., Z. Blach-Olszewska, and E. Gejdel. 1995. Production of cytokines with antiviral activity by endothelial cells. *J Interferon Cytokine Res* 15:811-814.
146. Chang, Y.S., E. di Tomaso, D.M. McDonald, R. Jones, R.K. Jain, and L.L. Munn. 2000. Mosaic blood vessels in tumors: frequency of cancer cells in contact with flowing blood. *Proc Natl Acad Sci U S A* 97:14608-14613.
147. Janeway, C.A., Travers, P., Walport, M., and M.J. Scholmchik. 2001. Innate Immunity. *In* Immunobiology. Garland Publishing, New York. 35-92.
148. Monsky, W.L., D. Fukumura, T. Gohongi, M. Ancukiewcz, H.A. Weich, V.P. Torchilin, F. Yuan, and R.K. Jain. 1999. Augmentation of transvascular transport of macromolecules and nanoparticles in tumors using vascular endothelial growth factor. *Cancer Res* 59:4129-4135.
149. Debbage, P.L., J. Griebel, M. Ried, T. Gneiting, A. DeVries, and P. Hutzler. 1998. Lectin intravital perfusion studies in tumor-bearing mice: micrometer-resolution, wide-area mapping of microvascular labeling, distinguishing efficiently and inefficiently perfused microregions in the tumor. *J Histochem Cytochem* 46:627-639.
150. Heise, C.C., A. Williams, J. Olesch, and D.H. Kirn. 1999. Efficacy of a replication-competent adenovirus (ONYX-015) following intratumoral injection: intratumoral spread and distribution effects. *Cancer Gene Ther* 6:499-504.
151. Grote, D., S.J. Russell, T.I. Cornu, R. Cattaneo, R. Vile, G.A. Poland, and A.K. Fielding. 2001. Live attenuated measles virus induces regression of human lymphoma xenografts in immunodeficient mice. *Blood* 97:3746-3754.
152. Janeway, C.A., Travers, P., Walport, M., and M.J. Scholmchik. 2001. Adaptive Immunity to Infection. *In* Immunobiology. Garland Publishing, New York. 381-424.
153. Palmer, G.A., J.L. Brogdon, S.L. Constant, and P. Tattersall. 2004. A nonproliferating parvovirus vaccine vector elicits sustained, protective humoral immunity following a single intravenous or intranasal inoculation. *J Virol* 78:1101-1108.

154. Ebert, O., K. Shinozaki, T.G. Huang, M.J. Savontaus, A. Garcia-Sastre, and S.L. Woo. 2003. Oncolytic vesicular stomatitis virus for treatment of orthotopic hepatocellular carcinoma in immune-competent rats. *Cancer Res* 63:3605-3611.
155. Schirrmacher, V., Ahlert, T., Heicappel, R., Appelhans, B. and P. von Hoegen. 1986. Successful application on non-oncogenic viruses for antimetastatic cancer immunotherapy. *Cancer Reviews* 5:19-49.
156. Schirrmacher, V., L. Bai, V. Umansky, L. Yu, Y. Xing, and Z. Qian. 2000. Newcastle disease virus activates macrophages for anti-tumor activity. *Int J Oncol* 16:363-373.
157. Janeway, C.A., Travers, P., Walport, M., and M.J. Scholmchik. 2001. T-Cell mediated immunity. *In* Immunobiology. Garland Publishing, New York. 295-340.
158. Washburn, B., M.A. Weigand, A. Grosse-Wilde, M. Janke, H. Stahl, E. Rieser, M.R. Sprick, V. Schirrmacher, and H. Walczak. 2003. TNF-related apoptosis-inducing ligand mediates tumoricidal activity of human monocytes stimulated by Newcastle disease virus. *J Immunol* 170:1814-1821.
159. Vidalain, P.O., O. Azocar, B. Lamouille, A. Astier, C. Rabourdin-Combe, and C. Servet-Delprat. 2000. Measles virus induces functional TRAIL production by human dendritic cells. *J Virol* 74:556-559.
160. Clarke, P., S.M. Meintzer, S. Gibson, C. Widmann, T.P. Garrington, G.L. Johnson, and K.L. Tyler. 2000. Reovirus-induced apoptosis is mediated by TRAIL. *J Virol* 74:8135-8139.
161. Lorence, R.M., P.A. Rood, and K.W. Kelley. 1988. Newcastle disease virus as an antineoplastic agent: induction of tumor necrosis factor-alpha and augmentation of its cytotoxicity. *J Natl Cancer Inst* 80:1305-1312.
162. Bussfeld, D., M. Nain, P. Hofmann, D. Gemsa, and H. Sprenger. 2000. Selective induction of the monocyte-attracting chemokines MCP-1 and IP-10 in vesicular stomatitis virus-infected human monocytes. *J Interferon Cytokine Res* 20:615-621.
163. Tseng, J.C., B. Levin, T. Hirano, H. Yee, C. Pampeno, and D. Meruelo. 2002. In vivo antitumor activity of Sindbis viral vectors. *J Natl Cancer Inst* 94:1790-1802.
164. Grote, D., R. Cattaneo, and A.K. Fielding. 2003. Neutrophils contribute to the measles virus-induced antitumor effect: enhancement by granulocyte macrophage colony-stimulating factor expression. *Cancer Res* 63:6463-6468.
165. Sveinbjornsson, B., C. Rushfeldt, R. Olsen, B. Smedsrod, and R. Seljelid. 1997. Cytotoxic effect of cytokines on murine colon carcinoma cells involves TNF-mediated apoptosis. *Biochem Biophys Res Commun* 233:270-275.
166. Manda, T., K. Shimomura, S. Mukumoto, K. Kobayashi, T. Mizota, O. Hirai, S. Matsumoto, T. Oku, F. Nishigaki, J. Mori, and et al. 1987. Recombinant human tumor necrosis factor-alpha: evidence of an indirect mode of antitumor activity. *Cancer Res* 47:3707-3711.
167. Tsutsumi, Y., S. Tsunoda, Y. Kaneda, H. Kamada, T. Kihira, S. Nakagawa, Y. Yamamoto, Y. Horisawa, and T. Mayumi. 1996. In vivo anti-tumor efficacy of polyethylene glycol-modified tumor necrosis factor-alpha against tumor necrosis factor-resistant tumors. *Jpn J Cancer Res* 87:1078-1085.

168. Mahadevan, V., S.T. Malik, A. Meager, W. Fiers, G.P. Lewis, and I.R. Hart. 1990. Role of tumor necrosis factor in flavone acetic acid-induced tumor vasculature shutdown. *Cancer Res* 50:5537-5542.
169. Tsuruo, T., H. Iida, S. Tsukagoshi, T. Oku, and T. Kishida. 1982. Different susceptibilities of cultured mouse cell lines to mouse interferon. *Gann* 73:42-47.
170. Sidky, Y.A., E.C. Borden, C.E. Weeks, M.J. Reiter, J.F. Hatcher, and G.T. Bryan. 1992. Inhibition of murine tumor growth by an interferon-inducing imidazoquinolinamine. *Cancer Res* 52:3528-3533.
171. Sakurai, F., T. Terada, M. Maruyama, Y. Watanabe, F. Yamashita, Y. Takakura, and M. Hashida. 2003. Therapeutic effect of intravenous delivery of lipoplexes containing the interferon-beta gene and poly I: poly C in a murine lung metastasis model. *Cancer Gene Ther* 10:661-668.
172. Ozawa, S., W. Lu, C.D. Bucana, H.O. Kanayama, H. Shinohara, I.J. Fidler, and Z. Dong. 2003. Regression of primary murine colon cancer and occult liver metastasis by intralesional injection of lyophilized preparation of insect cells producing murine interferon-beta. *Int J Oncol* 22:977-984.
173. De Bouard, S., J.S. Guillamo, C. Christov, N. Lefevre, P. Brugieres, E. Gola, P. Devanz, S. Indraccolo, and M. Peschanski. 2003. Antiangiogenic therapy against experimental glioblastoma using genetically engineered cells producing interferon-alpha, angiostatin, or endostatin. *Hum Gene Ther* 14:883-895.
174. von Marschall, Z., A. Scholz, T. Cramer, G. Schafer, M. Schirner, K. Oberg, B. Wiedenmann, M. Hocker, and S. Rosewicz. 2003. Effects of interferon alpha on vascular endothelial growth factor gene transcription and tumor angiogenesis. *J Natl Cancer Inst* 95:437-448.
175. Izawa, J.I., P. Sweeney, P. Perrotte, D. Kedar, Z. Dong, J.W. Slaton, T. Karashima, K. Inoue, W.F. Benedict, and C.P. Dinney. 2002. Inhibition of tumorigenicity and metastasis of human bladder cancer growing in athymic mice by interferon-beta gene therapy results partially from various antiangiogenic effects including endothelial cell apoptosis. *Clin Cancer Res* 8:1258-1270.
176. McCarty, M.F., D. Bielenberg, C. Donawho, C.D. Bucana, and I.J. Fidler. 2002. Evidence for the causal role of endogenous interferon-alpha/beta in the regulation of angiogenesis, tumorigenicity, and metastasis of cutaneous neoplasms. *Clin Exp Metastasis* 19:609-615.
177. Dvorak, H.F., and I. Gresser. 1989. Microvascular injury in pathogenesis of interferon-induced necrosis of subcutaneous tumors in mice. *J Natl Cancer Inst* 81:497-502.
178. Zeh, H.J., and D.L. Bartlett. 2002. Development of a replication-selective, oncolytic poxvirus for the treatment of human cancers. *Cancer Gene Ther* 9:1001-1012.
179. Sauthoff, H., J. Hu, C. Maca, M. Goldman, S. Heitner, H. Yee, T. Pipiya, W.N. Rom, and J.G. Hay. 2003. Intratumoral spread of wild-type adenovirus is limited after local injection of human xenograft tumors: virus persists and spreads systemically at late time points. *Hum Gene Ther* 14:425-433.

180. Tsirigotis, M., S. Thurig, M. Dube, B.C. Vanderhyden, M. Zhang, and D.A. Gray. 2001. Analysis of ubiquitination in vivo using a transgenic mouse model. *Biotechniques* 31:120-126, 128, 130.

Contributions of Collaborators

Jen Reynard provided general assistance with mouse work, including all intravenous injections and slow infusions, as well as some intratumoural injections and establishment of mouse tumours. Alison McGuire provided significant assistance with several experiments. Alison infected cells and titred virus in tissue culture media for Figures 6B and 7C. Alison also homogenized and titred VSV in all of the tissues from the kinetic biodistribution experiment (Figure 11), as well as a some samples from Figure 12. Alison also aided with some tumour sectioning and immunohistochemical staining (Figures 16, 17 and 18). Alison performed the majority of the sectioning and staining presented in Appendix X (EMT6). Shane Knowles prepared the AV1 VSV used in Figures 13, 14 an 17. David Stojdl provided the G-less WT VSV GFP used in Figure 10. Brian Lichty constructed and rescued WT VSV GFP.

Appendices

Appendix I: Comparison of GFP expression in lung tumour-bearing animals before and after perfusion.

CT26 lung-tumour bearing animals were treated with Δ51 VSV GFP for 1 day. Lungs and heart were removed and photographed, then the lungs were perfused with PBS, and photographed again. Shown are overlays of GFP and white light picture.

Before perfusion

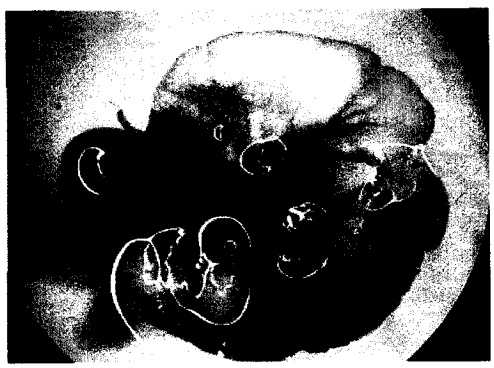

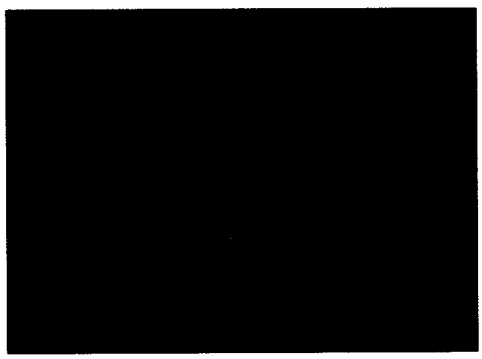

After perfusion

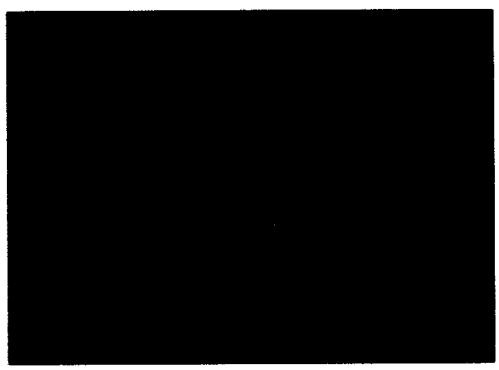

Appendix II: Immunohistochemistry of complete panel of two-day VSV treated tumours used for quantification in Figure 16D and E.

CT26 subcutaneous tumour-bearing mice were intravenously injected with $5x10^8$ PFU of IFN inducing VSV mutants (either AV1 VSV, or recombinant reporter gene expressing Δ51 VSVs). Two days later, mice were euthanized, and frozen tumour sections were immunohistochemically stained for VSV and active caspase 3.

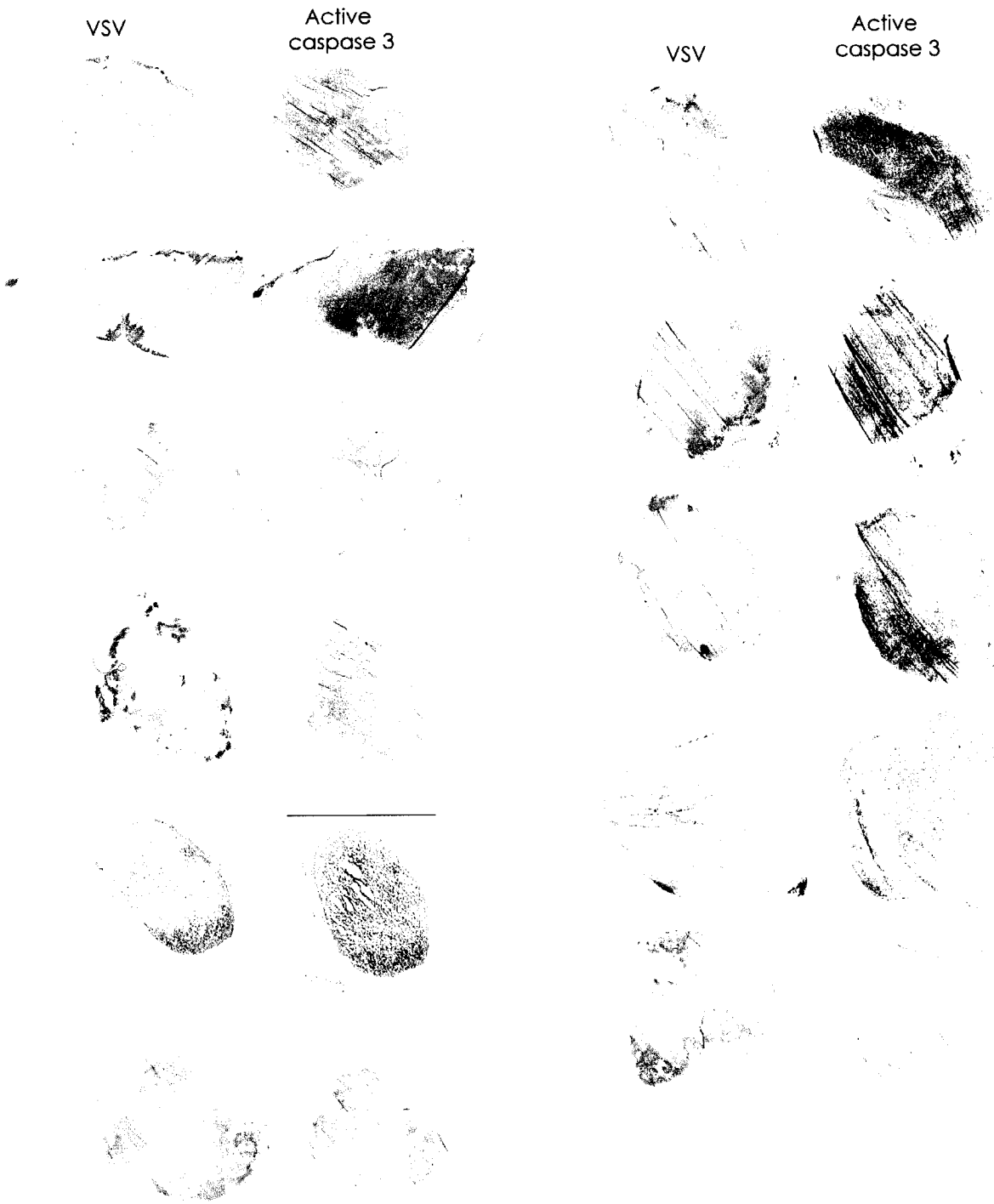
VSV
Active caspase 3
VSV
Active caspase 3

Appendix III: Immunohistochemistry of complete panel of untreated treated tumours used for quantification in Figure 16E.

CT26 subcutaneous tumour-bearing mice were euthanized, and frozen tumour sections were immunohistochemically stained for active caspase 3.

Active caspase 3 staining

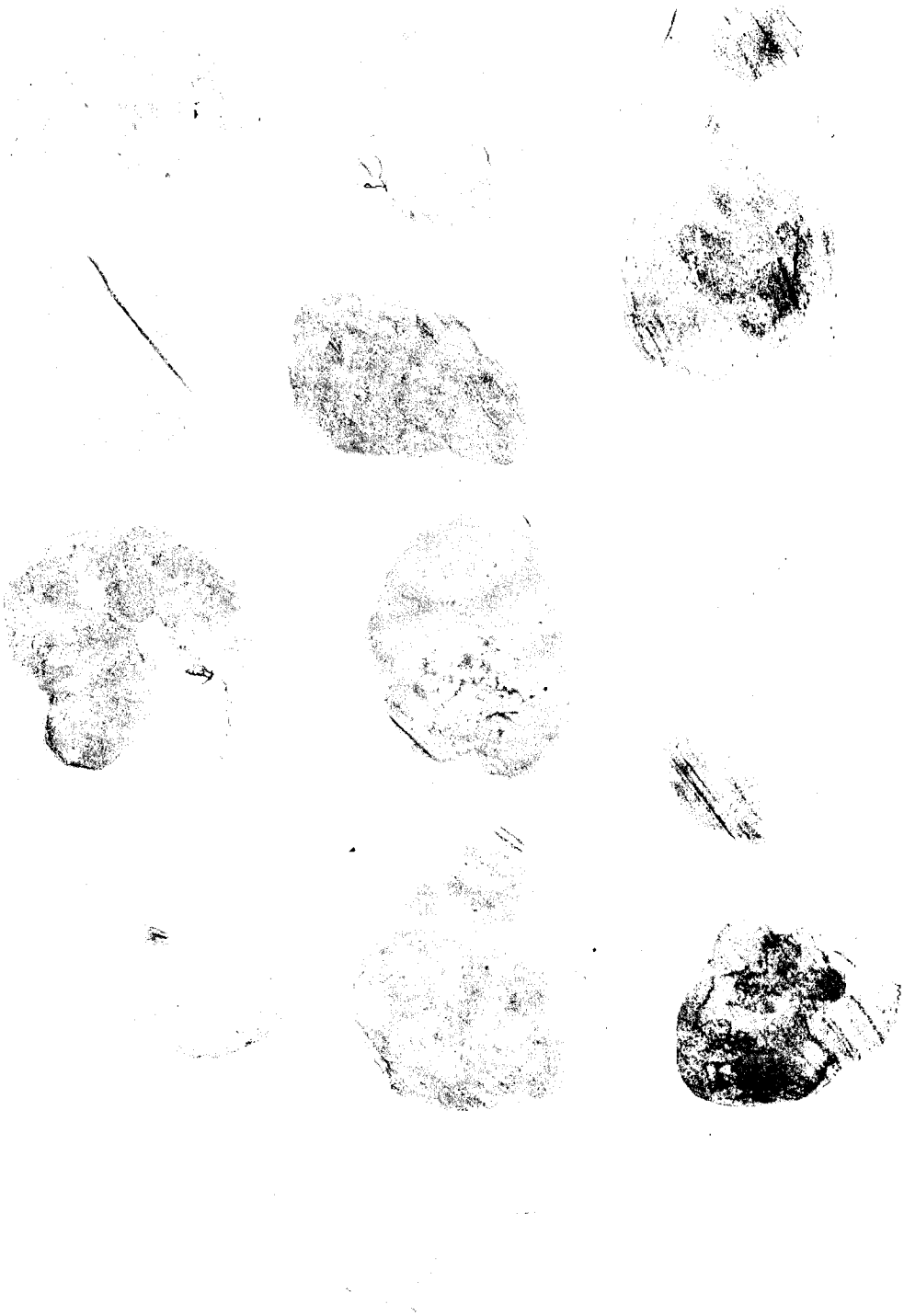

Appendix IV: Immunohistochemistry of complete panel of 5-day treated tumours used for quantification in Figure 16D and E.

CT26 subcutaneous tumour-bearing mice were intravenously injected with $5x10^8$ PFU of IFN inducing VSV mutants (either AV1 VSV, or recombinant reporter gene expressing Δ51 VSVs). Five days later, mice were euthanized, and frozen tumour sections were immunohistochemically stained for VSV and active caspase 3.

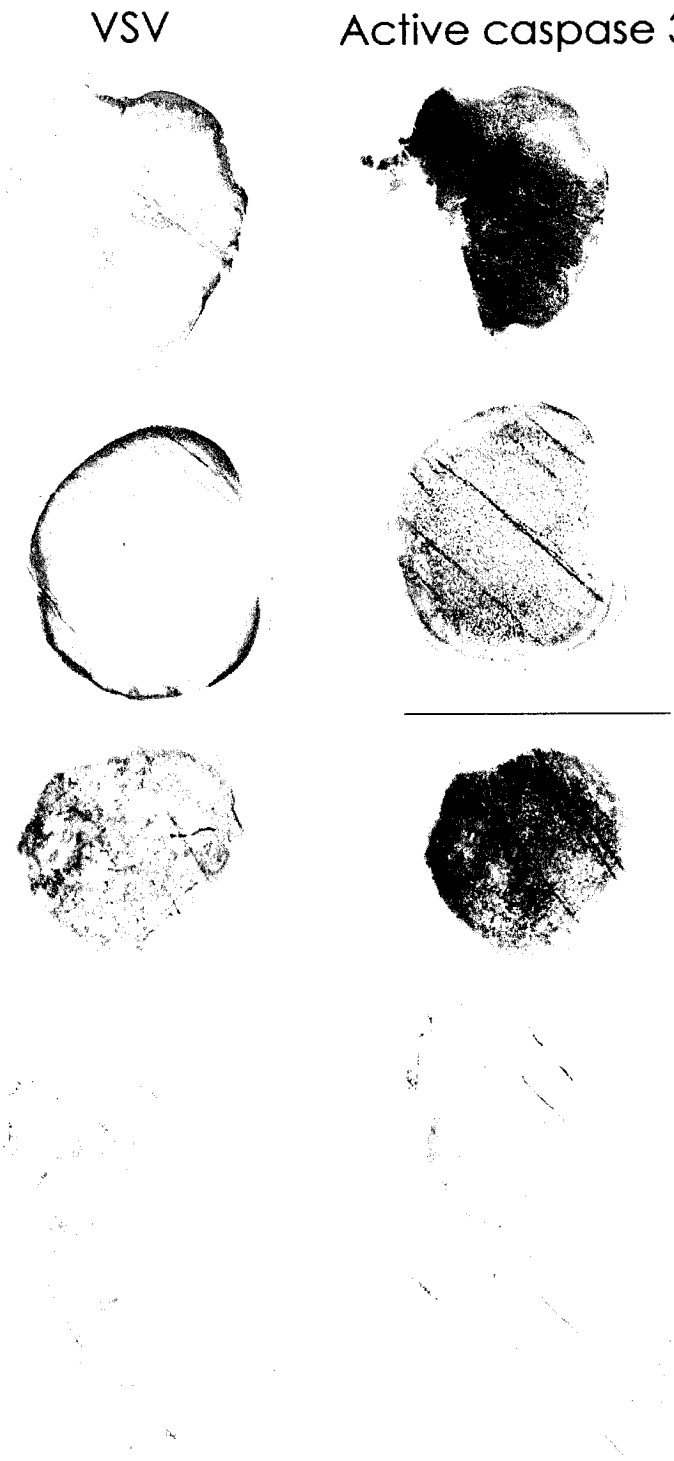
VSV
Active caspase 3

Appendix V: Immunohistochemistry of CT26 subcutaneous tumours treated with WT VSV for 2 days.

CT26 subcutaneous tumour-bearing mice were intravenously injected with $5x10^8$ PFU of WT VSV GFP. Two days later, mice were euthanized, and frozen tumour sections were immunohistochemically stained for VSV and active caspase 3.

VSV

Active caspase 3

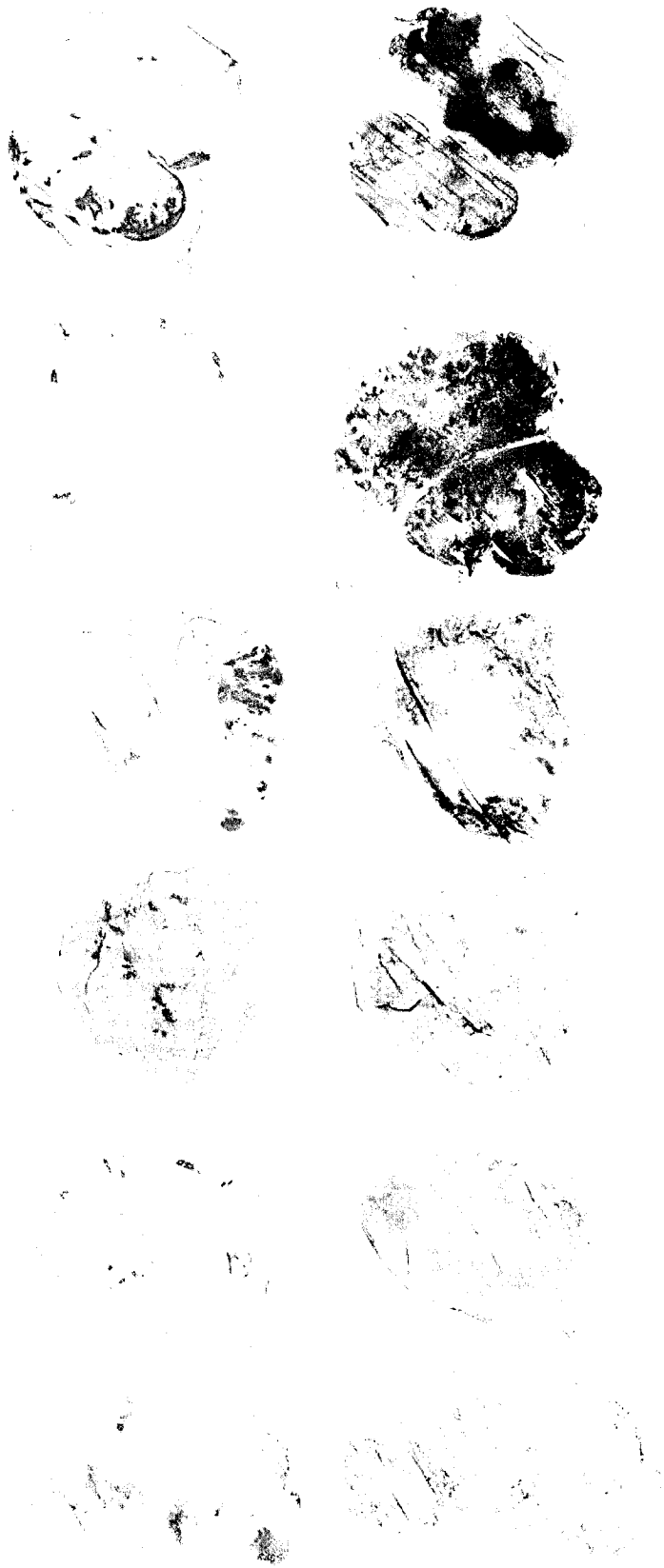

Appendix VI: Immunohistochemistry of CT26 subcutaneous tumours treated IT with Δ51 VSVs or PBS for 2 days.

CT26 subcutaneous tumour-bearing mice were intratumourally injected with $5x10^8$ PFU of IFN inducing VSV mutants (A) or PBS (B), both in 35 ul. Two days later, mice were euthanized, and frozen tumour sections were immunohistochemically stained for VSV and active caspase 3.

A

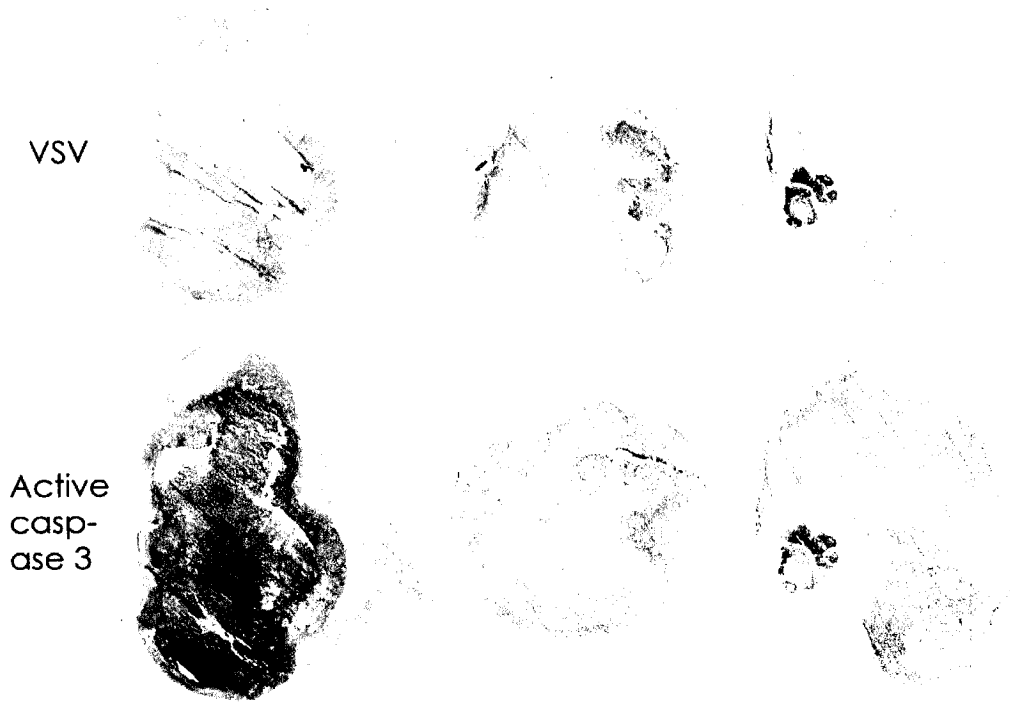

B

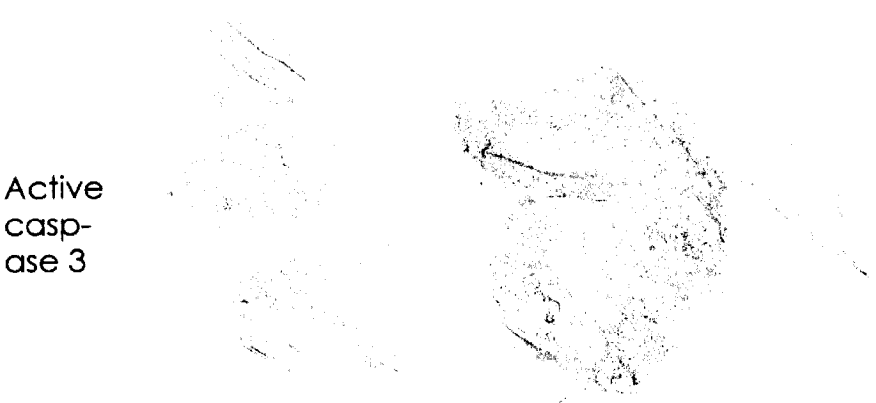

Appendix VII: Immunohistochemistry of CT26 subcutaneous tumours in Balb/c nude mice treated with recombinant Δ51 VSVs IV for 2 days, or untreated.

Balb/c nude mice were injected with CT26 cell subcutaneously. After tumours developed, animals were intravenously injected with $5x10^8$ PFU of IFN inducing VSV mutants (**A**). Five days later, mice were euthanized, and frozen tumour sections were immunohistochemically stained for VSV and active caspase 3. **B** shows the tumours of untreated nude mice.


A
VSV
Active
casp-
ase 3
B
Active
casp-
ase 3

Appendix VIII: Illustration of VSV, active caspase 3, hypoxia, and perfusion in all tumours from Figure 17 experiment.

CT26 subcutaneous tumour-bearing mice were intravenously injected with $5x10^8$ PFU AV1 VSV or PBS and 48 hours later, animals were treated with Hypoxyprobe (intraperitoneally) to assess hypoxia and fluorescent microspheres (intravenously) to assess tumour perfusion. Further details are provided in the text and in *Materials and Methods*. **A** illustrates microsphere distribution, active caspase 3 staining and hypoxyprobe staining in the tumours of animals treated with PBS. **B** illustrates the tumours of animals treated with VSV.

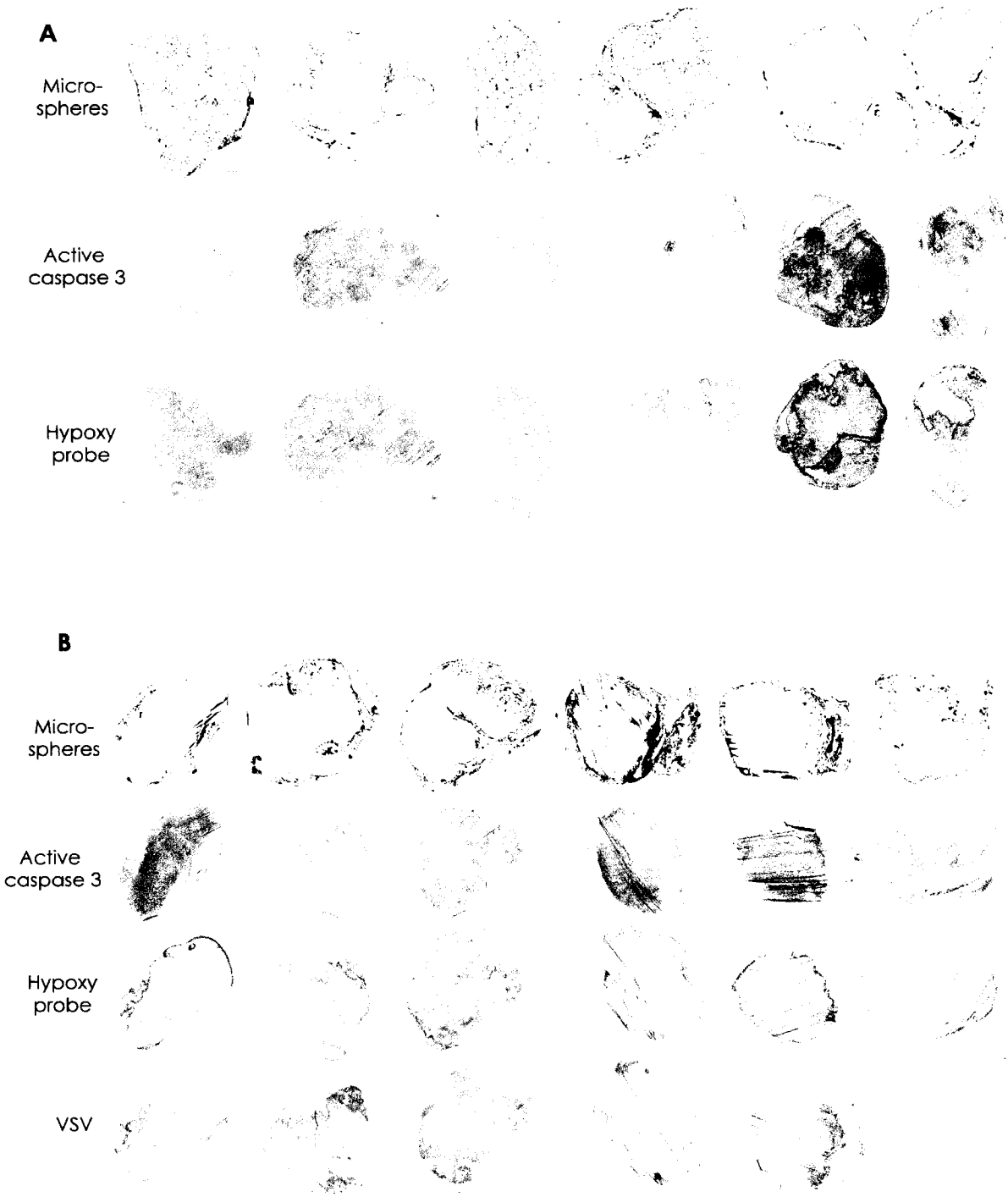
A
Micro-
spheres
Active
caspase 3
Hypoxy
probe
B
Micro-
spheres
Active
caspase 3
Hypoxy
probe
VSV

Appendix IX: Illustration of VSV, active caspase 3, hypoxia, and perfusion in two tumours 15 hours after AV1 VSV treatment.

CT26 subcutaneous tumour-bearing mice were intravenously injected with $5x10^8$ PFU AV1 VSV or PBS and 15 hours later, animals were treated with Hypoxyprobe (intraperitoneally) to assess hypoxia and fluorescent microspheres (intravenously) to assess tumour perfusion. Further details are provided in the text and in *Materials and Methods*. Microsphere distribution, active caspase 3, hypoxyprobe, and VSV staining in tumour cryosections are shown.

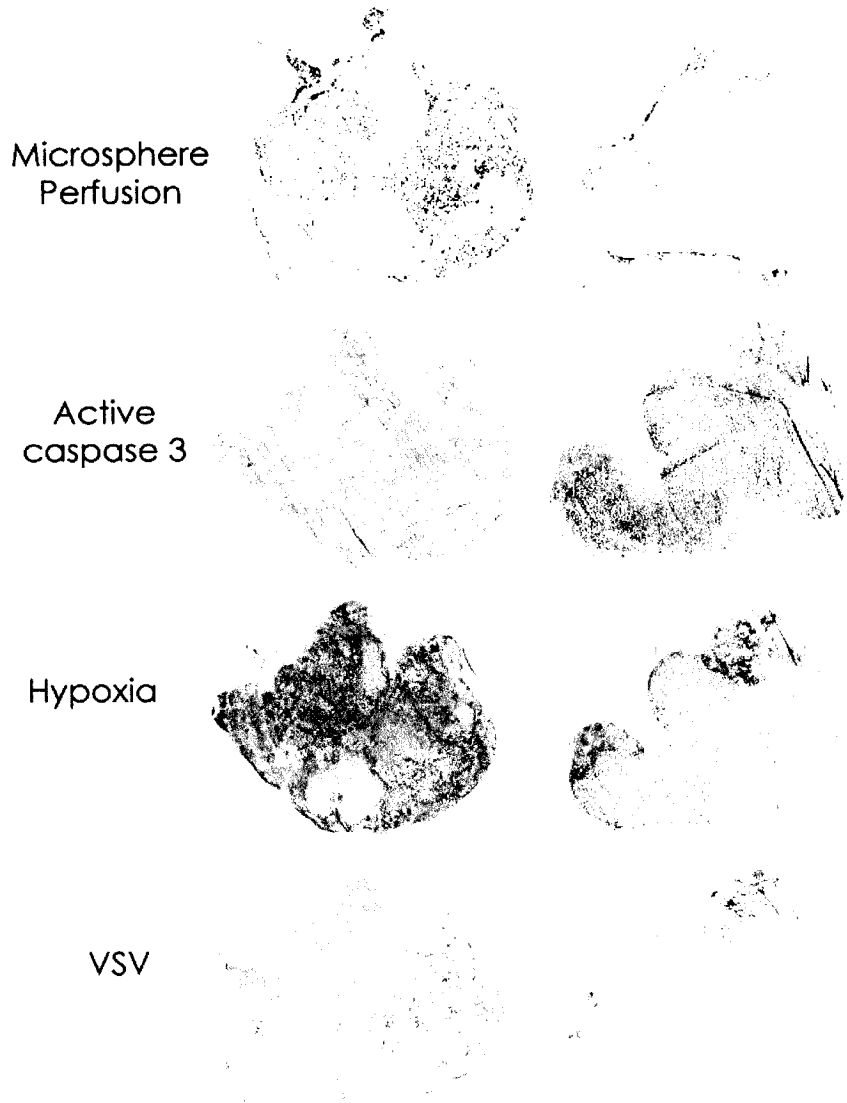
Microsphere Perfusion
Active caspase 3
Hypoxia
VSV

Appendix X. Anti-VSV immunohistochemistry in EMT6 subcutaneous tumours 2 days after treatment with VSV by IV or IT route.

Balb/c mice were injected with $3x10^5$ EMT6 cells. Once tumours formed, animals were treated intravenously or intratumourally with $5x10^8$ PFU of IFN-inducing mutants of VSV. Tumour cryosections were immunohistochemically stained for VSV.

Intratumoural

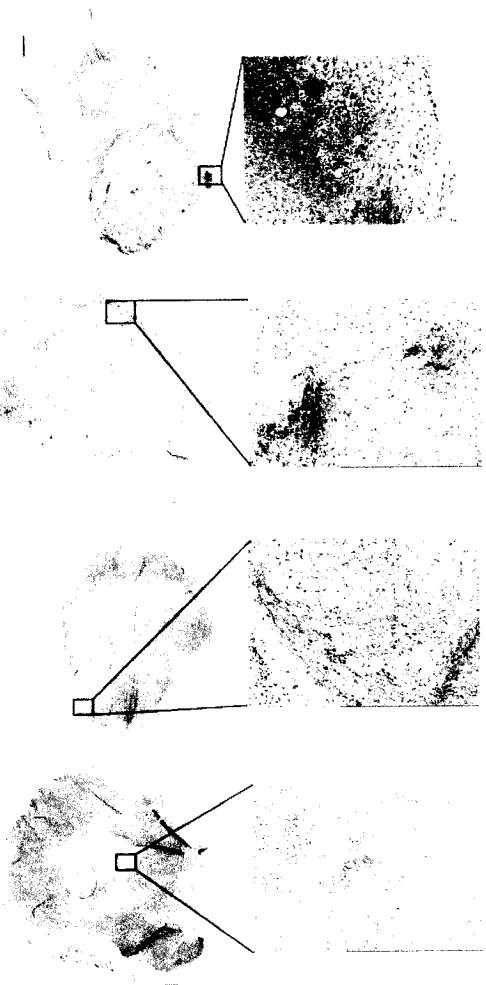

Intravenous

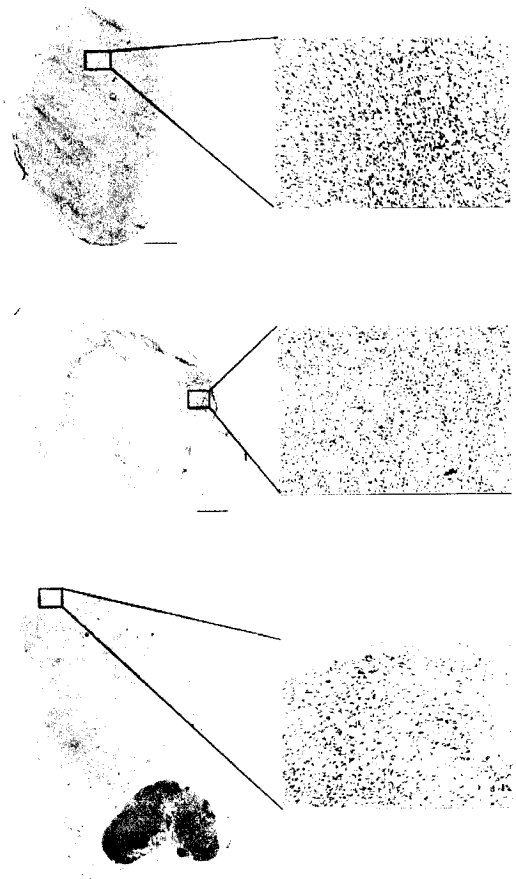

Appendix XI. Anti-VSV immunohistochemistry in CT26 subcutaneous tumours between 7 and 15 hours after intravenous infection.

CT26 subcutaneous tumour-bearing mice were intravenously injected with $5x10^8$ PFU of VSV. 7-15 hours later (as indicated) mice were euthanized, and frozen tumour sections were immunohistochemically stained for VSV.

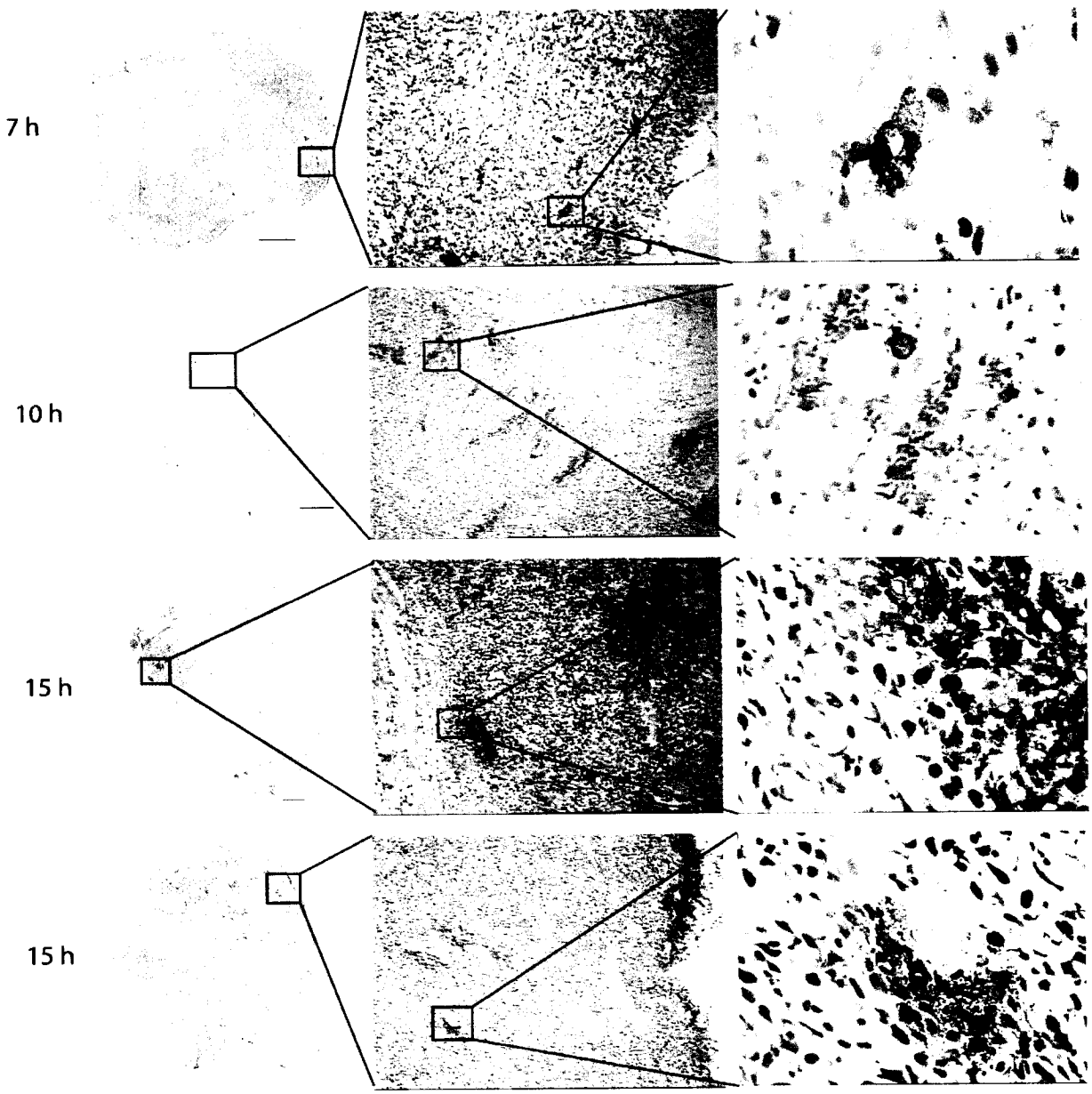
7 h
10 h
15 h
15 h

Curriculum Vitae

Education

Institution:	University of Ottawa (Ottawa, ON)
Date:	Sep. 2002 – current
Degree:	M.Sc. Candidate in Biochemistry, Microbiology and Immunology
Awards:	NSERC Post Graduate Scholarship A ($34,600 over two years) University of Ottawa National Excellence Scholarship

Institution:	University of Ottawa (Ottawa, ON)
Date:	Sep. 2000 – Jun. 2002
Degree:	B.Sc. in Biochemistry (Honours) completed in Jun. 2002
Grades:	Cumulative GPA 9.1
Awards:	Admission Scholarship of $2,500 annually NSERC Undergraduate Student Research Award ($5,000) held Summer of 2001

Institution:	Queen's University (Kingston, ON)
Date:	Sep. 1998 – Jun. 2000
Degree:	First two years of Biochemistry degree completed
Grades:	Cumulative average of 87%
Awards:	Principal's Entrance Scholarship of $8,000 annually

Institution:	Earl of March S.S. (Kanata, ON)
Date:	1993 - 1998
Degree:	Ontario Secondary School Diploma, with Certificate of French Immersion
Grades:	Graduating average of 96%
Awards:	OAC Staff Awards (highest mark) in Chemistry, Biology, Physics, English, French, History

Work Experience

Employer:	Dr. J. Bell, Ottawa Regional Cancer Center, University of Ottawa
Date:	Sep. 2001 – current
Position:	M.Sc. candidate (Sep. 2002 – current) Research Assistant (Jun. – Sep. 2002) Undergraduate Honour's Student Researcher (Sep. – May 2002)

Employer:	Dr. L. Bonen, Department of Biology, University of Ottawa (Ottawa, ON)
Date:	May – Sep. 2001
Position:	NSERC Undergraduate Student Researcher

Employer:	Kymata Canada Ltd. (Ottawa, ON)
Date:	Jun. – Sep. 2000
Position:	Administrative Assistant

Employer:	Nidacon Canada Inc. (Ottawa, ON)
Date:	May 2000, May – Sep. 1999
Position	Research Assistant

Publications

Stojdl DF, Lichty BD, tenOever BR, Paterson JM, Power AT, Knowles S, Marius R, Reynard J, Poliquin L, Atkins H, Brown EG, Durbin RK, Durbin JE, Hiscott J, Bell JC. VSV strains with defects in their ability to shutdown innate immunity are potent systemic anti-cancer agents. Cancer Cell. 2003 Oct;4(4):263-75.

Poster presentations

Investiagtion of VSV oncolysis in murine cancer models.
BioNorth 2003, Ottawa, ON

Fluorescent proteins provide a sensitive method of assessing Vesicular stomatitis virus oncolysis in vivo.
Oncolytic Viruses as Cancer Therapeutics 2003, Banff, AB

Skills and Strengths

I have a wide range of biological laboratory skills, including animal work, cell culture, molecular cloning, and analysis of gene expression. During my work at the Ottawa Regional Cancer Centre, I also had frequent opportunity to present my research formally to a large audience of peers. Science outreach volunteer work with the group *Lets talk science* has helped me develop skills in explaining science to the public. On a similar note, I was also a frequent contributor to the science section of the *Queen's Journal* when I attended university there.